Theoretical and Experimental Relationships between Stress Dilatancy and IDS Strength Components

By

KUM-HUNG HO

A DISSERTATION PRESENTED TO THE GRADUATE COUNCIL OF THE UNIVERSITY OF FLORIDA IN PARTIAL FULFILLMENT OF THE REQUIREMENTS FOR THE DEGREE OF DOCTOR OF PHILOSOPHY

UNIVERSITY OF FLORIDA
1971

To my wife, Nancy, for her constant support and encouragement without which this dissertation would not have been completed.

ACKNOWLEDGEMENTS

The author gratefully expresses his appreciation to Dr. John H. Schmertmann, Chairman of his Supervisory Committee,for the encouragement and guidance during the course of this study. The writer is also indebted to Dr. M. W. Self and Dr. F. G. Martin for serving on his Supervisory Committee.

This investigation was supported by National Science Foundation Grant No. GK-1908X which provided the research assistantship to make this work financially possible.

Thanks are due Mr. William Whitehead who provided general assistance in the laboratory.

TABLE OF CONTENTS

LIST OF TABLES

LIST OF FIGURES

NOTATION

a	zero intercept of Rowe's stress path plot
A	average area at point of contact of particles
A_c	area of specimen after consolidation phase
A_p	cross section area of piston
A_m	initial cross section area of membrane
A_s	cross section area of specimen
c	cohesion term in Coulomb's equation
c_e	Hvorslev effective or 'true' cohesion
c_f	cohesion corrected for dilatancy, interparticle cohesion
c_g	Gibson's modified Hvorslev c_e parameter
c_o	zero cohesion intercept
c_μ	interparticle cohesion strained at minimum energy
C	conditions of formation of soil
C.I.	confidence interval
d	slope of constant structure envelope = tan ϕ_ε
D_ε	dilatancy factor = $(1 + \lambda)$
D	effective stress Dependent component of mobilised shear resistance
D_{50}	diameter of particle at which 50% of the soil is finer
e	void ratio of specimen
e_c	void ratio after consolidation phase
e_f	final void ratio
e_i	initial void ratio
E	Young's modulus

E_R	energy ratio
g_f	dilatancy component in direct shear test
G_s	specific gravity of soil solids
h	height of spicimen
H	stress history
IDS	Independent-Dependent-Strain
I_m	maximum value of I_ε component in IDS test
I_o	bond strength
I_ε	effective stress Independent component of mobilised shear resistance
I^*_ε	I_ε component corrected for dilatancy
K	correction factor for filter paper
K_{af}	$\tan^2 (45 - \phi_f/2)$
K_{pf}	$\tan^2 (45 + \phi_f/2)$
m_1	ratio of length of projected solid path to number of contact points in vertical direction
m_3	ratio of length of projected solid path to number of contact points in horizontal direction
M	slope of Roscoe's p vs q line
n	porosity
n_s	number of samples
N	normal load at point of contact of particles
p'	mean principal stress = $\frac{\sigma'_1+2\sigma'_3}{3}$
P	vertical force
q	shear stress
Q	horizontal force
r_f	sample correlation coefficient for τ^*_t vs $\bar{\sigma}^{*\prime}_t$
r_i	sample correlation coefficient for I_ε vs $\bar{\sigma}'_t$ relationship

r^*	sample correlation coefficient for I_ε^* vs $\bar{\sigma}_t^{*\prime}$ relationship
r_s	radius of sample
R	principal stress ratio = σ_1'/σ_3'
R_o	uplift on piston
s	degree of saturation
s_c	degree of saturation after consolidation phase
s_f	final degree of saturation
s_i	initial degree of saturation
s_s	sample standard deviation
S	soil structure, geometric arrangement of soil particles
t_m	thickness of membrane
t_{100}	time to end of primary consolidation
T	temperature
u	pore water pressure
w	water content of specimen
w_c	water content after consolidation phase
w_f	final water content
w_i	initial water content
x	horizontal relative movement or abscissa
y	vertical height or movement or ordinate
$\bar{y}$	sample mean

Greek Alphabet

α_R	Rowe's structural parameter
α_s	Schmertmann's soil structure parameter in constant structure envelope
β_m	slope of I_m vs $\bar{\sigma}'_t$ line and also parameter in constant structure envelope
β_0	zero intercept of linear model
β_1	slope of line in linear model
$\delta\varepsilon_1$	increment of major principal strain, defined as positive in compression
$\delta\varepsilon_3$	increment of minor principal strain, defined as positive in compression
$\Delta\sigma'_1$	$= \sigma'_{1h} - \sigma'_{1_0}$, difference in major principal effective stress in IDS test
ε	strain
ε_{at}	axial strain due to consolidation and undrained deformation
ε_r	error component
ε_v	volumetric strain, positive for volume increase
ε_1	strain in same direction as σ_1, positive for compression
ε_3	strain in same direction as σ_3, negative for horizontal decrease
$\dot{\varepsilon}$	strain rate
κ	slope of c_e vs σ'_e line
λ	rate of change of volumetric strain to vertical strain $= \dfrac{d\varepsilon_v}{d\varepsilon_1}$
μ	population mean
ρ_f	population correlation coefficient for τ^* vs $\bar{\sigma}^{*\prime}_t$ relationship

ρ_i	population correlation coefficient for I_ε vs $\bar{\sigma}'_t$ relationship
ρ^*	population correlation coefficient for I^*_ε vs $\bar{\sigma}^{*\prime}_t$ relationship
ρ_p	effective stress component derived from primary chemical bonds
ρ_s	effective stress component derived from van der Waal's forces and electrostatic forces
σ^2	variance of error component
σ'	$\sigma - u$, where ' indicates effective stress
σ'_c	effective consolidation pressure
σ'_e	equivalent effective consolidation pressure
σ_f	pressure normal to failure plane
σ_h	hydrostatic cell pressure
$\bar{\sigma}'_t$	average normal effective stress at any strain between the two points of common Mohr circle tangency in an IDS test
$\bar{\sigma}^{*\prime}_t$	$\bar{\sigma}'_t$ corrected for dilatancy
σ'_1	major principal effective stress
σ'_{1h}	major principal effective stress at high pressure level
$\sigma'_{1\ell}$	major principal effective stress at low pressure level
σ'_3	minor principal effective stress
$(\sigma_1-\sigma_3)$	deviator stress
$\bar{\sigma}'_1$	$= \frac{1}{2}(\sigma'_{1h} + \sigma'_{1\ell})$, average major principal effective stress
τ	$= \frac{1}{2}(\sigma_1 - \sigma_3)$, shear stress
τ_f	shear stress on failure plane
τ_t	average shear stress at any strain between two points of common Mohr circle tangency in an IDS test
τ^*_t	τ_t corrected for dilatancy

T	shear force at point of contact of particles
ϕ	angle of internal friction in Coulomb's equation
ϕ_{cv}	interparticle friction angle sheared at constant volume
ϕ_e	Hvorslev effective or 'true' angle of internal friction
ϕ_f	angle of internal friction corrected for dilatancy, interparticle friction
ϕ_g	Gibson's modified Hvorslev ϕ_e parameter
ϕ_{Rs}	friction angle from Roscoe's Critical State Concept
ϕ_r	Coulomb's ϕ after deduction of external work by dilation
ϕ_α	friction angle applied to α_R plane
ϕ_ε	rate of change of D_ε component of mobilised shear resistance
ϕ^*_ε	ϕ_ε corrected for dilatancy
ϕ_μ	physical angle of friction between the minerals
ψ	slope of Rowe's stress path plot

Abstract of Dissertation Presented to the Graduate Council of the University of Florida in Partial Fulfillment of the Requirements for the Degree of Doctor of Philosophy

THEORETICAL AND EXPERIMENTAL RELATIONSHIPS BETWEEN STRESS DILATANCY AND IDS STRENGTH COMPONENTS

By

Kum-Hung Ho

August 1971

Chairman: Dr. John H. Schmertmann

Major Department: Civil Engineering

The object of this study is to establish the relationships between Schmertmann's IDS components of I_ε, tan ϕ_ε and α_s, and Rowe's interparticle parameters of c_f, tan ϕ_f and α_R. Both investigators realised the importance of soil structure but took entirely different approaches to account for this effect. Both sets of parameters are claimed to be more fundamental than Hvorslev's 'true' parameters of c_e and ϕ_e and, moreover, they are obtained as a function of strain.

The IDS test was extended to include measurement of volume changes during shear so that both sets of parameters can be computed from the data on the same sample. The linear relationship between the I_ε component and $\bar{\sigma}'_t$, the average normal effective stress at each strain, has been shown to be valid for the three types of materials investigated, i.e. kaolinite, glass beads and glass beads with hydrocal.

The average shear stress and average normal effective stress corrected for dilatancy, τ_t^* and $\bar{\sigma}_t^{*\prime}$, are also demonstrated to be linearly related at each strain for the three materials with still higher positive correlation coefficients than the I_ε versus $\bar{\sigma}_t^{\prime}$ correlation at each strain.

Both the IDS and Stress Dilatancy Methods can be employed to determine 'bond strength' I_o and c_f respectively, as a function of strain. Their difference lies in the effect of dilatancy, which is small. The choice of the method depends on the individual since each method has some advantages over the other. Introducing a dilatancy correction into Schmertmann's method, giving I_ε^* and $\bar{\sigma}_t^{*\prime}$, is not recommended for the determination of bond strength because of the larger scatter.

ϕ, ϕ_ε, ϕ_f and ϕ_α friction angles are presented on the same Mohr diagram for cohesionless materials. The two α parameters show some correlation for the three materials tested.

The application of small sample procedures in statistics provides a rational means of analysing and drawing conclusions from the data obtained from this work.

CHAPTER I
INTRODUCTION

The concept of shear strength occupies an important position in the field of soil mechanics. The most frequent problem encountered by a soils engineer is that of stability, which requires knowledge of the shear strength of soils. The selection of the proper value of shear strength to suit a particular field problem is sometimes difficult, especially for fine grained soils.

In practice, the shear strength parameters at failure, c and ϕ are determined from a series of test samples and these are then substituted into the expressions for bearing capacity or slope stability.

The separation of shear resistance into components of 'cohesion' and 'friction' has recieved wide attention. Following Taylor (1948), energy corrections have been used for the analysis of shear data by many investigators (Penman, 1953; Gibson, 1953; Bishop, 1954; Newland and Allely, 1957; Roscoe, Schofield and Wroth, 1958; Bjerrum, 1961) and have been made only for failure or ultimate conditions.

To better understand the mobilization of shear strength, Schmertmann and Osterberg (1960) introduced a new laboratory technique and Rowe (1962) independently put forward a new mathematical theory to separate shear resistance into

components at any stage of deformation. These two entirely different approaches resulted in different parameters. A unifying concept is needed to relate the parameters obtained from these two methods.

The object of this dissertation is to determine the relationships between the two sets of parameters obtained by Schmertmann's IDS Concept and Rowe's Stress Dilatancy Theory so that greater understanding into the mobilization of shear strength with strain will result.

The experimental part of this study is confined to triaxial compression tests on three types of materials, i.e. kaolinite (cohesive), glass beads (cohesionless) and glass beads with hydrocal (artificial bonds). Three different stress paths of constant-σ_1', p' and volume were imposed on the extruded kaolinite while constant-σ_3' IDS tests were made on the other two materials.

CHAPTER II
REVIEW OF PREVIOUS WORK

Historical Background

Although Coulomb had introduced his shear strength equation almost 200 years ago (1776), the present-day concept of shear strength is still built around his original form of equation where the maximum shear resistance was given by

$$\tau_f = c + \sigma_f \tan \phi \qquad (2\text{-}1)$$

where c and ϕ are the apparent cohesion and angle of shearing resistance respectively and σ_f, the pressure normal to the failure plane.

Mohr, in 1882, proposed a more general criterion of failure based on shear stress. He assumed that at failure the shear stress, τ_f and the normal stress on the failure plane, σ_f, are uniquely related

$$\tau_f = f(\sigma_f) \qquad (2\text{-}2)$$

This relation is represented on the shear stress versus normal stress diagram by the envelope of all possible Mohr circles of stress for the material. When the relation of the Mohr criterion is linear, it becomes identical with the Coulomb criterion, i.e.

$$\tau_f = c + \sigma_f \tan \phi \qquad (2\text{-}3)$$

This is referred to as the Mohr-Coulomb failure criterion.

In 1923, Terzaghi showed that effective stress, σ',

controls the deformation behaviour of saturated soils and it is equal to the total stress, σ,minus the pore water pressure,u,

$$\sigma' = \sigma - u \qquad (2\text{-}4)$$

The Mohr-Coulomb failure criterion for saturated soils is therefore unique when expressed in terms of effective stresses.

$$\tau_f = c' + (\sigma_f - u) \tan \phi' \qquad (2\text{-}5)$$

This equation remains one of the most controversial in soil mechanics in the sense that the parameters c and ϕ are not unique.

Methods of Separating Shear Resistance

Hvorslev's 'True'Strength Parameters

The triaxial test is most commonly used in research work and in routine testing for the determination of effective stress parameters. The standard types of triaxial tests are the undrained or UU test, the consolidated-undrained test (CD) with pore pressure measurements and drained test. The undrained test in saturated clay gives a horizontal Mohr envelope where no volume or intergranular stress changes take place. This yields the undrained shear strength for the $\phi = 0$ method of analysis. Effective stress parameters are obtained by comparing samples having different intergranular stresses and volume changes at failure (or void ratio). Such conventionally determined strength parameters vary, among other factors, with stress

history (normally or overconsolidated) and drainage conditions at the time of test. Since the series of tests defining the envelope are of different void ratio and also different soil structures, their strength components are also different. Thus the effective strength parameters obtained conventionally are empirical factors and not fundamental properties of the soil material.

Working with remolded clays, Hvorslev in 1937 came a little closer to obtaining the true cohesion and friction of a soil. He compared normally consolidated and overconsolidated samples having the same water content (void ratio) at failure. He obtained linear shear strength versus normal stress at failure lines whose slopes are equal and their inclination gives the effective angle of internal friction, ϕ_e. The zero intercept on the shear strength axis yields the effective cohesion component, c_e, for the particular void ratio. Different c_e values were obtained for different void ratios and it was found that they vary linearly with the equivalent consolidation pressure, σ_e', for clays remolded at high water contents. Bjerrum (1954) found that for clays remolded at low water contents, a zero cohesion intercept, c_o, exists.

$$c_e = c_o + \kappa\sigma_e' \qquad (2\text{-}6)$$

where κ is the slope of the c_e vs σ_e' line.

Thus, on the basis of Hvorslev's work, Coulomb's equation becomes

$$\tau_f = c_e + \sigma_f' \tan \phi_e \qquad (2\text{-}7)$$

where c_e is a function of the water content and ϕ_e was approximately constant and σ'_f = normal effective stress at failure.

Gibson (1953) proposed a failure criterion based upon energy considerations in direct shear tests. He retained the form of Hvorslev's equation but the meaning of the fundamental parameters is changed. The equation becomes

$$\tau_f = c_g + \sigma'_f \tan\phi_g + \sigma'_f g_f \qquad (2\text{-}8)$$

where c_g and ϕ_g are the modified parameters, g_f the dilatancy component.

Scott (1963) commented that Gibson's use of direct shear tests instead of triaxial tests was because of the difficulty of calculating or measuring the work done against the confining pressure from the gradient of the motion of the particles perpendicular to the failure plane. He refers to Gibson's dilatancy component as 'geometric factor' which for any one soil will be reflected in the variation of void ratio and the grain orientations of the soil.

Trollope et al.(1965) suggested that the open, 3-dimensional random structure of aggregate units of organic molecules of brown coal may be related to the open structural sensitive clays which have a 3-dimensional card-house structure. The major difference between brown coals and sensitive clays is that the structure of brown coal units is more fibrous than platy as in clays and the existence of primary chemical bonds between elements of brown coal.

They proposed a generalised effective stress equation

whereby the cohesion term may be considered as of a frictional nature and shear strength is given by

$$\tau = (\rho_\rho + \rho_s + \sigma'_f) \tan \phi_e \qquad (2\text{-}9)$$

where ρ_ρ = effective stress component derived from primary chemical bonds which is zero for clays.

ρ_s = effective stress component derived from van der Waals' forces and electrostatic forces.

ϕ_e = similar to friction angle of Hvorslev and is constant for a given structural arrangement of particles.

It should be noted that tan ϕ_e includes a geometric component as well as a coefficient of interpartical friction.

Schmertmann's IDS Concept

Schmertmann was the first to realise that any fundamental cohesion and friction components must vary with strain, and to devise a test procedure to investigate such variation. The development of the IDS curve-hopping technique (Schmertmann and Osterberg, 1960) in the separation of I_ε and D_ε components from shear resistance is one phase of research into the stress-strain-time response of cohesive soils dealing with stress-strain but with the time element held constant (method of testing, strain rate, specimen storage time, and any time dependent effects).

The formulation of the effective stress principle implies a unique relationship between τ_f and σ'_f. Actually shear strength, based on present knowledge (1971) of soil

behaviour is a function of a large number of factors:

$$\tau_f = f(e,\varepsilon,\dot{\varepsilon},\sigma',S,T,H,s,C,\lambda) \qquad (2\text{-}10)$$

where
- e = void ratio
- ε = strain
- $\dot{\varepsilon}$ = strain rate
- σ' = effective stress
- S = soil structure
- T = temperature
- H = stress history
- s = degree of saturation
- C = condition of formation of soil
- λ = rate of change of volumetric strain to vertical strain

Though the list of factors affecting shear strength looks formidable, fortunately not all of the factors are independent. Moreover, most of the factors are variable during deformation. For example, soil structure, S is a function of H, C, e, σ' and ε. Void ratio is a function of σ', H, C, and S. With the IDS technique, a given type of soil is sheared under constant temperature and strain rate at an identical soil structure where the void ratio change is negligible after a small variation in effective stress, the shearing resistance at any strain can be expressed as

$$\tau = f(\sigma',\lambda) \qquad (2\text{-}11)$$

Realising that Hvorslev's parameters were obtained at failure by comparing specimens at equal e (but not necessarily of the same structure), Schmertmann invented his curve-hopping technique to separate shear resistance into I_ε and D_ε components at any strain. Schmertmann (1963a, 1963b) found favourable agreement between $(\tan \phi_\varepsilon)_{max}$ with Hvorslev's $\tan \phi_e$ for remolded kaolinite, an undisturbed and remolded glacial lake clay and undisturbed Leda clay and suggested that I_ε and D_ε components are generalisations of

Hvorslev's parameters. It may be noted that at large strains where the comparisons of Hvorslev and Schmertmann components were made, the rate of volume changes of the samples would likely be small or negligible.

The separation of shear resistance at a certain strain requires the fitting of a tangent to two Mohr circles having the same structure. The zero tangent intercept on the shear stress axis gives the I_ε component while the slope, tan ϕ_ε,is a measure of the shear resistance sensitivity to a change in effective stress at the particular soil structure. The D_ε component is the difference between the total shear resistance and I_ε

$$D_\varepsilon = \tau_t - I_\varepsilon = \bar{\sigma}'_t \tan \phi_\varepsilon \qquad (2\text{-}12)$$

where $\bar{\sigma}'_t$ is the average normal effective stress at the tangential points to the two Mohr circles.

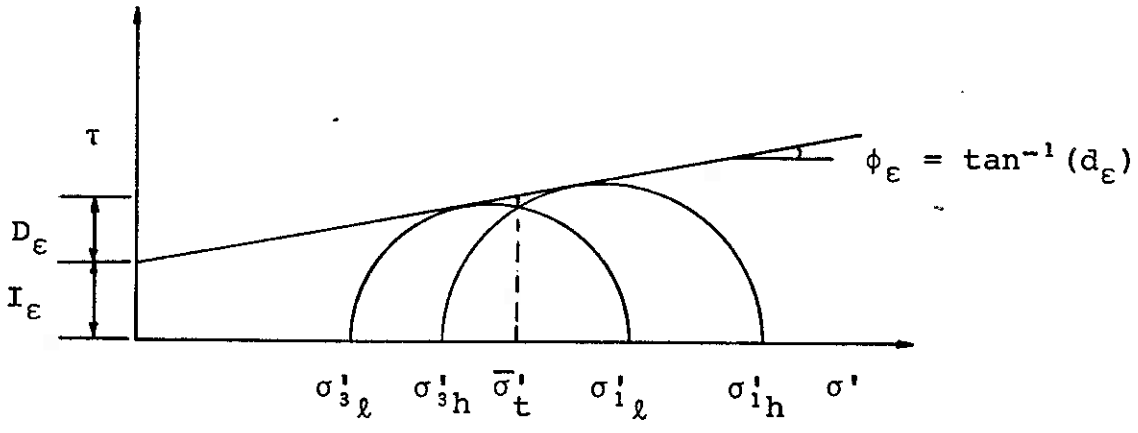

Figure II-1 I_ε and D_ε Components of Shear Resistance

Schmertmann and Osterberg (1960) had shown that the I_ε component (then called cohesion, c_ε) reaches a maximum at low strains (1% or less) while ϕ_ε increases with strain. For remolded soils, the maximum value of I_ε, I_m had been found to be quite stable, being independent of the mineralogy, time for primary and secondary consolidation, rate of strain suitable for IDS test, previous creep behaviour, stress history and type of pore fluid. However, I_m was found to be linearly related to the average normal effective stress! This confirmation was obtained for remolded and a few undisturbed clays as well as reassembled silts and sands. Thus I_m must have contained part of the shear strength due to curvature of the stress envelope.

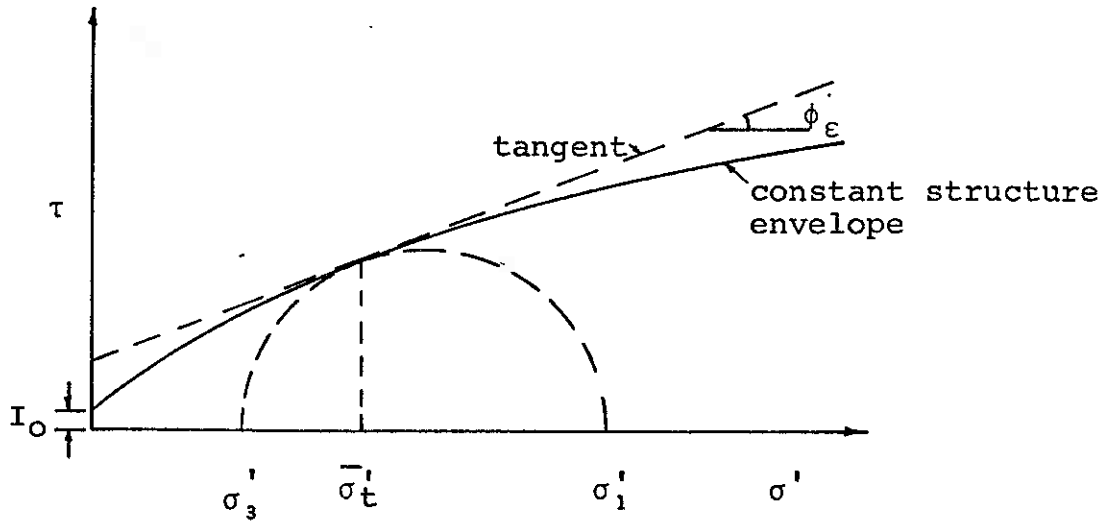

Figure II-2 Constant Structure Envelope

Based on the linear relationship between I_m and $\bar{\sigma}_t'$, a hypothetical Mohr envelope at constant structure was derived from the differential equation

$$\frac{d\tau_t}{d\bar{\sigma}_t'} = \frac{\tau_t - I_o - \beta_m \bar{\sigma}_t'}{\bar{\sigma}_t'} \qquad (2\text{-}13)$$

giving the solution as

$$\tau_t = I_o + \alpha_s \bar{\sigma}_t' - \beta_m \bar{\sigma}_t' \ell n(\bar{\sigma}_t') \qquad (2\text{-}14)$$

where I_o = bond strength

α_s = soil structure parameter varying with strain, stress ratio, density, etc.

β_m = soil constant varying seemingly with grain size only (value increasing with decreasing grain size)

Tests to date (Schmertmann, 1966a) indicate that β_m varies between limits of 0.15 and 0.22. For cohesive soils, bond strength I_o contributes to I_m in addition to the effect of envelope curvature. It is also assumed that maximum bond strength occurs at I_m. Topshoj (1970) concluded that bond strength of remolded kaolinite does not differ significantly for both triaxial compression and extension constant-σ_1' IDS tests. More detail considerations of the IDS Concept will be presented in Chapter III.

Rowe's Stress Dilatancy Theory

Rowe (1962) was not satisfied with the traditional approach to the problem of shear strength of soils involving the use of the Mohr-Coulomb Theory and the implications carried with it in respect to the manner of failure and slip

planes. He considered Coulomb's ϕ which includes both the frictional and dilatancy components of strength cannot properly define the behaviour of the material and came up with a theory that considers the effect of friction and dilatancy separately.

The basis of his Stress Dilatancy Theory is derived from the study of ideal assemblies of rods and uniform spheres under deviatoric stress systems. He considers the medium as discrete particles rather than as a continuum and derives relationship for stress and strain in terms of packing geometry, α_R, and ϕ_μ, the physical angle of friction between the particle surfaces.

He assumed that the form of law which applies to any uniform packing is also applicable to a mixture of packings. By minimising the ratio of energy input to energy output in a triaxial test, Rowe obtained the stress dilatancy relation for cohesionless soils.

$$\frac{\sigma_1'}{\sigma_3'(1+\lambda)} = \tan^2(45+\phi_\mu/2) \qquad (2\text{-}15)$$

where σ_1', σ_3' are the major and minor principal stresses respectively

λ is the rate of change of volumetric strain to vertical strain

For any state of packing other than very dense, the particles undergo rearrangement prior to failure involving further energy expended. To fit the above equation, ϕ_μ is replaced by ϕ_f where ϕ_f is greater than ϕ_μ. The upper

limit of ϕ_f is reached when at large strains, no volume change takes place and $\phi_f = \phi_{cv}$. The relation between ϕ_μ, ϕ_f and ϕ is given by Rowe (1962) for medium fine sand.

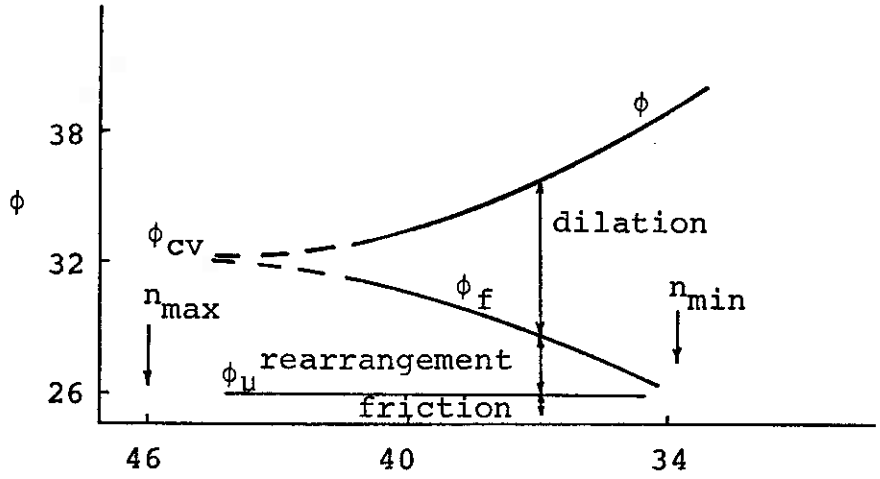

Figure II-3 ϕ Values as a Function of Porosity (After Rowe, 1962)

In the derivation of his theory, Rowe (1962) made the following assumptions:

i) Volume change due to ambient or mean principal stress change, associated with particle slides or elastic compression at contact point, is neglected.

ii) Shearing resistance is given by sliding of particles at their contact points and that rolling of particles is neglected.

iii) The measured volume change applies to the whole volume of the sample before any formation of slip planes.

Rowe (1962) also extended his theory to clays by introducing the interparticle cohesion term, c_f, resulting in the following expression:

$$\frac{\sigma_1'}{(1+\lambda)} = \sigma_3' \tan^2(45+\phi_f/2) + 2c_f \tan(45+\phi_f/2) \quad (2\text{-}16)$$

Rowe et al. (1963) found that the stress dilatancy performance of two clays, West water clay (12% clay fraction) and Derwent clay (50% clay fraction) was similar to that of sands. The c_f term was very small (1.7 psi) even when the clay had been consolidated anisotropically and had allowed secondary consolidation to take place.

On the practical application of his theory, Rowe (1963) introduced a method of earth pressure and slope stability calculation based on the effective interparticle friction angle, ϕ_f, and the degree of interlocking of the soil structure, α_R. The improvements of this proposed method are

i) It gives a better insight into the mechanism of shear strength of soils where the effect of dilatancy is taken directly into account and not taken as a correction to shear strength.

ii) The stress dilatancy equation is valid at any stage of deformation including the peak and residual states. For the special case of no volume change, the solution becomes identical to the well known solution based on Coulomb.

Horne (1965a) in his series of papers further extended the stress dilatancy work of Rowe. He assumed that the assembly consists of rotund, rigid and cohesionless particles and elastic, plastic deformation, crushing and cracking are ignored. Individual particles acting as 'rollers' between groups of particles do not occur significantly in a deforming assembly.

Horne (1965b) introduced the concept of mean-projected-solid-path (m.p.s.p.) to describe the changing state of anisotropy existing in a deforming assembly through the triaxial test. The degree of aniosotropy denoted by m_1/m_3 is the ratio of the m.p.s.p. in the axial (m_1) and radial (m_3) directions. This ratio increases to a maximum close to the peak stress ratio and then decreases until the condition of no further volume change causes the degree of aniosotropy to become stabilised so that

$$m_1/m_3 = (\pi/4)\ \tan(45+\phi_{cv}/2) \qquad (2\text{-}17)$$

where ϕ_{cv} = interparticle friction angle sheared at constant volume.

Horne (1969), in his third paper of the series, obtained a theoretical prediction of ϕ_{cv} based on ϕ_μ, and showed that his prediction is more accurate than the expressions of Caquot (1934) and Bishop (1954) given by

$$\tan \phi_{cv} = (\pi/2)\ \tan \phi_\mu \qquad (2\text{-}18)$$

$$\sin \phi_{cv} = (15 \tan \phi_\mu)/(10+3 \tan \phi_\mu) \qquad (2\text{-}19)$$

respectively.

Although Newland and Allely (1957) had proposed a dilatancy theory before Rowe, their theory had been relatively ignored. King and Dickin (1970) stated the reasons for this unpopularity.

i) Their theory was not based on rigorous analysis and their experimental results were not so reliable.

ii) Their theory was intended to apply at peak stress ratio only while Rowe's theory is applicable at all stages of deformation up to formation of slip plane.

King and Dickin extended Newland and Allely's theory to be applicable at all stress ratios and showed that the stress and volume change equations of the two theories are the same, their difference occuring in the final assumptions made in the interpretation of the results. Rowe postulated that for incremental deformation to occur, the ratio of the work done on the assembly by the major principal stress to that done on the minor principal stresses should be a minimum,while Newland and Allely adhered to the Mohr-Coulomb principal of failure. The theoretical relationships of the two parameters ϕ_f and α are obtained as follows:

$$\frac{\tan \phi_f \text{ (Newland \& Allely)}}{\tan \phi_f \text{ (Rowe)}} = \frac{2\sqrt{D}}{D + 1} \qquad (2\text{-}20)$$

$$\frac{\tan \alpha \text{ (Newland \& Allely)}}{\tan \alpha \text{ (Rowe)}} = \frac{1}{\sqrt{D}} \qquad (2\text{-}21)$$

where $D = (1 + \lambda)$.

Rowe (1971) pointed out that Newland and Allely's assumption of $\alpha = (45 + \phi/2)$ is invalid for soils which change in volume during shear. It is only applicable for stress paths in which $\lambda = 0$.

Rowe (1962) showed that for medium dense sand his ϕ_f compared favourably with those of Newland and Allely at high porosities, their differences increasing with decreasing porosities. This was confirmed by King and Dickin (1970).

Rowe et al.(1964) derived stress dilatancy equations for triaxial compression tests, triaxial extension tests and direct shear tests. They showed theoretically the differences between Coulomb ϕ, ϕ_r after Taylor and Bishop energy correction and Rowe's ϕ_f. It was pointed out that ϕ_r is the equivalent Coulomb ϕ after deduction of the external work done by dilation and ϕ_f is obtained after further reduction of internal work done by dilation from ϕ_r. The external work done in dilation is the energy spent in overcoming cell pressure while the internal work done in dilation is the energy required to rearrange the particles during sliding friction.

Barden and Khayatt (1966) further confirmed the validity of the Stress Dilatancy Theory by imposing different stress paths during triaxial compression and extension tests where mean stress was either increasing or decreasing. The stress ratio σ_1'/σ_3', denoted R, increased during all the tests.

El-Sohby (1964) showed that for paths of increasing R elastic (recoverable) strains are small compared with slip strains (irrecoverable) and therefore may be neglected. However, data are lacking for stress paths of decreasing R where the elastic deformation may possibly be as important as slip strains.

Barden et al.(1969) confirmed that the elastic component of shear strain is negligible in the case of first loading and rebound shear paths. They showed that isolation of elastic from total strain is not possible using loading and unloading cycles because of marked changes in structural

arrangement of particles. Employing constant R tests and cycling between chosen values of mean stress p', they attempted to separate total strain into elastic and slip components on the assumption that unloading defines the elastics.

Lee (1966) put the Stress Dilatancy Theory on a firmer footing by extending the confirming experimental data to a material (feldspar) with an extremely high value of interparticle friction of 37^0. Previous studies (Rowe 1962) had established the validity of the stress dilatancy equation for granular materials with ϕ_μ values varying from 7^0 (steel balls) to 26^0 (graded sand).

Summarising, Rowe's Stress Dilatancy Theory has been confirmed for a wide range of cohesionless materials with friction angles of ϕ_μ varying from 7^0 to 37^0. As for cohesive materials, only two clays had been investigated (Rowe et al.1963) besides the extruded kaolinite and glass beads with hydrocal used in this study. All the above work were triaxial compression tests with a few extension tests (Barden and Khayatt, 1966).

Other Methods

Other methods that may be used to separate shear resistance into components include

a) The Critical State Concept

b) Theory of Rate Process

c) Stress Loci Method

a) The Critical State Concept

Though the Critical State Concept invented by Roscoe et al.(1958) was never intended to separate shear resistance into components, Rowe (1964) demonstrated the correlation of his ϕ_f and α_R parameters with Roscoe et al's M and ϕ_{RS} values for cohesionless soils. Though there is some common meeting ground between the two theories, Rowe pointed out that the fundamental difference lies in his particulate mechanics approach and Roscoe's continuum approach to the shear strength problem.

b) Theory of Rate Process

Mitchell (1964), using the theory of rate process, derived an expression for shear resistance of a soil as a function of the frictional (includes dilation) and cohesive properties, effective stress, soil structure, rate of strain and temperature at any stage of deformation. He assumed solid particle to particle contacts.

This approach, however, requires much improvement and modification before soil behaviour can be completely understood within the framework of the theory because of the many assumptions and speculations involved. Nevertheless, its potential appears great.

c) Stress Loci Method

Yong and Vey (1962) presented a graphical method for the determination of effective stress parameters by stress

loci. They claimed that the method is applicable to normally consolidated as well as sensitive clays.

Definition of Parameters

Soil Structure

The concept of soil 'structure' or the arrangement of the soil particles was put forward by Terzaghi in 1925 to explain the great variations of void ratio and behaviour of soils. Casagrande (1932) proposed that undisturbed sensitive clays have flocculated structures and a compound honeycomb structure for silt grains. Present-day terminology of soil structure is taken to include the orientation and distribution of particles as well as the electrochemical forces between adjacent soil particles. (Lambe and Whitman, 1969)

The particulate nature of soils distinguishes itself from that of solid mechanics and fluid mechanics in that the soil particles are not strongly bonded together in the way that the crystals of a metal are and are therefore relatively free to move with respect to one another. Thus the resistance to shear deformation of a soil mass is controlled by the interactions between adjacent particles, or soil structure. The sliding and probably rolling of adjacent particles results in deformation and therefore soil structure varies with strain, besides other factors as effective stress, void ratio, etc.

The development of Schmertmann's IDS Concept on curve-

hopping was based on the assumption that two effective stress conditions can be imposed on a soil at approximately constant structure and at the same strain and thereby permit separation of the shear resistance into I_ε and D_ε components. The complex nature of the arrangement of particles has defied many researchers to express soil structure quantitatively.

Rowe (1962) defined tan α_R as "the ratio of sliding contacts of an assembly in the principal directions." Schmertmann (1966a) called α_s in his 'constant structure envelope' a structural parameter but gave no physical explanation of its meaning. Mitchell (1964) defined S as a "structural factor represented by the number of interparticle contacts per unit cross-sectional area." Horne (1965b) introduced the concept of mean-projected-soil-path and proposed the ratio m_1/m_3 (see page 15) as a measure of the anisotropy of an assembly of particles. This ratio is equivalent to Rowe's tan α_R.

Bond Strength

It is well recognised that a portion of the shear resistance of a cohesive soil is due to cohesion or 'sticking together' of adjacent particles without externally applied normal pressure. The nature of such bonding has been the subject of considerable research, supplemented by extensive investigation in the fields of colloid science (Kruyt, 1952; Rosenquist, 1959). It is agreed that bonding between

particles may be the result of van der Waals' forces of attraction, Coulombic forces of electrostatic attraction and repulsion and in some cases by hydrogen or potassium bonds or from cementation by organic or inorganic compounds.

Though formulas showing variation of attraction and repulsive forces with distance and system characteristics for the simplified case of parallel platelets have been developed by colloid chemists (Kruyt, 1952), these are of limited quantitative value to the soils engineer who has to deal with random arrangements of irregular particles with variable spacings. As yet there is still no reliable expression for determining the bond strength of a cohesive soil.

Lambe (1960) presented a theoretical consideration of the mechanism of shear resistance in cohesive soils with an equation relating the various pressures acting across a shear surface between adjacent soil particles. This equation is helpful in understanding qualitatively soil volume change and shear strength characteristics because,at the present state of knowledge, several of the terms cannot be evaluated.

Since Hvorslev's work, there has been some speculation that c_e and ϕ_e may be descriptive of the actual internal mechanisms of shear resistance and c_e was thought to be an indication of the magnitude of the bonding between the particles. Schmertmann (1963c) introduced a method to determine bond strength from the zero intercept of a I_m vs $\bar{\sigma}'_t$ plot.

He defined bond strength as the shear strength at zero effective stress on the plane of envelope tangency, at the same structure. Schmertmann (1966b) showed that c_e consists of the effect of constant structure envelope in addition to bond strength. The constants κ in equation (2-6) and β_m in equation (2-14) are both believed to be a measure of envelope curvature. Rowe's interparticle cohesion, c_f, may be thought of as shear strength at zero effective stress or bond strength with dilatancy effect removed.

Christensen and Wu (1964) defined bond strength as the force required to produce relative displacement between two particles at a contact point. Contact refers to a point at which a bond is formed between two particles and does not necessarily mean that the particles are in solid-to-solid contact. The mechanism of shear resistance was pictured as slippage occurs first at contacts with weak bonds under a given stress. The breaking of these weak bonds transfers load to other existing stronger bonds or new bonds formed as a result of strain. This concept of shear deformation and creep is similar to that propounded by Rowe (1962).

Applying the Rate Process Theory, Christensen and Wu (1964) postulated that the activation energy required to move a particular unit from one minimum energy position to the next minimum energy position represents the bond strength of the contact. This bond strength would include the

dilatant component as well as the adhesion and friction at the contacts. As expected, they found that bond strength of remolded specimens is lower than undisturbed ones and that the low initial bond strength of remolded clays increase with deformation as a result of stronger bonds.

Mitchell et al. (1969), in their study of stress-strain-time response of soils, also made use of the activation energy in Rate Process Theory to determine the number of interparticle bonds under a variety of conditions. However, they assumed solid-to-solid contact between particles with different number of bonds per contact and the individual bonds are of equal strength. These assumptions differ from those of Christensen and Wu.

Mitchell et al. found that the number of bonds per square cm. is linearly proportional to the effective consolidation pressure. They also postulated that the number of bonds at zero effective consolidation pressure is the source of true cohesion. They showed that strength and the number of bonds are linearly related irrespective of whether the material is undisturbed or remolded, and normally consolidated or overconsolidated San Francisco Bay mud, wet or dry illite and dry medium fine sand. The experimental evidence cannot be said to prove the validity of the theory which still has to stand the test of time because of the many assumptions involved.

In summary, the definitions of bond strength given by Mitchell et al. and Christensen and Wu are similar to

Schmertmann's definition in that it includes the effect of dilatancy. Rowe's definition of interparticle cohesion, c_f,differs from the above in that it is free of dilatancy effect.

Frictional Strength

The effective frictional component is generally defined as the remaining part of shear resistance, dependent upon the magnitude of effective stress. Associated with this component is the angle of friction expressed as the ratio of shear stress to normal effective stress.

Coulomb's ϕ angle is the slope of the envelope which compares samples at different void ratios and effective stresses at failure. It had been known that c and ϕ vary with the types of shear tests. Following Hvorslev's work, the friction angle ϕ_e was thought to be representative of the true mechanism of friction of soils at failure but it was shown by Gibson (1953) and later by Rowe (1963) to contain the effect of dilatancy.

Schmertmann and Osterberg (1960) in developing the IDS technique of separating shear resistance into components as a function of strain defined tan ϕ_ε as : "The angle of internal friction,ϕ_ε, at any strain, is the angle whose tangent is the ratio of the change in shear stress to change in normal intergranular (effective) stress occuring on the plane of Mohr envelope tangency at that strain, during a stress change occuring without significant change in

soil structure." This slope is now seen to be slope of imaginery constant structure envelope (See Figure II-2), tan $\phi_\varepsilon = d_\varepsilon$. ϕ_ε, therefore, does not take into account the effect of dilatancy.

Rowe (1962) introduced the following three friction angles (Figure II-3) in his Stress Dilatancy Theory:

ϕ_μ is the physical angle of friction between minerals,

ϕ_f is ϕ_μ plus the effect of rearrangement of particles or interlocking but with dilatancy effect removed,

ϕ_{cv} is ϕ_μ plus the effect of particle rearrangement for samples sheared at constant volume. Rowe (1964) suggested a friction angle ϕ_{Rs} which resulted from the 'boundary energy correction' proposed by Roscoe et al. (1958).

The following table summarises the various definitions of the angle of friction:

Definitions	Corrected for	not Corrected	Remarks
Coulomb ϕ	none	ε,e,S, dilatancy	at failure
Bishop ϕ_r	ε, dilatancy (external)	e,S dilatancy (internal)	any strain
Hvorslev ϕ_e	e	ε,S, dilatancy	at failure
Schmertmann $\phi_\varepsilon=\tan^{-1}$ (d)	S,ε	e,dilatancy	any strain
Rowe ϕ_f	ε,dilatancy (internal & external)	S,e	any strain
Roscoe ϕ_{Rs}	ε,dilatancy (external)	S,dilatancy (internal)	any strain

Table II-1 Definitions of ϕ Angles

To date, the IDS Concept and the Stress Dilatancy Theory are the only two available laboratory methods of determining bond strength. Since both methods were developed to measure the fundamental components of shear resistance as a function of strain, there should exist a theoretical relationship between the two sets of parameters. To achieve this goal, one must examine in greater detail the underlying assumptions and considerations of the two theories.

CHAPTER III
THEORETICAL CONSIDERATIONS OF SCHMERTMANN AND ROWE THEORIES

Schmertmann's IDS Concept

The IDS Concept is based on the fact that by keeping all the variables listed in expression (2-10) constant except effective stress σ', then at a certain strain, the shear strength will be a function of effective stress at that particular soil structure. The change between two levels of effective stress is so chosen that the soil structure is not significantly altered and can be considered constant at that strain.

The I_ε and D_ε components are dependent on the magnitude of the jump selected, the larger the jump the smaller will be the computed I_ε value (Figure III-1). A study of the effect of the magnitude of the jump for constant-σ_1' IDS tests on computed I_m values was made by Schmertmann (1966a) who considered that the high level of σ_1' was fixed and the jump was then decreased to a lower level of σ_1'. Considering the jump of $\Delta\sigma_1'$=20% σ_{1h}' as the standard, he compared I_m values for extruded kaolinite, Enid clay and sandy kaolinite with curve-hopping ratio of $\Delta\sigma_1'/\sigma_{1h}'$ varying from 10% to 60% resulting in almost identical theoretical and experimental (I_m/I_m20%) ratios varying from 1.1 to 0.6 respectively. He confirmed the use of the curve-hopping ratio

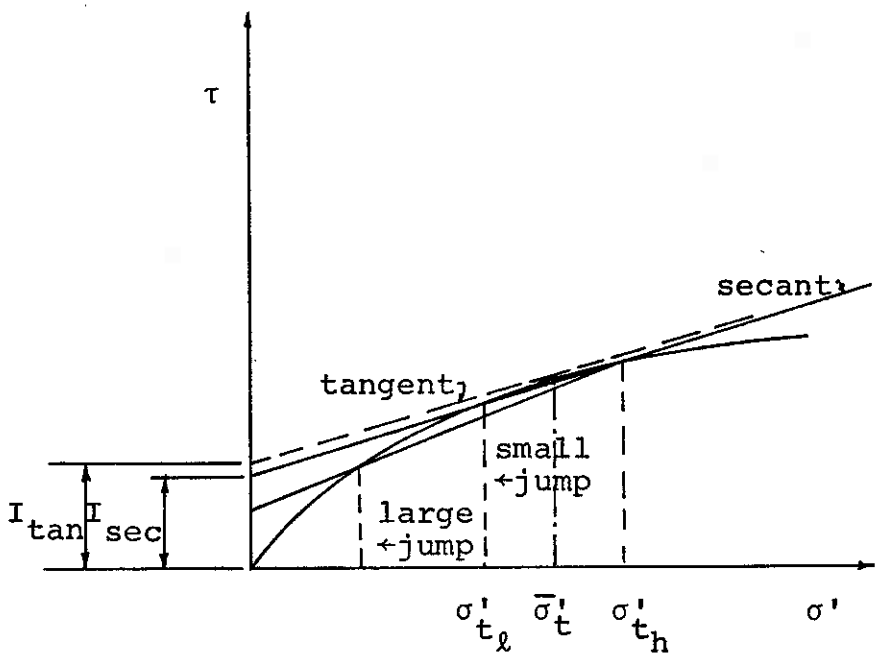

Figure III-1 Constant Structure Envelope Showing Fitted Secant and Tangent to Obtain I_ε Components

of 20% in the constant-σ_1' IDS test as a compromise between conflicting requirements. A small increment will minimise the effect of soil structural changes and also decrease the difference between the tangent and the secant slope of the constant structure envelope resulting in more accurate separation of the strength components. A larger increment will enable the line of common tangency to be drawn with better precision. The same curve-hopping ratio of 20% was also recommended for constant-σ_3' or constant pore pressure versions of IDS tests. For constant-volume IDS tests, an increase in volume of 0.25 % was employed to obtain the lower stress-strain curve. For the kaolinite, this will result in a drop of σ_1' varying from about 18% to 10% for strains ranging from 1% to 5%. The error involved in the computation of the I_ε component with the assumption that the fitted secant is the correct tangent to the envelope, is about 1.5% too low when compared to the theoretical constant structure envelope with $I_o = 0$. (Figure III-1)

The IDS test is neither a drained nor undrained test in the conventional sense. Because of the imposed stress conditions, the sample is not completely free draining and volume changes occur with changes between two levels of effective stress. The validity of the one-sample curve-hopping technique had been shown for nine soils, seven being remolded and two undisturbed (Schmertmann, 1962). The applicability of the one-specimen test eliminates one of the fundamental variables inherent in testing a natural soil deposit.

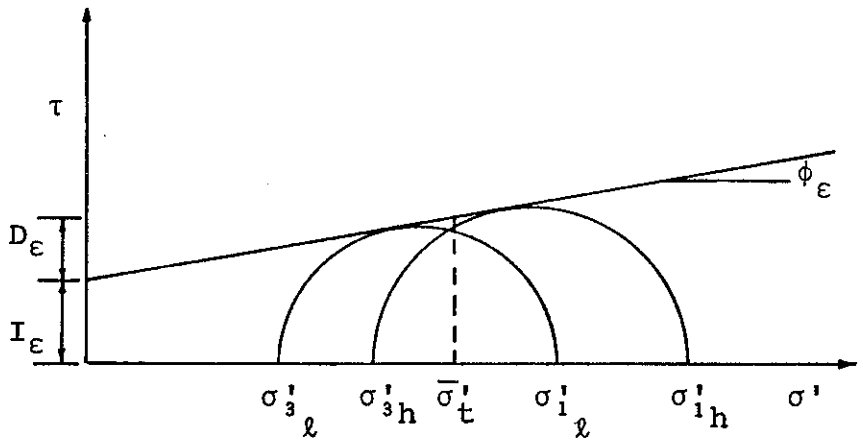

Figure III-2 Separation of Shear Resistance into I_ε and D_ε Components at Constant Structure and Strain

From the geometry of the two Mohr circles at the same strain, the I_ε and D_ε components as well as the average normal stress at the plane of tangency, $\bar{\sigma}'_t$ are computed from the following:

$$\phi_\varepsilon = \sin^{-1}\left[\frac{(\sigma_1-\sigma_3)_h - (\sigma_1-\sigma_3)_\ell}{2(\sigma'_{1h}-\sigma'_{1\ell})-\{(\sigma_1-\sigma_3)_h-(\sigma_1-\sigma_3)_\ell\}}\right] \quad (3\text{-}1)$$

$$\bar{\sigma}'_t = \tfrac{1}{2}\left[(\sigma'_{1_h}+\sigma'_{1_\ell})-(1+\sin\phi_\varepsilon)\left(\frac{(\sigma_1-\sigma_3)_h}{2}+\frac{(\sigma_1-\sigma_3)_\ell}{2}\right)\right] \quad (3\text{-}2)$$

$$D_\varepsilon = \bar{\sigma}'_t \tan\phi_\varepsilon \quad (3\text{-}3)$$

$$I_\varepsilon = \tau_\varepsilon - D_\varepsilon \quad (3\text{-}4)$$

where subscripts h and ℓ denote high and low effective stress conditions. Subscripts 1 and 3 denote major and minor principal stresses respectively.

Schmertmann (1966a) demonstrated the stability of the

I_m value which, however, is found to be a function of the magnitude of effective stress. The linear relationship between I_m and effective stresses, existing even for sands, indicates that I_m must include some other component besides the bond strength between particles. The introduction of the concept of the imaginary constant-structure envelope helps to explain this paradox. The curvature of the constant-structure envelope results in a contribution to the I_ε component and it was found that in the remolded clays and sands investigated (Schmertmann, 1966a), almost all the I_m values result from envelope curvature. I_m, besides being effective stress dependent, was also found to be affected by the size of the soil particles, I_m decreasing with increasing average grain size defined by D_{50}. Schmertmann's work included tests in assorted glass beads. He proposed that it is the radius of particles at their contact points rather than the particle size that is significant.

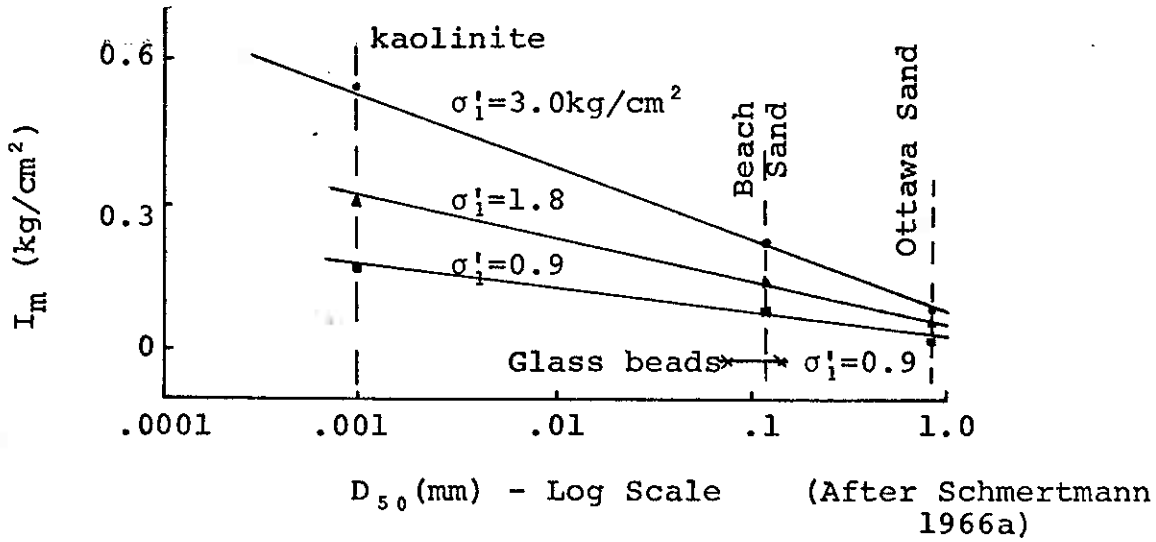

Figure III-3 I_m vs D_{50} Grain Size at Constant Effective Stress

Rowe's Stress Dilatancy Theory

Terzaghi (1920) wrote about the fallacy of Coulomb's equation,"The fundamental assumptions of the traditional earth pressure theories cannot, in fact, stand even superficial examination. The fundamental error was introduced by Coulomb, who purposely ignored the fact that sand consists of individual grains and who dealt with the sand as if it were a homogeneous mass with certain mechanical properties. Coulomb's idea proved very useful as a working hypothesis for the solution of one special problem of the earth pressure theory, but it developed into an obstacle against further progress as soon as its hypothetical character come to be forgotten by Coulomb's successors.

"The way out of the difficulty lies in dropping the old fundamental principles and starting again from the elementary fact that the sand consists of individual grains."

Rowe (1962) indeed made a fresh start by considering the particulate nature of the particles. Starting with two particles in limiting sliding equilibrium, he derived a stress dilatancy relation between stress ratio, σ_1'/σ_3', the physical angle of friction between minerals, ϕ_μ, the ratio of changes in volumetric strain to vertical strain, $d\varepsilon_v/d\varepsilon_1$ and the angle of interlocking, α_R.

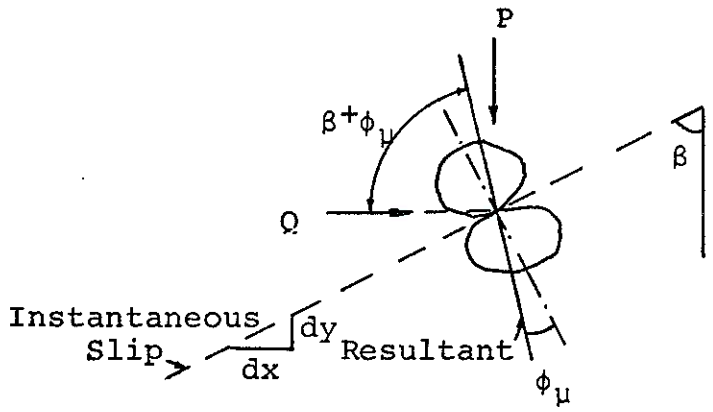

Figure III-4 Two Cohesionless Particles at Instant of Slip

The two particles having a physical angle of friction ϕ_μ, slide at an angle of β to the vertical under the action of forces P and Q acting in the vertical and horizontal directions respectively. From geometry,

$$P/Q = \tan(\beta+\phi_\mu) \qquad (3\text{-}5)$$

$$dx/dy = \tan\beta \qquad (3\text{-}6)$$

therefore

$$(P\ dy)/(Q\ dx) = \tan(\beta+\phi_\mu)/\tan\beta = E_R \qquad (3\text{-}7)$$

where E_R is called the energy ratio.

In a triaxial compression test, summing forces vertically and horizontally for a random assembly of particles having n sliding contacts,

$$\frac{\Sigma_1^n P(dy)}{\Sigma_1^n Q(dx)} = + \frac{\sigma_1' d\varepsilon_1}{2\sigma_3' d\varepsilon_3} = \frac{\tan(\beta+\phi_\mu)}{\tan\beta} = E_R \qquad (3\text{-}8)$$

where all contacts are at minimum energy condition. For

a given energy input, the minimum energy ratio is given by $dE_R/d\beta = 0$ whence $\beta = (45 - \phi_\mu/2)$

$$+\frac{\sigma_1' d\varepsilon_1}{2\sigma_3' d\varepsilon_3} = \tan^2(45 + \phi_\mu/2) \qquad (3\text{-}9)$$

For small strains,

$$+d\varepsilon_v = -d\varepsilon_1 + 2d\varepsilon_3 \qquad (3\text{-}10)$$

$$\frac{\sigma_1'}{\sigma_3'} = \left(1 + \frac{d\varepsilon_v}{d\varepsilon_1}\right) \tan(45+\phi_\mu/2) \qquad (3\text{-}11)$$

This is the stress dilatancy equation for a cohesionless soil deforming under the minimum energy condition. The sign convention adopted is positive for volume increase and positive for vertical compression.

The above equation gives the lower limit of interparticle friction angle, ϕ_f, when all contacts are sliding at critical angle β. This condition occurs for very dense packing of particles. For densities other than very dense, ϕ_μ is replaced by ϕ_f in equation (3-11) and at large strains when the sample is shearing at constant volume, ϕ_μ is replaced by ϕ_f where ϕ_f lies between the lower and upper limits of ϕ_μ and ϕ_{cv} respectively. Whatever ϕ_f may be, the deformation is always conceived of as occuring such that the ratio of energy absorbed in friction to energy supplied is a minimum.

Rowe (1962) introduced the α_R parameter to describe the soil structure or geometry of packing of the particles. He defined α_R as the ratio of the number of contacts per unit area in the principal directions. Referring to Figure III-5,

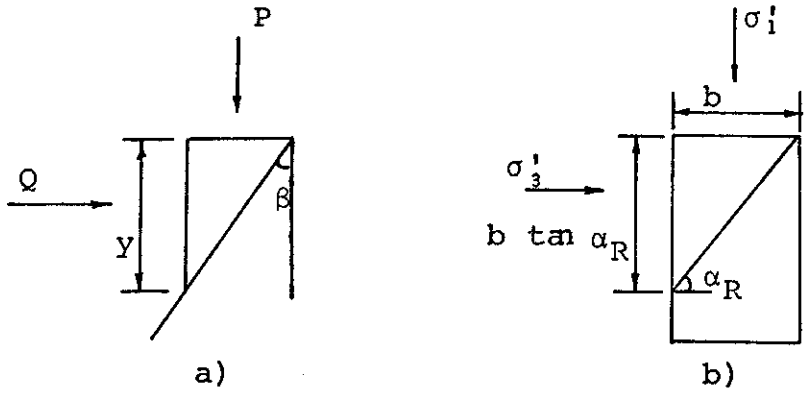

Figure III-5 Stress Summation over α_R Plane in Triaxial Sample

$$P/Q = \frac{\sigma_1' b}{\sigma_3' b \tan\alpha_R} = \tan(\beta+\phi_\mu) \qquad (3\text{-}12)$$

$$\frac{\sigma_1'}{\sigma_3'} = \tan\alpha_R \tan(45+\phi_f/2) \qquad (3\text{-}13)$$

Combining with equation (3-11)

$$\tan\alpha_R = (1+\frac{d\varepsilon_v}{d\varepsilon_1}) \tan(45+\phi_f/2) \qquad (3\text{-}14)$$

The α_R parameter is a variable quantity and depends on the magnitude of the stress and stress system because the geometry of packing is altered with stress and strain. The α_R lines are not slip planes although there is no great harm in considering them as a kind of slip line. It should be noted that α_R can be equated to $(45+\phi/2)$ only if $\phi_f = \phi$ at the critical void ratio state which is ϕ_{cv}.

Rowe et al.(1963) extended the Stress Dilatancy Theory to include cohesive soils by assuming that shear force between points of contact of adjacent particles follows the law

$$T = c_f A + N \tan \phi_f \qquad (3\text{-}15)$$

where A = average area of contact

N = normal load of contact

c_f, ϕ_f = interparticle cohesion and friction.

Introducing the interparticle cohesion into the two sliding cohesionless particles in Figure III-4 and resolving forces,

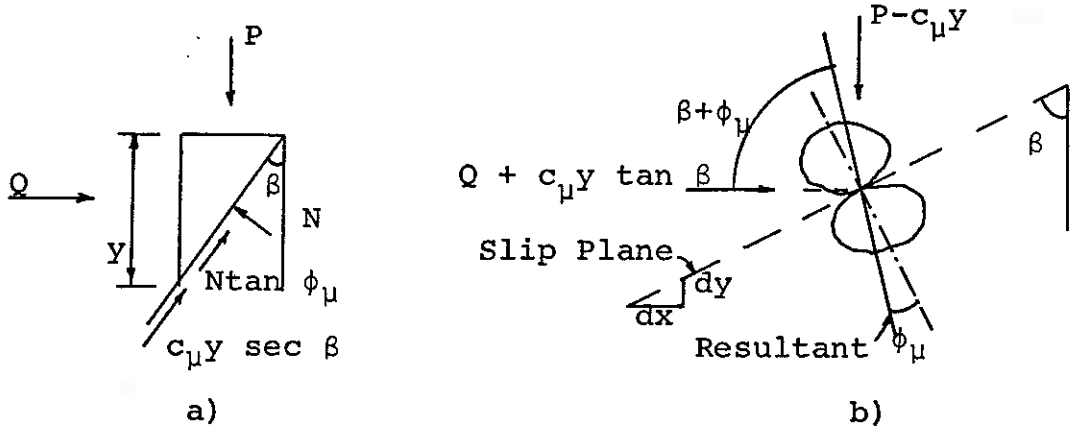

Figure III-6 Two Cohesive Particles at Instant of Slip

$$P/Q = \tan(\phi_\mu + \beta) + \frac{c_\mu y \sec^2 \beta}{Q(1-\tan \phi_\mu \tan \beta)} \qquad (3\text{-}16)$$

$$dx/dy = \tan \beta \qquad (3\text{-}6)$$

dividing,

$$\frac{Pdy}{Qdx} = \frac{\tan(\phi_\mu+\beta)}{\tan \beta} + \frac{c_\mu y \sec^2 \beta}{Q \tan \beta(1-\tan\phi_\mu \tan\beta)} \qquad (3\text{-}17)$$

Again, if there are n particle contacts,

$$\frac{\Sigma_1^n P(dy)}{\Sigma_1^n Q(dx)} = + \frac{\sigma_1' d\varepsilon_1}{2\sigma_3' d\varepsilon_3} = \frac{\tan(\phi_\mu+\beta)}{\tan\beta}$$

$$+ \frac{c_\mu b \tan\alpha_R}{\sigma_3' b \tan\alpha_R \sin\beta\cos\beta(1-\tan\phi_\mu \tan\beta)} \qquad (3\text{-}18)$$

Minimising E_R yields $\beta = (45-\phi_\mu/2)$ which together with the small strain equation (3-10) substituted in equation (3-18) gives

$$\frac{\sigma_1'}{(1+\frac{d\varepsilon_v}{d\varepsilon_1})} = \sigma_3' \tan^2(45+\phi_\mu/2) + 2c_\mu \tan(45+\phi_\mu/2) \qquad (3\text{-}19)$$

which is the stress dilatancy relation for a cohesive soil. The structural α_R parameter for a cohesive soil is given by (3-14).

Experimental Plots

For cohesionless soils, the stress dilatancy relation is usually displayed with the stress ratio, R as the ordinate and $(1+\frac{d\varepsilon_v}{d\varepsilon_1}) = D$ as the abscissa with the slope of the graph represented by $\tan^2(45+\phi_f/2) = K_{pf}$.

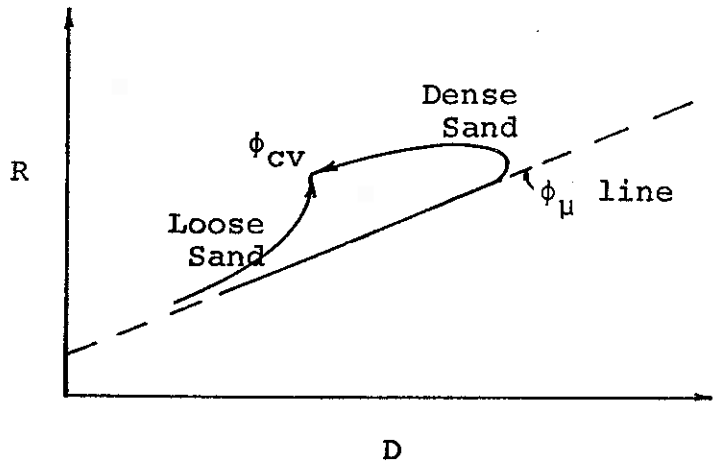

Figure III-7 Stress Dilatancy Relations for Loose and Dense Sand

For dense sands at low strains, the stress dilatancy relationship follows the minimum energy line when $\phi_f=\phi_\mu$ but as strain increases resulting in remolding or rearrangement of the particles, ϕ_f increases until the critical state when there is no volume change, $\phi_f=\phi_{cv}$.

For a loose sand, ϕ_f will always be greater than ϕ_μ and it increases as strain increases until at the peak stress ratio state, $\phi_f=\phi_{cv}$. The difference between ϕ_f and Coulomb's ϕ is attributed to the work done in overcoming the cell pressure as well as the rearrangement of the particles in dilation.

In the separation of the interparticle components c_f and ϕ_f of a cohesive soil as a function of strain, it is convenient to plot stress paths with $\{\sigma_1'/(1+\lambda)+\sigma_3'\}$ as abscissa and $\{\sigma_1'/(1+\lambda)-\sigma_3'\}$ as the ordinate. The parameters are then computed from (see Figure III-8,b)

$$\sin \phi_f = \tan \psi \qquad (3\text{-}20)$$

$$c_f = (a/2)\sec\phi_f \qquad (3\text{-}21)$$

For cohesionless soils, the stress dilatancy theory has been substantially verified for a wide spectrum of materials ranging from steel balls ($\phi_\mu = 9^0$), 0.25 mm diameter glass ballontini ($\phi_\mu = 17^0$), sands ($\phi_\mu = 23^0$ and 26^0), silt ($\phi_\mu = 31.5^0$) to feldspar ($\phi_\mu = 37^0$). On the other hand, only two clays had been tested and they were found to behave similarly as sands with zero or very small value of c_f.

Definition of Strain Paths

The meanings of strain paths for the two methods are explained as follows:

Stress Dilatancy Method

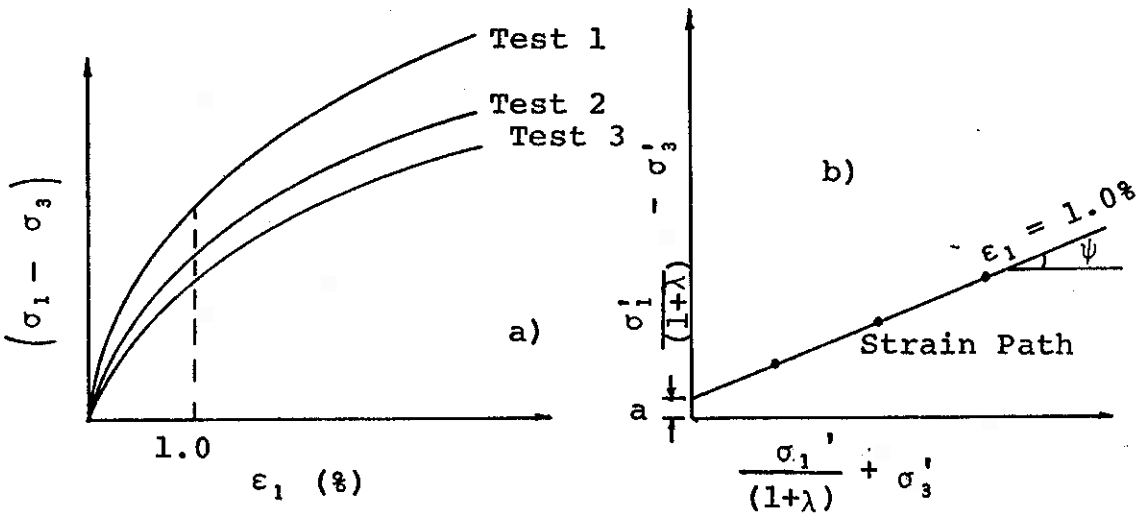

Figure III-8 Definition of Strain Path by Stress Dilatancy Method

Figure III-8 a) shows the stress-strain curves of a series of three triaxial tests conducted at different cell pressures. At a vertical strain of, say 1%, the principal stresses of the three tests were computed and the results were then presented on a $(\frac{\sigma_1'}{1+\lambda}-\sigma_3')$ vs $(\frac{\sigma_1'}{1+\lambda}+\sigma_3')$ plot (Figure III-8 b)). The line joining the three stress points at the same strain is then known as the strain path for the Stress Dilatancy Method.

IDS Method

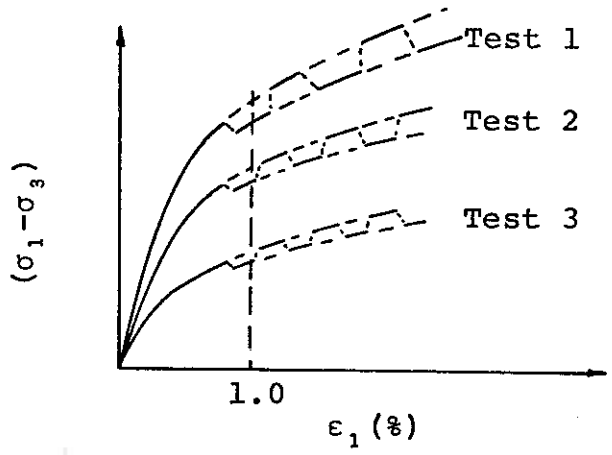

a)

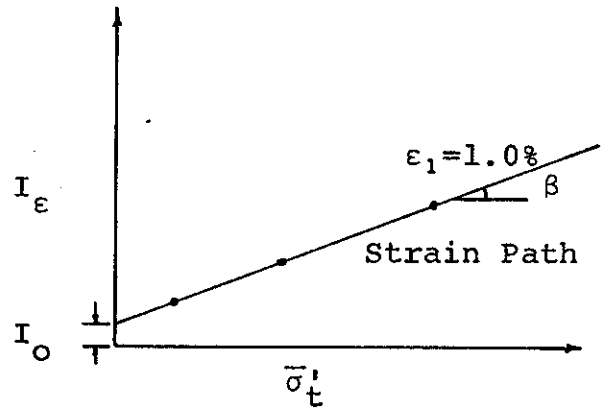

b)

Figure III-9 Definition of Strain Path by IDS Method

In the IDS method, a series of three IDS tests were performed at different confining pressures (Figure III-9 a)). The I_ε components are then determined at the same vertical strain, say 1%, for the three tests and the values plotted against the corresponding $\bar{\sigma}'_t$. The line joining these $(I_\varepsilon, \bar{\sigma}'_t)$ points at the same strain is then known as the strain path for the IDS Method.

Need for Establishing Linearity

Before the relationship between the two theories can be established, it is necessary to prove that the 'strain paths' are linear for both methods of determining bond strength. This is because that the Stress Dilatancy Theory is derived on the assumption of a linear stress law between the particle contacts (equation (3-15)) while the IDS Concept does not assume any such linear stress-strain behaviour. Secondly, linearity of strain paths in both methods will simplify the relationships between the two sets of parameters.

CHAPTER IV
TEST METHOD, EQUIPMENT AND EXPERIMENTAL PROGRAM

Test Method

In order to extablish a link-up between the parameters of the IDS and Stress Dilatancy Methods, it is convenient if a method of test can be developed so that both sets of parameters can be computed from the experimental data obtained from the same specimen.

Most of IDS tests performed to date on remolded and undisturbed cohesive and cohesionless soils have been the 'standard' constant-σ_1' version IDS compression tests and it was established that the one-specimen curve-hopping technique gives essentially two separate stress-strain curves at different effective stress levels.

In the derivation of the Stress Dilatancy Theory, it was assumed that interparticle slips are caused by increasing stress ratios, R, where total strains are considered to be slip strains with negligible elastic strains.

Most investigations made to date to verify the Stress Dilatancy Theory had been based on drained tests (Rowe, 1962; Rowe et al., 1963; Lee, 1966). Barden and Khayatt (1966) employed loading and unloading stress paths in compression and extension tests on a fine sand to investigate the conditions under which the upper $\phi_f, (\phi_{cv})$ and lower $\phi_f, (\phi_\mu)$

values are reached.

The types of IDS tests made in this investigation consist of constant-σ_1', σ_3', p', and constant-volume tests which yield increasing R values. All the tests result in increasing p' while constant-σ_1' tests give decreasing p' with strain. It is thus postulated that the data obtained from IDS tests with volume change measurements can be used to compute Rowe's interparticle parameters c_f and ϕ_f as well as the I_ε and D_ε components.

To date it has not been claimed that the c_f and ϕ_f parameters are unique nor has the effect of stress paths on these parameters been investigated.

I_ε and D_ε Components with Dilatancy Corrections

Using the IDS tests with volume change measurements, the IDS components corrected for dilatancy can be calculated from the following equations:

$$\phi_\varepsilon^* = \sin^{-1}\left[\frac{\left(\frac{\sigma_1'}{1+\lambda}\right)_h - \left(\frac{\sigma_1'}{1+\lambda}\right)_\ell - (\sigma_{3h}' - \sigma_{3\ell}')}{\left(\frac{\sigma_1'}{1+\lambda}\right)_h - \left(\frac{\sigma_1'}{1+\lambda}\right)_\ell + (\sigma_{3h}' - \sigma_{3\ell}')}\right] \quad (4\text{-}1)$$

$$\bar{\sigma}_t'^* = \tfrac{1}{2}\left[\left(\frac{\sigma_1'}{1+\lambda}\right)_h + \left(\frac{\sigma_1'}{1+\lambda}\right)_\ell - \frac{(1+\sin\phi_f^*)}{2}\left(\left(\frac{\sigma_1'}{1+\lambda}\right)_h + \left(\frac{\sigma_1'}{1+\lambda}\right)_\ell - \sigma_{3h}' - \sigma_{3\ell}'\right)\right] \quad (4\text{-}2)$$

$$D^*_\varepsilon = \bar{\sigma}'^*_t \tan \phi^*_\varepsilon \qquad (4\text{-}3)$$

$$I^*_\varepsilon = \tau^*_\varepsilon - D^*_\varepsilon \qquad (4\text{-}4)$$

where the superscript * denotes values after correction for dilatancy. It should be noted that the maximum shear stress of each circle falls on a 45° line from its uncorrected position after dilatancy correction.

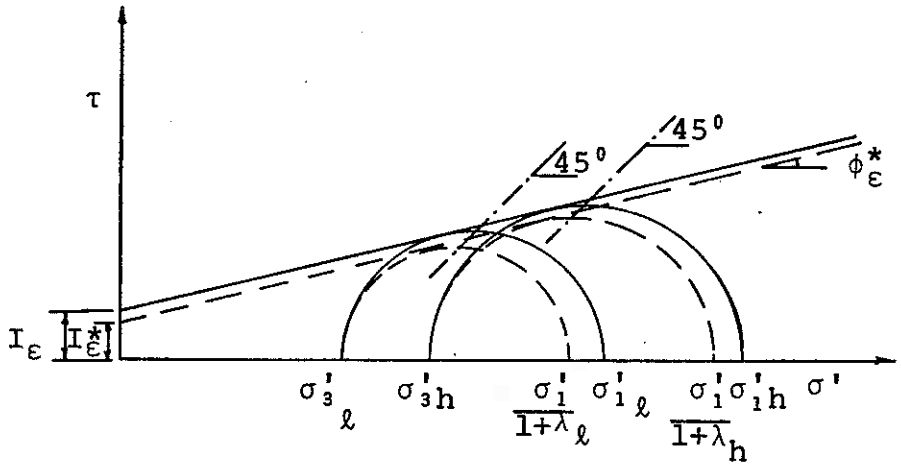

Figure IV-1 Separation of Shear Resistance at Contant Structure and Strain with Correction for Dilatancy

When the rates of volumetric strain to vertical strain for both the 'high' and 'low' Mohr circles are equal, i.e. $\lambda_h = \lambda_\ell = \lambda$, then it can be shown analytically that

$$I^*_\varepsilon = \frac{I_\varepsilon}{\sqrt{1+\lambda}} \qquad (4\text{-}5)$$

$$\bar{\sigma}'^*_t = \frac{2}{2+\lambda(1-\sin\phi_\varepsilon)}\,\bar{\sigma}'_t \qquad (4\text{-}6)$$

where $\lambda = \dfrac{d\varepsilon_v}{d\varepsilon_1}$

Equipment

The 'Geonor' triaxial equipment used in this research was developed by Norwegian Geotechnical Institute and has been described by Andresen and Simons (1960). The following modifications were made to the triaxial equipment to give the necessary precision required for this work.

Vertical Load Measurement

Strain gage load cells are used to measure the piston load instead of the conventional proving rings for quicker response in IDS work. For cohesive soils, a 100-lb capacity Thwing-Albert load cell with a sensitivity of 0.0075301 Kg/microinch/inch was used, while for cohesionless soils, a 200-lb capacity load cell with a sensitivity of .0151515Kg/microinch/inch was employed. These load cells deflect much less than the proving rings although this factor would not have affected the accuracy of the vertical deformation measurements because of the design of the system which is described in the following paragraph.

Vertical Deformation

To eliminate the effects of cell expansion or contraction from the variation in cell pressure as well as the deformation of the load cell, the vertical deformation of the specimen is measured by the relative movement between the top of the piston and the bottom of the cell. A dial gage with an accuracy of 0.002 mm per division deflection

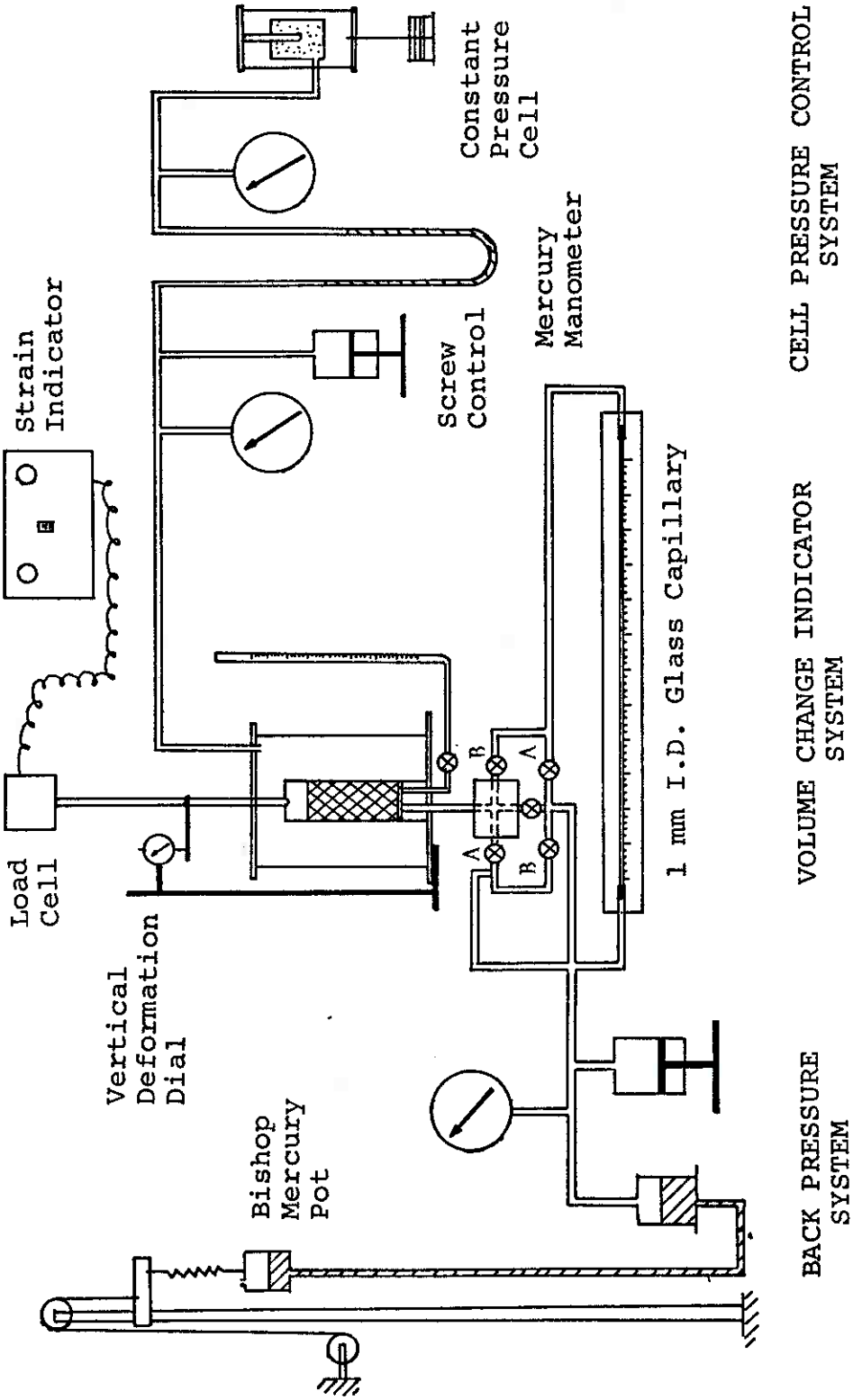

Figure IV-2 Schematic Diagram of Triaxial Apparatus for IDS Test with Volume Change Measurements

is used. With this set-up, corrections that still have to be made are bedding of the ball joint, compression of the top cap, grease and rubber discs or frictionless platens.

Back Pressure Saturation

To ensure the sample is 100% saturated before and during the shearing process, back pressure saturation technique was employed. This back pressure is supplied by the Bishop self-compensating mercury pot system which has the advantage over the Norwegian constant pressure system of no piston friction. The mercury pot has an accuracy of 1/15 psi pressure though the Bourdon gage can only be estimated to 1/4 psi.

Lowe and Johnson (1960) gave an expression for calculating the back pressure required to achieve any degree of saturation by increasing the pore pressure under the conditions of constant overall soil volume and increasing water content.

$$\Delta u = \frac{14.7}{14.22}\left(\frac{1-.98s_i}{1-.98s_p} - 1\right) \qquad (4\text{-}7)$$

where s_i = initial degree of saturation

s_p = degree of saturation desired

The following table shows the back pressure in kg/cm^2 required to achieve 100 and 99% saturation from an initial saturation of s_i.

S_i	Δu_{100}	Δu_{99}
100	0	-
98	1.05	0.35
95	2.53	1.34
90	5.06	3.09
88	6.05	3.73

Table IV-1 Required Back Pressure For Achieving 100% and 99% Saturation

All the kaolinite samples had an initial saturation of over 98% and most of them are close to 100% after consolidation. All kaolinite samples tested at an effective cell pressure of less than 4.0 kg/cm^2 had a back pressure of 4.0 kg/cm^2. Samples tested at 4.0 kg/cm^2 effective cell pressure had a back pressure of 3.0 kg/cm^2. Even this back pressure is high enough to ensure total saturation of the kaolinite samples.

Since the glass beads were boiled and then placed under water and vibrated in a mold, the possibility of air trapped in the sample is very low. However, a back pressure of 2.0 kg/cm^2 was used further to ensure the glass beads were totally saturated.

The glass beads with hydrocal samples were installed dry in the triaxial cell and then saturated by vacuum to 88% saturation. A back pressure of 4.0 kg/cm^2 was used

producing a saturation of 99.2%. A higher back pressure was not possible because the back pressure plus the maximum consolidating pressure of 3.0 kg/cm^2 give a total cell pressure of 7.0 kg/cm^2 which is the design capacity of the Geonor triaxial cell.

The back pressure was applied to all the samples after consolidation and then allowed to come to equilibrium (usually overnight) before the start of the shearing process.

Volume Change Measurements

The measurement of volume change is as important as the vertical deformation readings because of the incremental strain ratios used in the Stress Dilatancy Theory. The accuracy of the volume change measurements have to be compatible with the vertical deformation readings and at the same time, the system has to have the capacity to measure the large volume changes that take place.

The final design consists of a 46-in.-long glass capillary with an internal diameter of 1.0 mm connected to two pairs of Circle Seal valves which, by closing one pair and opening the other pair, reverse the movement of the air bubble in the glass capillary without changing the movement of the water into or out of the sample. A bubble displacement of one inch is equivalent to a volume change of 0.0238 cc and the movement can be read to the nearest 0.05 inch. For a sample having a height of 8.00 cm and a volume

of 80.00 cc, the ratio of the smallest units of measurable volumetric strain to vertical strain equals

$$\text{volumetric strain} = \frac{\left(\frac{.0238(.05)}{80}\right)}{} = 1.19$$

$$\text{vertical strain} = \left(\frac{.0001}{8.00}\right)$$

The above ratio indicates that both strains are determinable with similar precision.

The volume change of a sample during the shearing process is measured by the flow of water into and out of the sample, while the pore water pressure is kept constant. The importance of keeping a constant pore water pressure throughout the test is to ensure the amount of dissolved air and the volume of air bubbles, if any, to be constant.

The reader will see that extreme precision is required to determine volumetric strain with the accuracy required for the Stress Dilatancy calculations.

Sample Preparation and Testing

Three types of materials were used:

Kaolinite

Glass beads (no. 140 to 200 sizes)

Glass beads with hydrocal (10:1 ratio by weight)

Kaolinite Samples

This pure commercial clay and its characteristics have been described by Topshoj (1970). It consists of over 99 % of kaolinite clay minerals and has a specific gravity of 2.609.

The kaolinite powder was first mixed with distilled water to a predetermined water content of about 40 per cent and then cured overnight. It was then passed through an 'Vac-Aire' extruder five times to distribute the water evenly before it was cut to lengths of 10 cm, wrapped in wax paper and dipped into warm wax several times to prevent evaporation. The samples were numbered in ascending order as they came out of the machine. Water content samples were taken every five samples to check the uniformity of the batch. Each batch produces 50 to 55 samples and three batches were made in 1969.

All samples have three wool drains drawn through prepunched holes in a triangular pattern with a 0.18 cm. needle. Three O-rings were used both around the top cap and the pedestal to prevent cell water seeping into the sample. Previous tests (Schmertmann 1960) have indicated that as long as the duration of the cell pressure does not exceed two days, the effect of moisture migration is relatively minor.

The sample is then hydrostatically consolidated at preselected pressures for about a day, although the time for the end of primary consolidation, t_{100} is generally reached between 50 to 110 minutes for cell pressures between 1.0 and

4.0 kg/cm², using the Casagrande graphical method to determine t_{100}. The advantage of using an open burette during consolidation is to allow air bubbles trapped between the rubber membranes and the sample to escape. After consolidation is complete, a back pressure is applied through the volume change system and allowed to come to equilibrium before the subsequent compression phase of the test. The following three types of IDS tests were then performed on normally consolidated and overconsolidated kaolinite.

Constant-σ_1' series

To perform a constant-σ_1' IDS test, one can control the pore water pressure with a constant cell pressure or control the cell pressure with a constant pore pressure. The latter method was chosen because of the necessity of having a constant back pressure for reliable volume change measurements. However, this variation of cell pressure results in expansion and contraction of the triaxial cell and also variation of the uplift on the piston load. The system for obtaining vertical deformation has been designed to nullify this effect by measuring the relative movement between the piston and the immovable cell base. The variation in uplift is accounted for in the following formula for computation of deviator stress:

$$(\sigma_1-\sigma_3)_i = \frac{(R_i-R_o)-(\sigma_{3i}-\sigma_{3o})Ap}{A_s} \qquad (4\text{-}8)$$

where σ_{3o} = initial cell pressure

σ_{3i} = cell pressure at strain i

A_p = area of piston

A_s = area of sample at strain i

R_o = initial load cell reading

R_i = load cell reading at strain i

Constant-p' series

The method of testing for this series is similar to the constant-$\bar{\sigma}_1$ series by varying the cell pressure with constant back pressure. This series was suggested by one of Rowe's assumptions that the volume change due to mean stress change is neglected.

Constant-volume series

The correlation between the two methods of component separation depends mainly on λ, the rate of volumetric strain to vertical strain. When no volume change takes place, the λ term becomes zero and the I_ε and D_ε components remain unchanged.

The three types of tests involved different dilatancy rates during the shearing process and hence different energy input into the soil sample. The constant volume tests require the highest cell pressure of the three types of tests to maintain the sample volume constant. All three test types employ a back pressure of 4.0 kg/cm^2 except samples tested at a cell pressure of 4.0 kg/cm^2 when the back

pressure is reduced to 3.0 kg/cm^2 because of the design capacity of the cell.

Glass Bead Samples

It is anticipated that preparation of loose samples will be difficult because of their spherical shapes and cohesionless properties. It was then decided to place the saturated beads in a split mold and vibrated in five layers by a 'Burgess' vibrotool. The last layer of the sample was vibrated with a surcharge weight of 600 grams after placing of the top cap to eliminate necking of sample at the top when a small vacuum was applied. The dimensions of the sample were then measured optically with a travelling telescope with a vernier reading to 0.01 cm. The sample is then consolidated hydrostatically and tested.

Constant cell pressure with constant back pressure of 2.0 kg/cm^2 or constant-minor-effective-stress IDS tests were used for the shearing process because of the ease of control and the strain rate had been increased from 0.5% per hour for kaolinite to about 2½% per hour for glass beads.

Glass Beads with Hydrocal Samples

Several types of materials were experimented with before it was decided on hydrocal (gypsum) for the artificial bonding. Glass beads (140-200 sieve sizes) and hydrocal are mixed in the dry in the proportion of 140 grams to 14 grams and then 27 cc of distilled water added. The wet

mixture is then immediately compacted with a vibrotool in a split mold which had been lined with Saran wrap to prevent sticking of the sample to the sides of the mold. The sample was compacted in five layers and was then let to set for about half an hour before the mold was removed. It was then allowed to cure another 48 hours before the sample was installed in the triaxial cell.

A vacuum of 8.5 inches of murcury was then applied to the top of the sample while water is admitted from the bottom. If too high a vacuum is used it will cause cavitation of the bottom of the sample from the inrush of water. This method of saturation gives a degree of saturation of about 88% and to achieve over 99% saturation, a back pressure of 4.0 kg/cm^2 is required. The sample is then consolidated hydrostatically and tested at two levels of constant-σ_3' at a strain rate of 0.5% per hour. This slow rate was adopted to give a better definition of the stress-strain curves because of the failure of the sample at vertical strains of just over 2%.

Correction of Measured Data

Vertical Stress, σ_1'

Strength of filter strips

The correction is given by

$$\Delta\sigma_{fp} = - K(p/A_s) \qquad (4\text{-}9)$$

where p = perimeter of sample

A_s = area of sample

K = correction factor

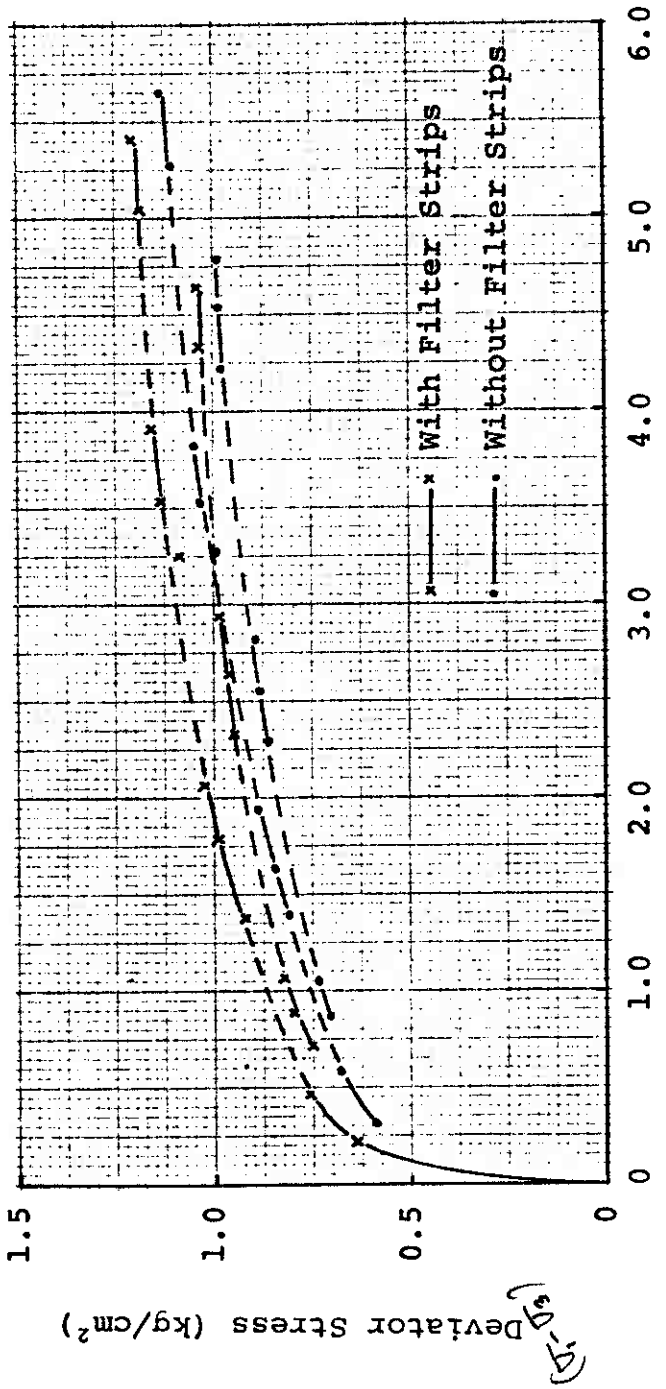

Figure IV-3 Effect of Filter Strips, Test Nos. 3-18-NC2, 3-17-NC2

The correction factor, K(kg/cm), is determined from the difference in deviator stress between kaolinite samples with and without filter strips at consolidating pressures of 1.0, 2.0 and 4.0 kg/cm^2. At strains varying from ½ to 5%, K varies from about 0.10 to 0.16kg/cm. This compares favourably with the value of 0.13 quoted by Duncan and Seed (1967).

Rubber membrane correction

From a consideration of elasticity, the membrane correction for vertical stress is given by

$$\Delta\sigma_{am} = -(2/3)E \left[1+2\varepsilon_{at} - \sqrt{\frac{(1-\varepsilon_v)}{(1-\varepsilon_{at})}} \right] \frac{A_m}{A_s(1-\varepsilon_v)} \quad (4\text{-}10)$$

with the assumption that

i) the membrane when held against the sample by cell pressure, was capable of taking compression.

ii) sample deforms as a right cylinder.

The extension modulus value of rubber membrane was determined as recommended by Bishop and Henkel (1964) and the Young's modulus was computed to be 175 psi which compares favourably with those given by Henkel and Gilbert (1952).

Weights of plunger and rod ... They are automatically accounted for during computation of deviator stress by taking the difference between the load cell reading at any strain and the initial reading.

Plunger friction

Appreciable friction can arise only as a result of lateral forces pushing on the plunger. Proper alignment of

triaxial assembly and the use of frictionless platens will diminish lateral forces that may develop. The lubricated plunger falls freely under its own weight through a brass bushing which rotates during the shearing process to reduce friction (Andresen and Simons, 1960) and therefore this effect is negligible.

Horizontal Stress, σ_3'

Rubber membrane correction is given by

$$\Delta\sigma_{hm} = -(2/3)E\left[2+\varepsilon_{at}-2\sqrt{\frac{1-\varepsilon_v}{1-\varepsilon_{at}}}\right]\frac{t_m}{r_s(1-\varepsilon_v)} \qquad (4\text{-}11)$$

where the same assumptions are made as deriving equation (4-10). All values on the right hand side of the equation are measurable.

Vertical Deformation

The measured vertical deformation had to be corrected for deflection of the top cap, ball joint and frictionless platens under load. This correction is obtained by replacing the sample with an aluminum dummy which is then loaded as in an actual test. It was found that if the plunger and top cap are brought into intimate contact with the dummy the deformation correction is linear with a slope of 3×10^{-6} cm per micro-inch per inch. The load applied to the dummy was of the same magnitude as the strength of the samples.

Volume Change Readings

Apparent membrane correction

Increase or decrease of cell pressure during an IDS test gives an apparent volume change of the sample due to

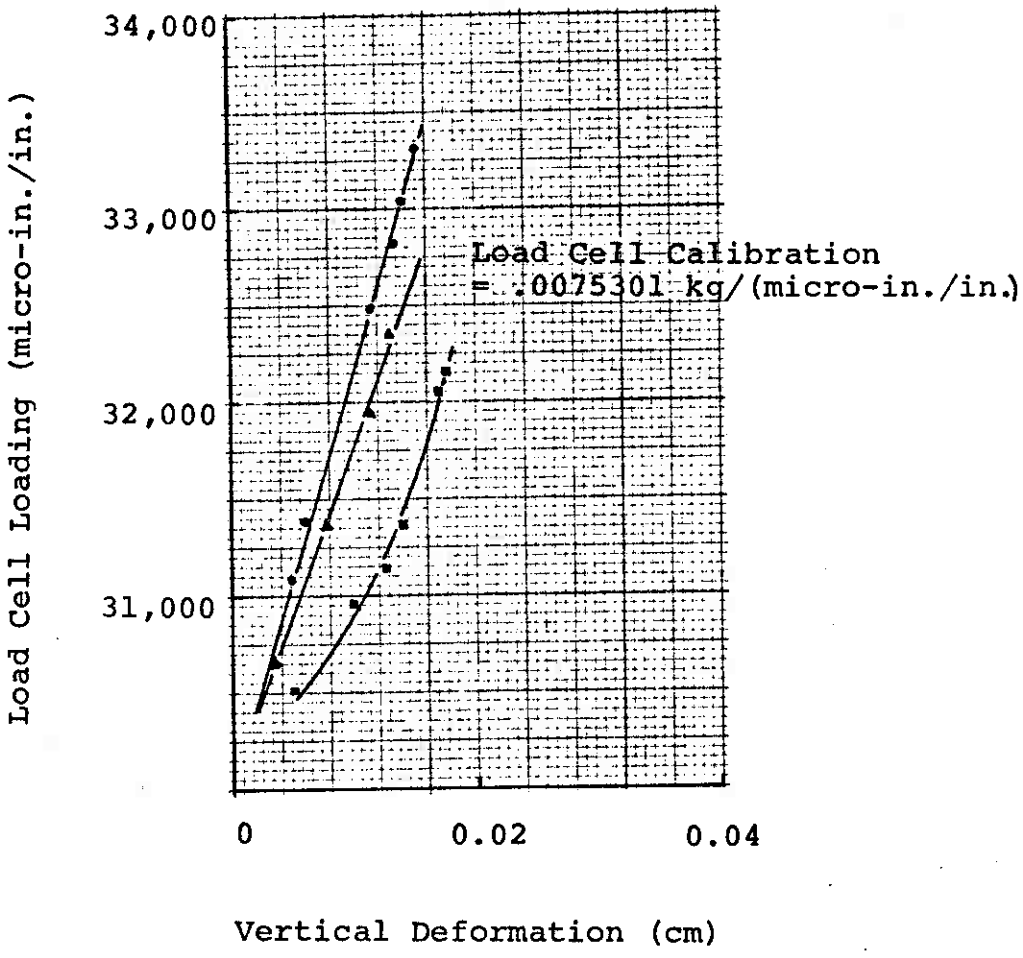

Figure IV-4 Bedding Correction of Top Cap, Ball Joint and Frictionless Platens

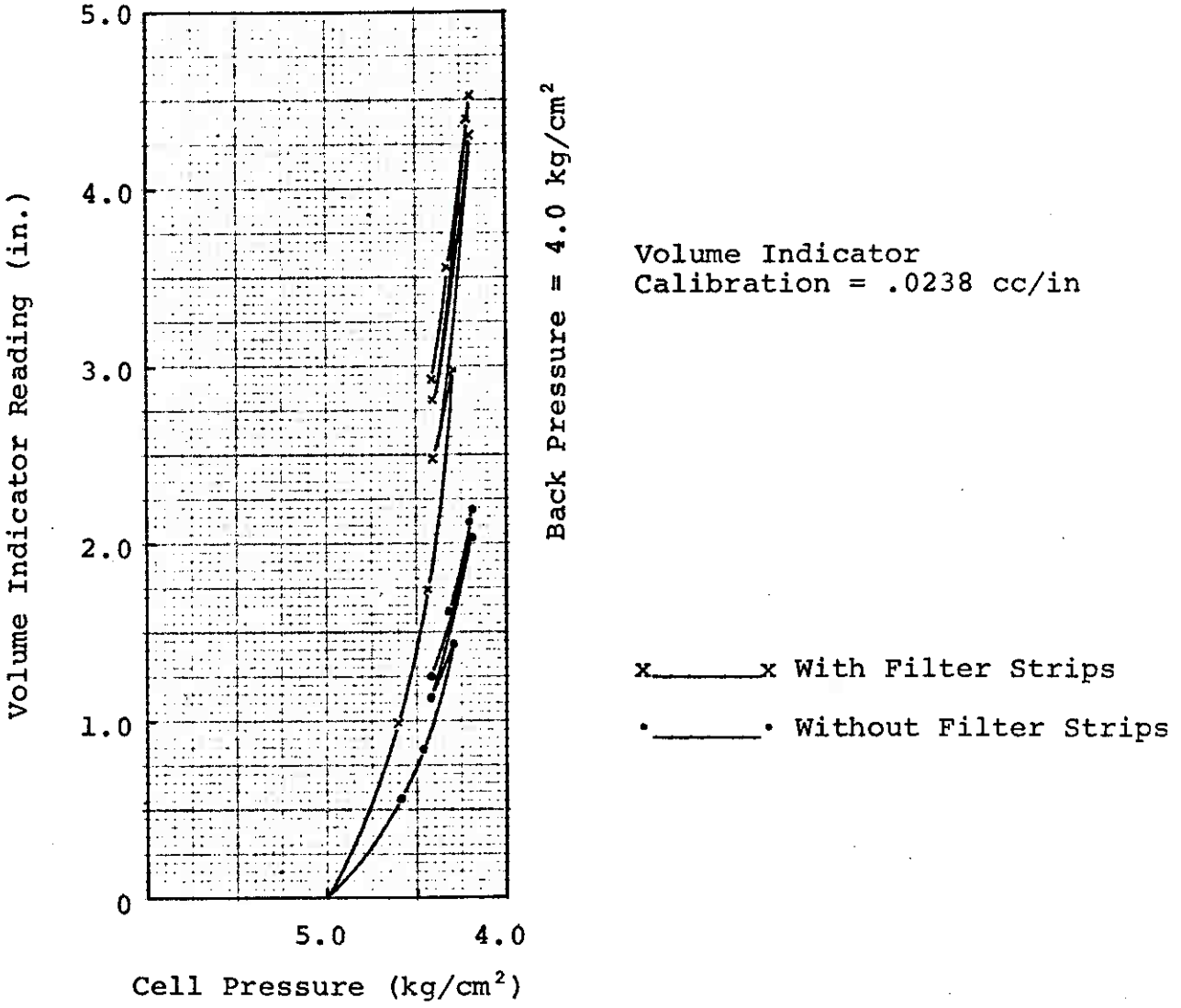

Figure IV-5 Apparent Membrane Correction at Normally Consolidated Condition

displacement of the membrane. This is calibrated with an aluminum dummy in place of a regular sample and then decreasing the cell pressure in the same manner as in an actual test. Dummies with and without external filter strips show a difference in volume change readings with greater volume increase for the latter. The greatest volume change correction occurs in samples with the lowest consolidating pressure.

Membrane penetration correction

This correction is applied only to cohesionless materials where the grains are large enough so that the membrane can penetrate the void between the particles under the action of the surrounding cell pressure. This correction will automatically include the correction mentioned in above for cohesive soils.

To determine this correction, a cohesionless sample is formed around an aluminum core of known dimensions and the volume changes under varying cell pressures noted. By comparing the volume changes of the entire sample with that of a cored sample and the membrane penetration common to both, the correction volume can be deduced.

Temperature

The variation of temperature has an unknown effect on volume change readings because of the different materials used in the construction of the volume change measuring system. The materials include brass Circle Seal valves, copper

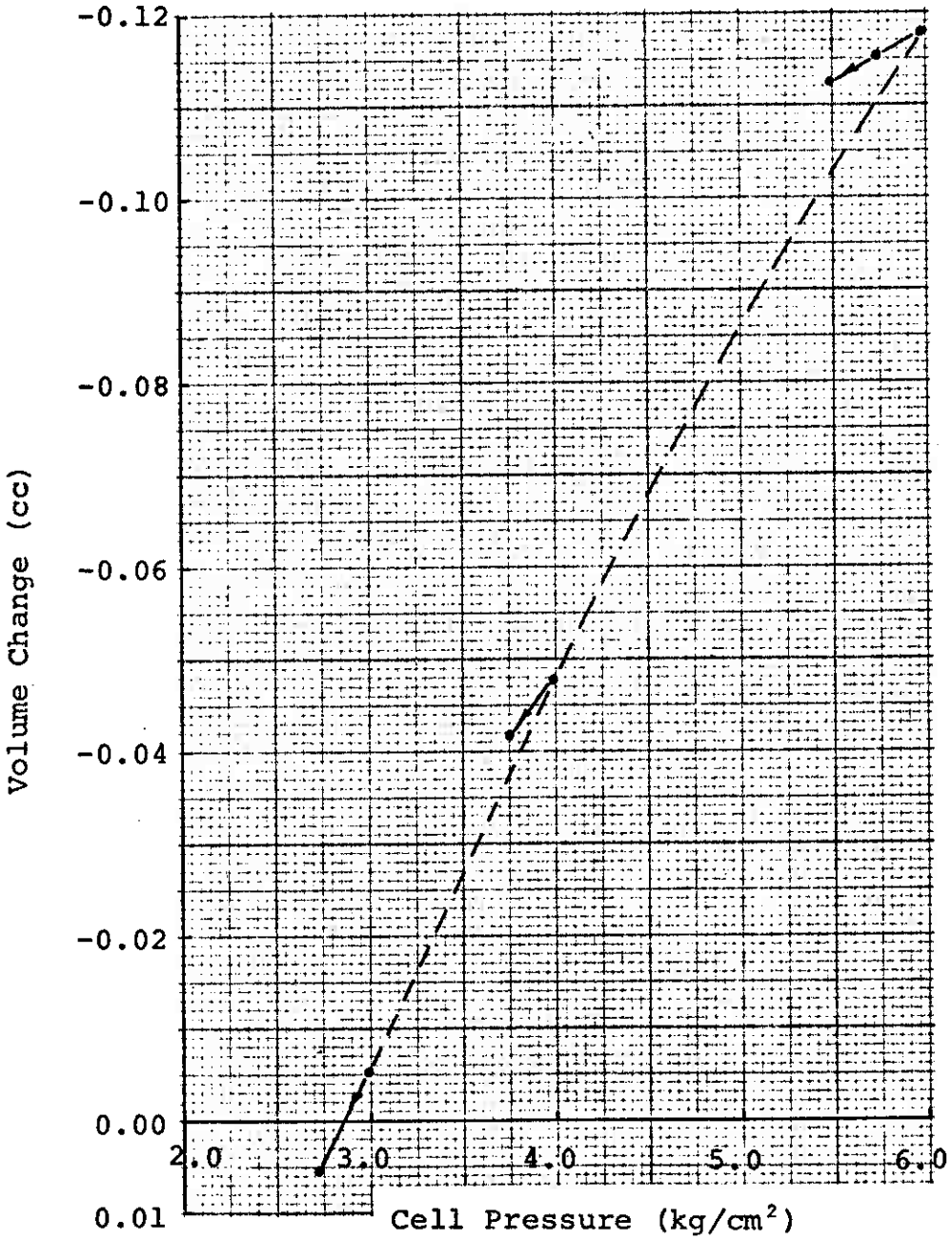

Figure IV-6 Membrane Penetration Correction for Glass Beads

lines, glass capillary, nylon lines and aluminum manifold. To diminish the increase in temperature as the test progresses, the motor was turned on the night before the test. This gives a maximum increase of $2^{0}C$ for a 12-hour test.

To investigate the effect of elevated temperature on the volume readings, the triaxial cell was assembled with an aluminum dummy and then heat was supplied to the triaxial cell and the surrounding system. Two 375W infrared radiation lamps and a 1320W portable heater placed about 3½ feet away provided the source of heat. Temperature was measured both in the triaxial cell and at the glass volume change indicator location. With one end of the volume change indicator open to the self-compensating mercury pot and the other end to the dummy sample, it was found that for an increase of $14^{0}C$ at the indicator location, the volume increase was 0.018 cc giving a volumetric strain of 0.0016% per degree C. This is negligible and hence no temperature correction was applied. The corresponding temperature increase within the cell from the above test was about $5^{0}C$.

CHAPTER V
PROOF OF LINEARITY OF STRAIN PATHS

Typical Experimental Results

A total of six drained tests and forty-six IDS tests with volume change measurements were performed. Each IDS test necessited two full days to perform, with the kaolinite requiring twelve full hours of continuous control to achieve 5½% strain. The glass beads with hydrocal require six hours to attain a strain of 2½%. A glass bead sample can be prepared and run within a day.

The following pages present the results of a typical test taken from each test material. The results of drained tests on kaolinite and glass beads are presented as deviater stress and volumetric strain against vertical strain plots. In the IDS tests on kaolinite, plots of deviator stress, cell pressure and volumetric strain against vertical strain are required. The missing parts of curves are interpolated to give two separate relationships, one for the 'high' and the other for the 'low' stress condition. At selected strains, the deviator stress, cell pressure and the incremental strain ratio, λ are obtained for both curves. The I_ε and D_ε components as well as the average shear and normal stress corrected for dilatancy, τ_t^* and $\bar{\sigma}_t^{*\prime}$ were computed

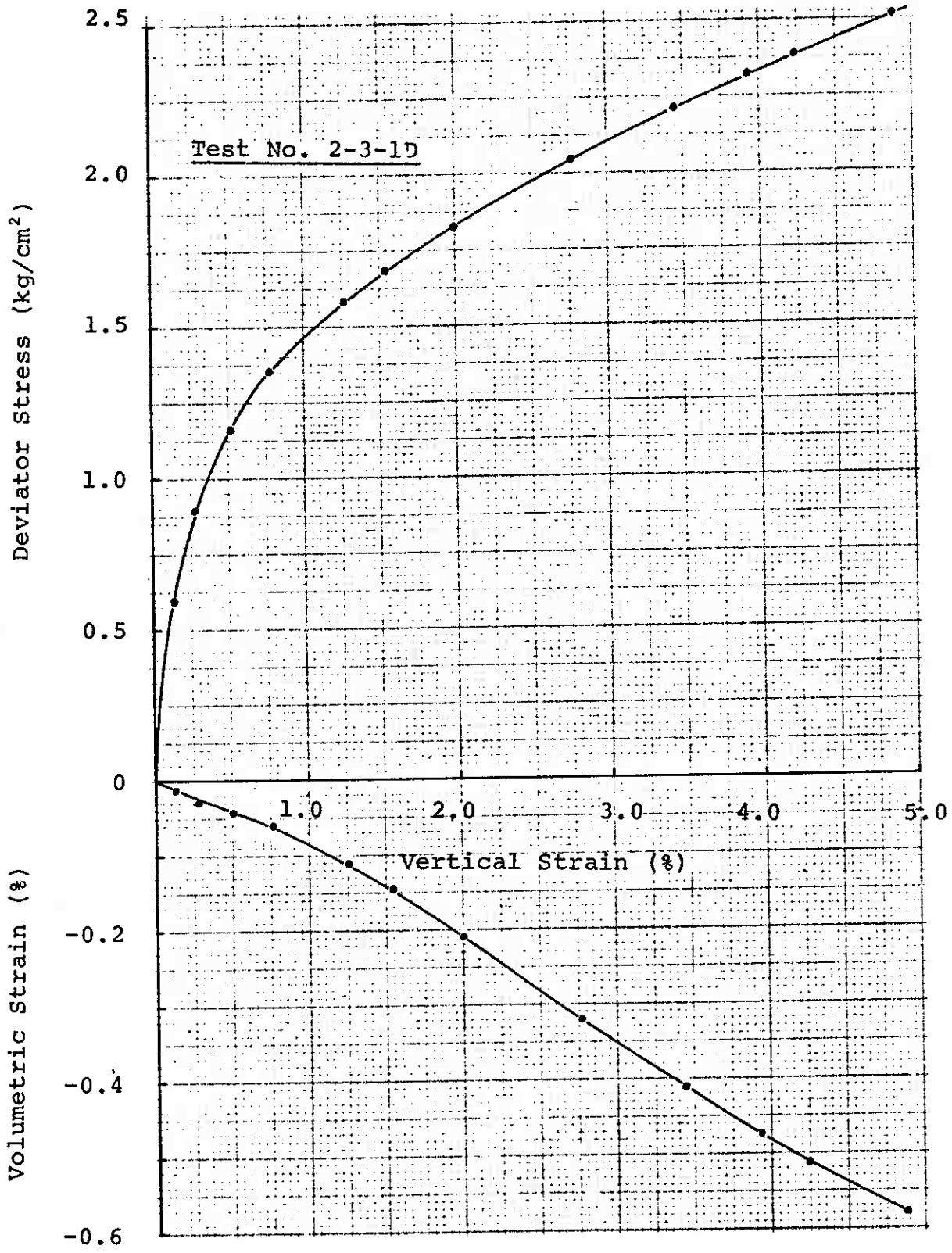

Figure V-1 Drained Test on O.C. Kaolinite

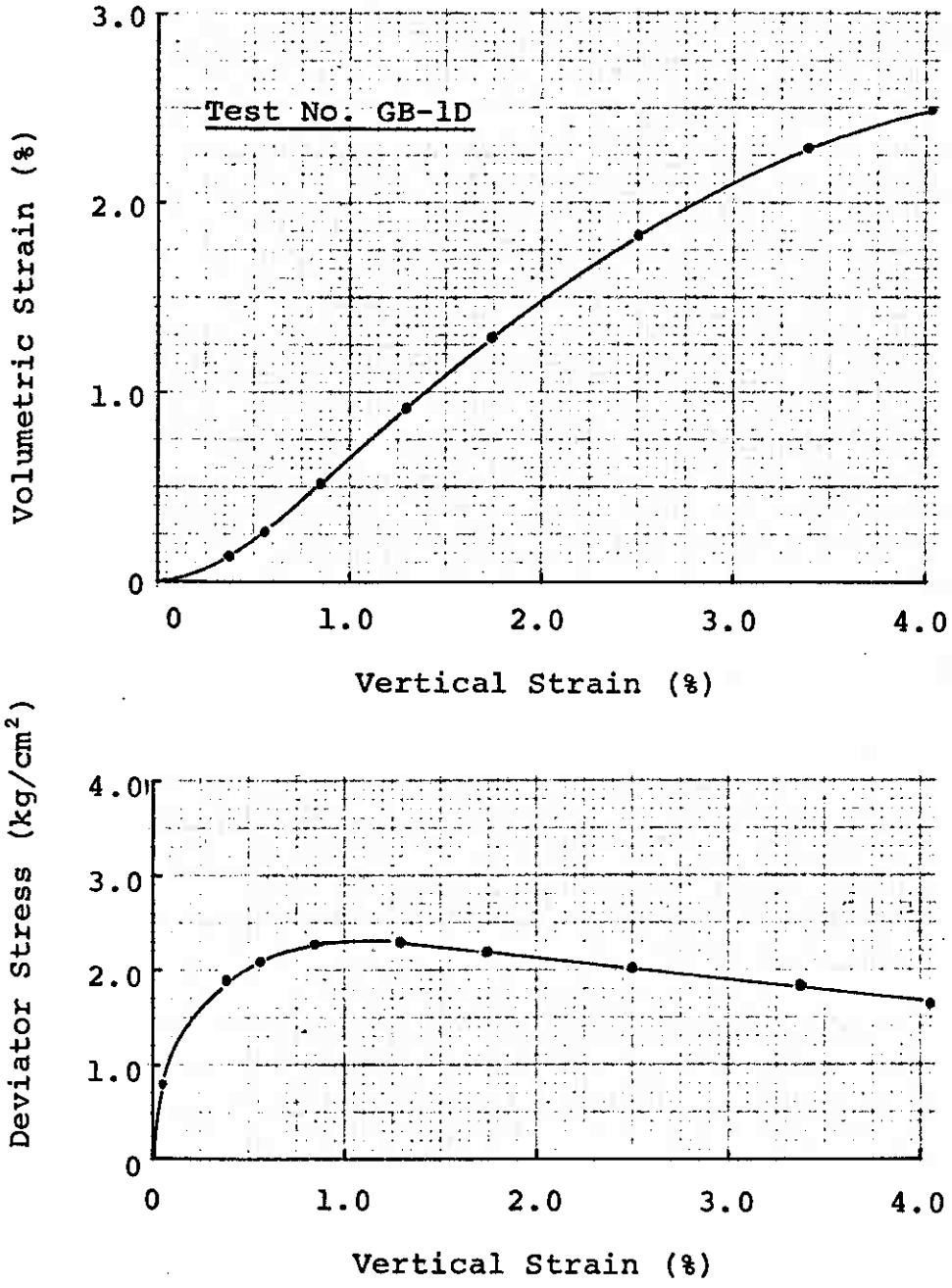

Figure V-2 Drained Test on Glass Beads

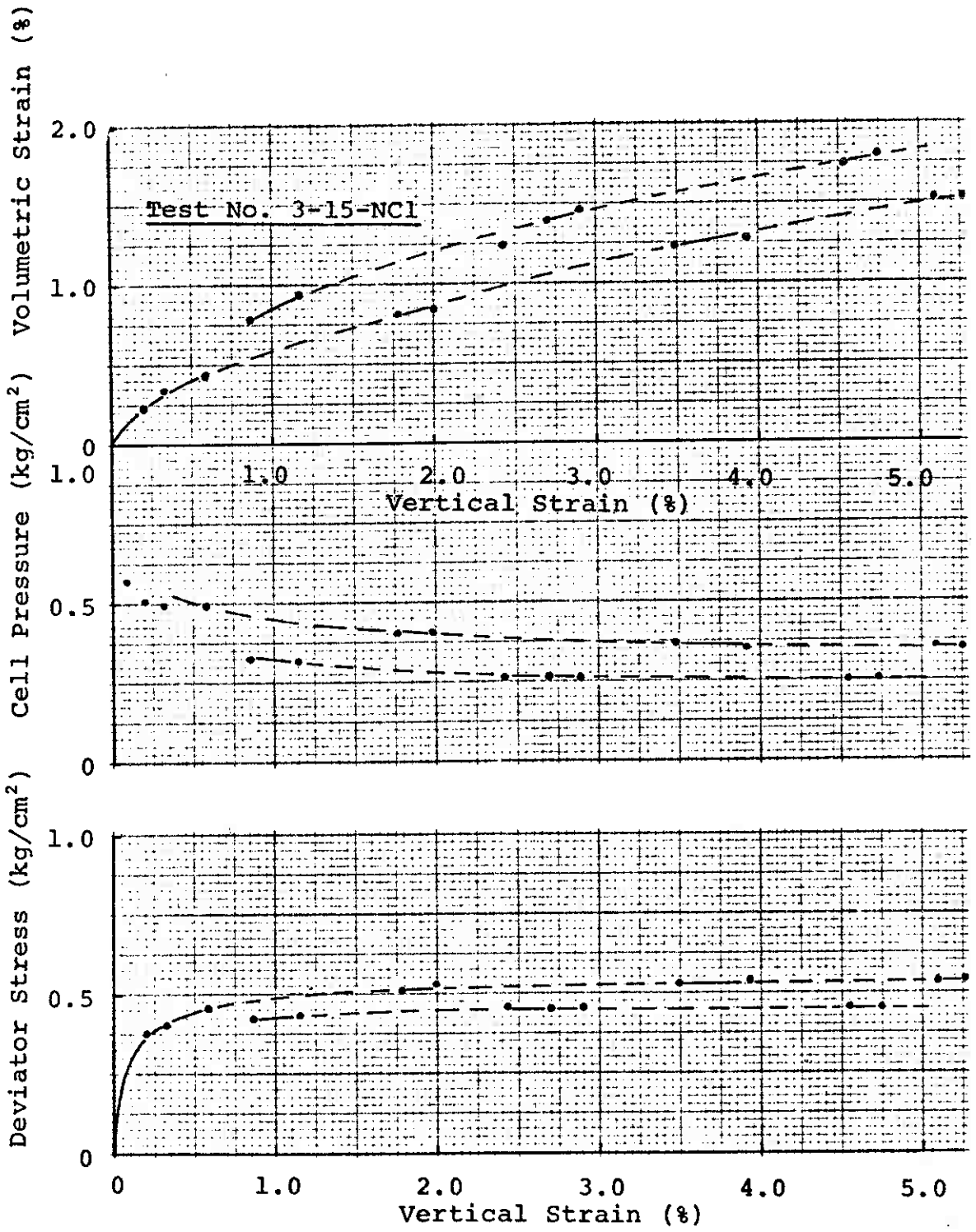

Figure V-3 Constant-σ_1' IDS Test on N.C. Kaolinite

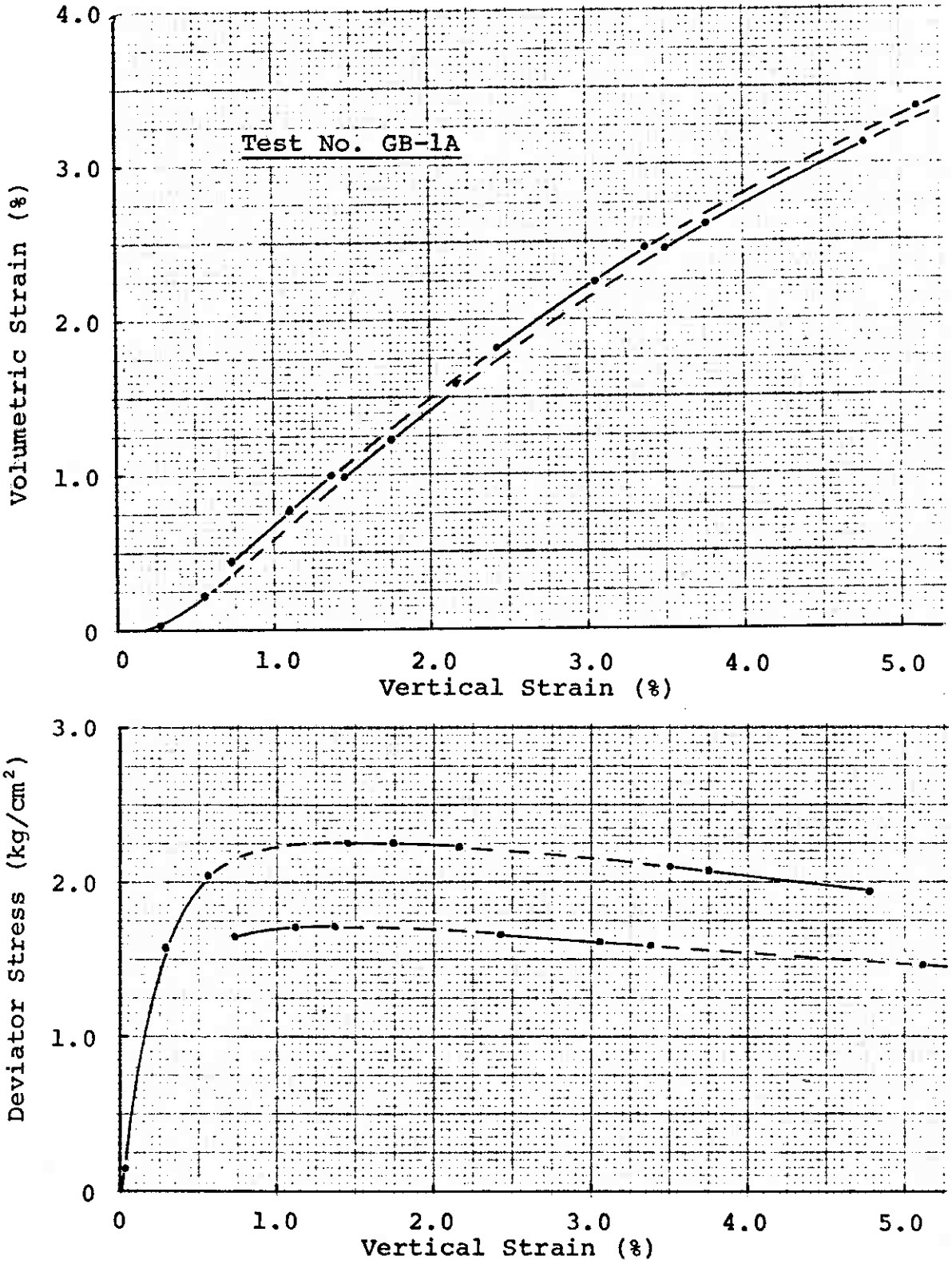

Figure V-4 Constant-σ_3' IDS Test on Glass Beads

using the Wang 700A calculator with the 701 IBM output typewriter. The output for all test results is presented in Appendix C.

For both glass beads and the glass beads with hydrocal only plots of deviator stress and volumetric strain versus vertical strain are required since the cell pressures are preselected at the two levels.

Statistical Analysis and Inference

As it is impossible to observe all conceivable events, the statistician must reason or infer from samples so as to be applicable to the entire population. Generally the exact laws of causes and effects are not known and therefore variation in the observed data will exist. The application of statistics herein consists of the analysis of experimental data, estimation of population parameters and drawing of inferences from these results.

In this statistical analysis, small sample inference procedures will be used because the maximum number of data points in any test series is less than 30 (Mendenhall, 1967). The number of test samples is limited mainly by the testing time involved to perform a complete test. The 't' statistic for small samples given by

$$t = \frac{\bar{y} - \mu}{s_s / \sqrt{n_s}} \qquad (5\text{-}1)$$

has a student's 't' distribution in repeated sampling. This distribution is mound-shaped and perfectly symmetrical

about t = 0. The variability of 't' is contributed by two random quantities, $\bar{y}$ and s_s. As n_s, the sample size increases, the 't' distribution tends towards the normal distribution.

Linear Regression and Correlation

A simple linear probabilistic model will be used in predicting the I_ε component of shear strength and τ_t^* with respect to $\bar{\sigma}_t'$ and $\bar{\sigma}_t^{*\prime}$ respectively. It has the form

$$y = \beta_0 + \beta_1 x + \varepsilon_v \qquad (5\text{-}2)$$

where ε_v is the error assumed to have zero mean and variance σ^2.

The parameters β_0 and β_1 computed by the method of least squares are given in the subsequent tables as I_o and β, c_f and $\tan \phi_f$ for I_ε vs $\bar{\sigma}_t'$ and τ_t^* vs $\bar{\sigma}_t^{*\prime}$ respectively. Figure V-6 and Figure V-7 show the parameters graphically and τ_t^* and $\bar{\sigma}_t^{*\prime}$ represent the average shear and normal effective stresses on the plane of tangency corrected for dilatancy. The corresponding linear sample correlation coefficients, r_i and r_f respectively, will vary between +1 and -1 where ±1 means perfect positive or negative linear association between the two variables considered. Associated with r, the sample correlation coefficient is the coefficient of determination, r^2 which when used in connection with regression analysis is the percentage variation in y attributable to the independent variable, x.

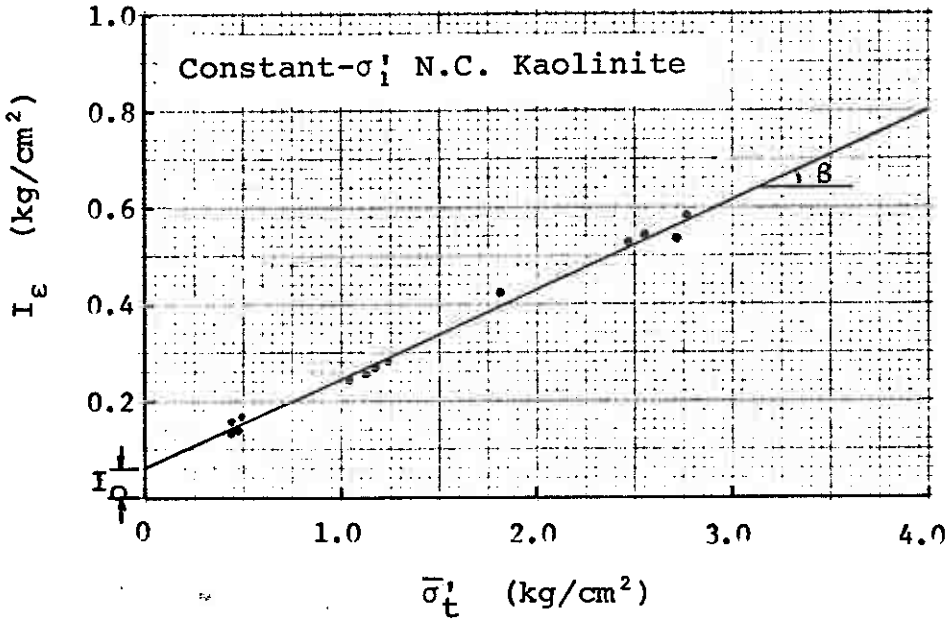

Figure V-6 I_ε vs $\bar{\sigma}_t'$ Plot

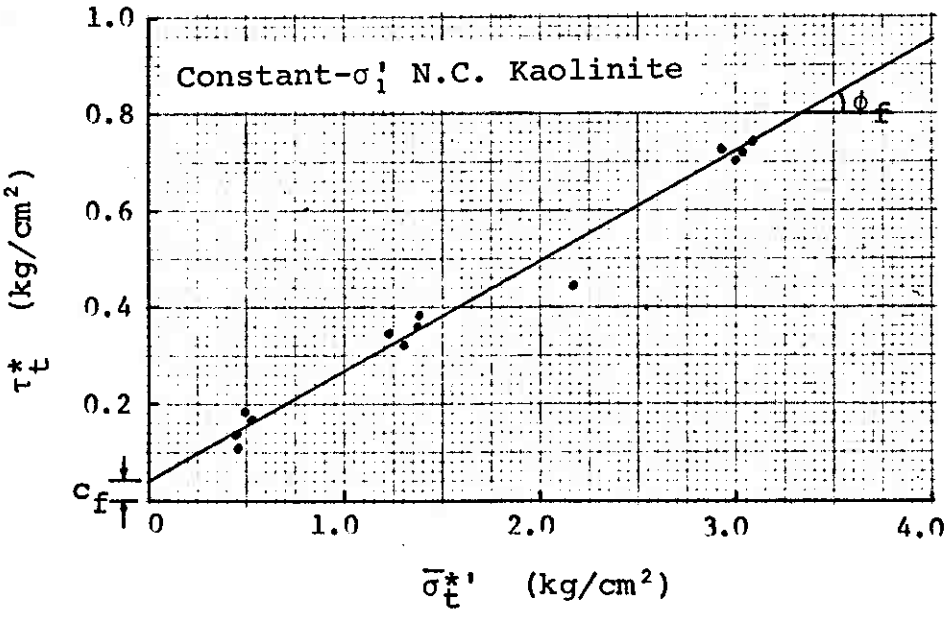

Figure V-7 τ_t^* vs $\bar{\sigma}_t^{*\prime}$ Plot

Comparison of Drained Tests and IDS Tests with Volume Change Measurements

To obtain experimentally a correlation between the two sets of parameters from the IDS test and Stress Dilatancy Theory, a test method must be able to yield data so that both sets of parameters can be calculated. The one-specimen IDS curve-hopping technique had been established (Schmertmann, 1962) to give two different stress-strain curves at two different preselected stress conditions. In the derivation of the stress dilatancy equations, it had been assumed that the specimen is sheared under increasing stress ratio R.

Constant-σ_1', σ_3', p' or constant-volume tests all involve increasing R ratios and hence it was postulated that the one-specimen IDS test with volume change measurements would provide the information necessary for the evaluation of the two sets of parameters.

Analysis of Experimental Data

Glass beads

To check the above postulation, a set of three drained tests and six constant-σ_3' IDS tests with volume change measurements were run and the interparticle parameters c_f and ϕ_f computed from the regression of $\frac{\sigma_1'}{1+\lambda} - \sigma_3'$ on $\frac{\sigma_1'}{1+\lambda} + \sigma_3'$ with the aid of expressions (3-20) and (3-21). The last column, r_f gives the sample correlation coefficient.

ε_1 (%)	c_f	tan ϕ_f	$\phi_f{}^0$	r_f
Drained (3 tests)				
1	-.0833	.3141	17.4	.9992
2	-.0350	.2977	16.6	.9994
3	-.0104	.3233	17.9	.9996
4	-.0435	.3649	20.0	.9983
Constant-σ_3' IDS (6 tests)				
1	-.025	.2817	15.7	.9979
2	-.006	.2824	15.8	.9990
3	-.010	.2833	15.8	.9985
4	-.052	.3282	18.2	.9937

Table V-1. Interparticle Parameters c_f and ϕ_f for Glass Beads

The physical angle of friction, ϕ_μ for glass beads (Rowe, 1962) is 17^0. Since the samples were prepared in a dense condition, the stress ratio R versus dilatancy D relation should follow the minimum energy line ϕ_μ at low strains before deviating from it at higher strains. The above table showed that for the drained tests, ϕ_f just exceeds 17^0 for strains from 1 to 3% while the corresponding values for IDS tests lie close to 16^0. It is felt that if more tests had been conducted, the agreement would have been better.

Applying the statistical method of hypothesis testing to check the null hypothesis of $c_f = 0$, it is found that there is insufficient evidence to reject the null hypothesis for all the strains investigated for both test series at 5% level of significance. This means at the 95% confidence level an investigator would conclude from the data that $c_f = 0$. The high r_f values indicate that the strain paths are linear.

Kaolinite

A set of three drained tests and another set of three constant-σ_1' IDS tests were made on overconsolidated kaolinite with the following results:

ε_1	c_f	tan ϕ_f	ϕ_f	r_f
Drained (3 tests)				
1	-.1064	.4449	24.0	.9971
2	-.0015	.3957	21.6	.9995
3	-.0057	.4334	23.4	.9998
4	-.0211	.4457	24.0	.9998
Constant-σ_1' IDS (3 tests)				
1	.0147	.1615	9.2	.9999
2	.0585	.2285	12.9	.9987
3	.0585	.2996	16.7	.9991
4	.0604	.3416	18.9	-

Table V-2. Interparticle Parameters c_f and ϕ_f for O.C. Kaolinite

The main distinction between these two series of tests is the difference in stress paths. Rowe et al.(1963) reported that two overconsolidated clays investigated behaved like sands with $c_f = 0$ for the isotropically consolidated clay and $c_f = .04$ kg/cm^2 for the anisotropically consolidated clay. For an overconsolidated clay as for a dense sand, the R versus D plot should fall on the ϕ_μ minimum energy line at low strains. From the drained test results, this would yield a ϕ_μ value for kaolinite of about 24^0. No available data on ϕ_μ of kaolinite had been published and the method of determining ϕ_μ for cohesionless materials (Rowe, 1962) is not applicable for clays.

Testing the null hypothesis of $c_f = 0$ for drained tests at 5% level of significance, it is found that there is insufficient evidence to reject the null hypothesis for all the strains investigated. Therefore $c_f = 0$.

On the other hand, the constant-σ_1' IDS tests yield c_f values of about 0.06 kg/cm^2 with corresponding lower ϕ_f values than drained tests. These results support the possibility that there is an effect of stress path on the interparticle parameters. The high r_f values for both test series indicate linearity of strain paths.

IDS Tests with Volume Change Measurements

Three types of materials were used in this experimental program:

i) Extruded kaolinite whose bond strength I_o had been

shown by previous studies to be between .06 and .08 Kg/cm^2.

ii) Glass beads passing U. S. sieve No. 140 and retained on No. 200. They are cohesionless and spherical shaped.

iii) Glass beads mixed with hydrocal (gypsum) in the proportion of 10 to 1 by weight to produce artificial bonding between the cohesionless glass beads.

Comparisons of Bond Strength I_o and c_f

Kaolinite

Three types of IDS tests were run on normally consolidated and overconsolidated kaolinite to determine the effect of stress paths on bond strength and interparticle parameters. The three types are constant-σ_1', constant-p' and constant-volume. The regression coefficients I_o, β and c_f, ϕ_f with corresponding linear correlation coefficients of r_i and r_f respectively are tabulated below for normally consolidated kaolinite. In all the following tables, vertical strain, ε_1, is in per cent, I_o and c_f are in kg/cm^2.

Constant-σ_1' IDS Tests (13 tests)

ε_1	I_o	β	r_i	c_f	$\tan\phi_f$	r_f
1	.0613	.1502	.9814	.0458	.2197	.9910
2	.0415	.1835	.9829	.0576	.2883	.9932
3	.0471	.1886	.9781	.0667	.3212	.9943
4	.0494	.2020	.9641	.0633	.3683	.9965
5	.0375	.2069	.9633	.0605	.3948	.9976
ave	.0479			.0588		

Constant-p'IDS Tests (6 tests)

ε_1	I_o	β	r_i	c_f	$\tan\phi_f$	r_f
1	.0804	.1413	.9902	.0270	.3036	.9955
2	.0898	.1527	.9826	.0032	.3780	.9987
3	.1025	.1573	.9686	.0542	.3678	.9904
4	.1206	.1581	.9267	.0804	.3656	.9895
5	.1230	.1596	.9379	.0914	.3754	.9894
	.1033			.0512		

Constant-Volume IDS Tests (3 tests)

ε_1	I_o	β	r_i	c_{cv}	$\tan\phi_{cv}$	r_f
1	.1303	.1148	.9633	.1381	.1819	.9952
2	.0817	.1375	.9799	.1387	.2532	.9973
3	.0870	.1525	.9892	.1296	.3107	.9989
4	.0878	.1487	.9995	.1188	.3554	.9995
5	.0540	.1553	.9836	.1152	.3848	.9999
	.0882			.1281		

Table V-3 Regression Coefficients of IDS and Stress Dilatancy Methods on N.C. Kaolinite

Similar parameters for the three stress paths on overconsolidated kaolinite follow:

ave .0796 .0799

Constant-σ_1' IDS Tests (3 tests)

ε_1	I_o	β	r_i	c_f	$\tan\phi_f$	r_f
1	.0550	.1686	.9956	.0147	.1615	.9999
2	.0433	.1683	.9581	.0585	.2285	.9997
3	.0376	.1780	.9916	.0585	.2996	.9991
4	.0576	.1639	-	.0604	.3416	-
5	.0880	.1318	-	.0489	.3867	-
	.0563			.0482		

Constant-p' IDS Tests (3 tests)

ε_1	I_o	β	r_i	c_f	$\tan\phi_f$	r_f
1	.0287	.2115	.9912	.0858	.1076	.9753
2	-.0078	.2539	.9921	.0326	.2934	.9997
3	-.0082	.2730	.9993	.0198	.3527	.9999
4	-.0723	.2892	.9999	.0155	.3932	.9994
5	-.0290	.3174	.9985	.0140	.4098	.9993
	-.0177			.0335		

Constant-Volume IDS Tests (3 tests)

ε_1	I_o	β	r_i	c_{cv}	$\tan\phi_{cv}$	r_f
1	.0405	.1491	.9849	.1966	.2071	.9947
2	.1647	.0753	.9839	.2089	.2611	.9931
3	.2189	.0518	.9959	.1846	.3133	.9933
4	.2025	.0756	.9825	.1412	.3635	.9922
5	.0880	.1415	.9986	.0926	.4099	.9889
	.1429			.1648		

Table V-4 Regression Coefficients of IDS and Stress Dilatancy Methods on O.C. Kaolinite

.0605 .0623

From the analysis of the three test types on both normally consolidated and overconsolidated kaolinite, the strain paths are found to be linear for both methods of analysis although more confidence can be placed on the constant-σ_1' test series where there are 13 tests. I_o values were less variable for normally consolidated than for overconsolidated kaolinite while c_f values for constant-volume tests are much greater than corresponding values for constant-σ_1' and constant-p' tests.

Testing the null hypothesis for the constant-σ_1' normally consolidated case that $I_o = 0$ at 5% level of significance, it was found that there was not sufficient evidence to indicate that I_o differs from zero at strains greater than 1%. This is to say that I_o is only significant at 1%. At the 10% significance level, I_o will be significant at 1.0, 2.0 and 3.0% strains.

Testing the null hypothesis of $c_f = 0$ at 5% significance level, it was found that there was insufficient evidence to indicate that $c_f = 0$ at all strains investigated. Therefore $c_f \neq 0$.

Glass beads

To eliminate the effect of the 'cohesion' variable, it was decided to test a cohesionless material with uniform particle sizes whose spherical shapes will also diminish the effect of interlocking.

A total of 6 tests with two samples at each of the

consolidating pressures of 1.0, 2.0 and 4.0 kg/cm^2 was performed. Correlation and regression analysis yield the following results:

ε_1	I_o	β	r_i	c_f	$\tan\phi_f$	r_f
1	-.081	.055	.9315	-.025	.2817	.9979
2	-.064	.0124	.4092	-.006	.2824	.9990
3	-.003	-.0076	-.4539	.010	.2833	.9985
4	.016	-.0202	-.5285	-.052	.3282	.9937

-.033 -.018

Table V-5. Regression Coefficients of IDS and Stress Dilatancy Methods on Glass Beads

In linear correlation when all the points lie on a horizontal line, the correlation coefficient will be zero indicating that the two variables are independent. Since I_o should be zero for the cohesionless glass beads, any I_ε component would reflect the magnitude of the error from extrapolation of the tangent during component separation. The slope β of the regression line indicates the rate of increase of this error. Testing the null hypothesis that $I_o = 0$ at 5% significance level, it was found that I_o is not significant at all the strains investigated. To test the null hypothesis that $\beta = 0$ at 5% level, it was found that there is insufficient evidence to reject the null hypothesis except at 1.0% strain.

The correlation between shear stress and normal stress corrected for dilatancy $(\tau_t^*, \bar{\sigma}_t^{*\prime})$ shows a high r_f value. A test of the null hypothesis that $c_f = 0$ at the 5% significance level indicated that there is not sufficient evidence

to indicate that c_f differs from zero at all strains investigated.

Glass beads with hydrocal

The addition of hydrocal to glass beads is to provide artificial bonding to the cohesionless beads greater than the bond strength obtained from kaolinite so that it can be defined more distinctly. A total of nine tests were made. Since failure planes were observed at about 2½% strain, only points up to 2% strain were analysed.

ε_1	I_o	β	r_i	c_f	$\tan\phi_f$	r_f
0.5	.2453	.3070	.9646	.1831	.6790	.9938
1.0	.2310	.2361	.9254	.1171	.6188	.9953
1.5	.2260	.1584	.9392	.1381	.5434	.9950
2.0	.2118	.1211	.9190	.1223	.5008	.9939
ave	.2285			.1402		

Table V-6. Regression Coefficients of IDS and Stress Dilatancy Methods on Glass Beads with Hydrocal

The r_f values are all consistently higher than r_i values. Testing the null hypothesis that I_o and c_f equal to zero, it was found that at 10% significance level both I_o and c_f are significant at all the strains except at 1% where the computed 't' value is very close to the critical value. It is felt that if more samples had been replicated, it would also result in the significance for I_o and c_f at 1% strain.

Confidence Limits on Bond Strength and Correlation Coefficients

From the sample data, it is possible to infer something about the location of the population mean, with the sample mean. A population consists of all possible values of a variable. However, the sample mean, $\bar{y}$ is variable and one would hesitate to say that μ is at $\bar{y}$. One would feel better if he can give an interval with $\bar{y}$ as the center and say with a stated degree of confidence that μ lies within that interval. The smaller the interval, the less variation will be the result.

It had been found in statistics that sample correlation coefficients, r_i and r_f are quite variable when computed from small sample sizes especially for low r values. Hence it is desirable to determine the probable confidence limits of the population correlation coefficients using Fisher's z transformation (Steel and Torrie, 1960).

Confidence limits on I_o and c_f, and also on ρ_i and ρ_f which are the population correlation coefficients corresponding to r_i and r_f respectively, are presented in the following tables.

Confidence Intervals for I_o and c_f

95% confidence intervals for I_o and c_f are presented for the two materials, normally consolidated kaolinite and beads with hydrocal:

Constant-σ_1' N.C. Kaolinite

ε_1	I_o ± C.I.	c_f ± C.I.
1	.061 ± .039	.046 ± .038
2	.042 ± .043	.058 ± .042
3	.047 ± .047	.067 ± .040
4	.049 ± .062	.063 ± .034
5	.038 ± .062	.060 ± .030

Glass Beads with Hydrocal

ε_1	I_o ± C.I.	c_f ± C.I.
0.5	.245±.283	.183 ± .211
1.0	.231±.320	.117 ± .176
1.5	.226±.183	.138 ± .155
2.0	.212±.160	.122 ± .154

Table V-7. Confidence Intervals for I_o and c_f

Confidence Limits for ρ_i and ρ_f

The following tables show the upper and lower limits of ρ_i and ρ_f at 95% confidence level for the three materials. The very small confidence intervals and high values of ρ_f for all three types of materials indicate that the strain paths are linear. For the same number of samples, the

confidence intervals for ρ_i are wider especially for beads with hydrocal samples.

Constant-σ_i' N.C. Kaolinite

ε_1	ρ_{iL} , ρ_{iU}	ρ_{fU} , ρ_{fU}
1	.9373 , .9946	.9693 , .9974
2	.9423 , .9950	.9767 , .9980
3	.9265 , .9936	.9805 , .9983
4	.8814 , .9895	.9880 , .9990
5	.8789 , .9892	.9917 , .9993

Glass Beads

ε_1	ρ_{fL} , ρ_{fU}
1	.9800 , .9999
2	.9904 , .9999
3	.9857 , .9999
4	.9411 , .9993

Glass Beads with Hydrocal

ε_1	ρ_{iL} , ρ_{iU}	ρ_{fL} , ρ_{fU}
0.5	.8361 , .9927	.9697 , .9987
1.0	.6778 , .9845	.9770 , .9990
1.5	.7311 , .9874	.9755 , .9990
2.0	.6544 , .9831	.9702 , .9988

Table V-8 Lower and Upper Confidence Limits of Population Correlation Coefficients ρ_i and ρ_f

I_ε^* versus $\bar{\sigma}_t^{*\prime}$ Relationships

The relationships between I_ε^* and $\bar{\sigma}_t^{*\prime}$ whose values were computed from equations (4-1) to (4-4) were analysed using linear regression where I_o^* and β^* denote the zero intercept and slope of the regression line respectively.

Constant-σ_3' N.C. Kaolinite

ε_1	I_o^*	β^*	r^*
1	.0241	.0119	.0843
2	-.0127	.1120	.6080
3	-.0148	.1340	.7675
4	-.0430	.1850	.8510
5	-.0233	.1730	.8705

Glass Beads

ε_1	I_o^*	β^*	r^*
1	.0615	-.0624	-.5716
2	-.1193	.0422	.6215
3	.0160	-.0265	-.7203
4	.1374	-.0936	-.7775

Glass Beads with Hydrocal

ε_1	I_o^*	β^*	r^*
0.5	.7266	-.0170	-.0806
1	.2535	.1252	.6569
1.5	.3330	.0615	.5680
2	.1851	.1008	.8491

Table V-9. Regression Coefficients for I_ε^* vs $\bar{\sigma}_t^{*\prime}$ Relationships

The above analysis showed that the correlation coefficients, r*, are much lower than the corresponding r_i and r_f values for kaolinite and glass beads with hydrocal. For the glass beads, the I_o^* are much greater than the corresponding I_o, which should be zero. r* values are much lower than corresponding r_f values because of the double extrapolation involved in obtaining I_o^*.

Table V-10 lists the upper and lower limits for ρ^*, the population correlation coefficient corresponding to sample correlation coefficient, r*, for both kaolinite and glass beads with hydrocal at 95% confidence level.

N.C. Kaolinite

ε_1	ρ_L^* ,	ρ_U^*
1	-.4892 ,	.6069
2	.0868 ,	.8680
3	.3757 ,	.9265
4	.5656 ,	.9544
5	.6144 ,	.9606

Glass Beads with Hydrocal

ε_1	ρ_L^* ,	ρ_U^*
0.5	-.7069 ,	.6163
1.0	-.0130 ,	.9197
1.5	-.1538 ,	.8947
2.0	.4244 ,	.9676

Table V-10 Lower and Upper Confidence Limits of Population Correlation Coefficient ρ^*

The lower confidence limits for ρ^* drops down even to a negative value indicating the variability and imprecision in this method of extrapolating for bond strength.

Linearity of Strain Paths

The above analysis has proven that the strain paths corresponding to both IDS and Stress Dilatancy Methods are linear with slightly greater linear correlation coefficient for the latter method.

CHAPTER VI
THEORETICAL RELATIONSHIPS BETWEEN IDS AND STRESS DILATANCY PARAMETERS

I_o and c_f Parameters

The previous chapter has shown that the strain paths for both methods of obtaining bond strength are linear. It now remains to express both I_o and c_f in terms of the same variables.

Taking two IDS test results at a certain strain with values of $\tau_{(1)}, \bar{\sigma}'_{(1)}, d_{(1)}, \lambda_{(1)}$ and $\tau_{(2)}, \bar{\sigma}'_{(2)}, d_{(2)}, \lambda_{(2)}$, the equation for I_ε is given by

$$I_\varepsilon = I_{(1)} + (\bar{\sigma}'_t - \bar{\sigma}'_{(1)}) \left(\frac{I_{(2)} - I_{(1)}}{\bar{\sigma}'_{(2)} - \bar{\sigma}'_{(1)}} \right) \qquad (6\text{-}1)$$

where $I = \tau - \bar{\sigma}' d$ (6-2)

From equation (6-1) at $\bar{\sigma}'_t = 0$,

$$I_o = I_{(1)} - \bar{\sigma}'_{(1)} \left(\frac{I_{(2)} - I_{(1)}}{\bar{\sigma}'_{(2)} - \bar{\sigma}'_{(1)}} \right) \qquad (6\text{-}3)$$

Substituting equation (6-2) for the two points into equation (6-3)

$$I_o = \frac{\tau_{(1)} \bar{\sigma}'_{(2)} - \tau_{(2)} \bar{\sigma}'_{(1)} - \bar{\sigma}'_{(1)} \bar{\sigma}'_{(2)} (d_{(1)} - d_{(2)})}{\sigma'_{(2)} - \sigma'_{(1)}}$$

$$= f(\bar{\sigma}'_{(1)}, \tau_{(1)}, \bar{\sigma}'_{(2)}, \tau_{(2)}, d_{(1)}, d_{(2)}) \qquad (6\text{-}4)$$

After correcting $\bar{\sigma}'_t$ and τ_t for the two points for dilatancy resulting in $\bar{\sigma}'^*_t$ and τ^*_t and working with principal stresses, then equations (3-21) and (3-22) are applied to yield

$$\sin \phi_f = \frac{\left(\frac{\sigma'_{21}}{1+\lambda_2} - \sigma'_{23}\right) - \left(\frac{\sigma'_{11}}{1+\lambda_1} - \sigma'_{13}\right)}{\left(\frac{\sigma'_{21}}{1+\lambda_2} + \sigma'_{23}\right) - \left(\frac{\sigma'_{11}}{1+\lambda_1} + \sigma'_{13}\right)} = \tan \psi \quad (6\text{-}5)$$

$$\text{and} \quad a = \left(\frac{\frac{\sigma'_{11}}{1+\lambda_1} - \sigma'_{13}}{2}\right) - \tan \psi \left(\frac{\frac{\sigma'_{11}}{1+\lambda_1} + \sigma'_{13}}{2}\right) \quad (6\text{-}6)$$

where first subscript denotes point number and second subscript denotes major (1) or minor (3) principal stress. But

$$c_f = a/\cos \phi_f \quad (6\text{-}7)$$

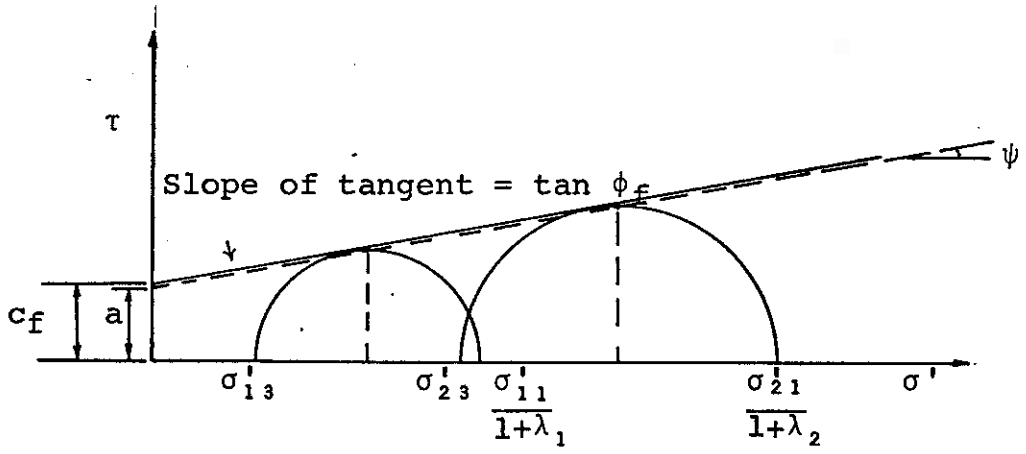

Figure VI-1 Isolation of Interparticle Parameters, c_f and ϕ_f

$$c_f = \frac{\left(\frac{\sigma_1'}{1+\lambda_1}\ \sigma_2' - \frac{\sigma_2'}{1+\lambda_2}\ \sigma_1'\right)}{2\sqrt{(\sigma_2' - \sigma_1')\left(\frac{\sigma_2'}{1+\lambda_2} - \frac{\sigma_1'}{1+\lambda_1}\right)}} \qquad (6\text{-}8)$$

But from the equation of the constant structure envelope, the principal stresses can be expressed in terms of the given values $\bar{\sigma}_t'$, τ_t and d.

$$\sigma_3' = \bar{\sigma}_t' + \tau_t(d - \sqrt{1+d^2}) \qquad (6\text{-}9)$$

$$\sigma_1' = \bar{\sigma}_t' + \tau_t(d + \sqrt{1+d^2}) \qquad (6\text{-}10)$$

Substituting equations (6-9) and (6-10) into (6-8) expression for c_f,

$$c_f = f(\bar{\sigma}_{(1)}', \tau_{(1)}, \bar{\sigma}_{(2)}', \tau_{(2)}, d_{(1)}, d_{(2)}, \lambda_{(1)}, \lambda_{(2)}) \qquad (6\text{-}11)$$

Equations (6-4) and (6-11) for I_o and c_f respectively are expressed in terms of the same variables with the extra λ terms for the c_f expression.

c_f and I_ε^* Parameters

The stress dilatancy equation for cohesive soils (2-16) can also be rewritten as

$$\frac{\left(\frac{\sigma_1'}{1+\lambda} - \sigma_3'\right)}{2} = \frac{\left(\frac{\sigma_1'}{1+\lambda} + \sigma_3'\right)}{2} \sin\phi_f + c_f \cos\phi_f \qquad (6\text{-}12)$$

From expressions for I_ε^* and D_ε^* (4-1 to 4-4), one can rewrite I_ε^* as

$$I_\varepsilon^* = \frac{\sigma_{3h}'\left(\frac{\sigma_1'}{1+\lambda}\right)_\ell - \sigma_{3\ell}'\left(\frac{\sigma_1'}{1+\lambda}\right)_h}{2\sqrt{\left(\left(\frac{\sigma_1'}{1+\lambda}\right)_h - \left(\frac{\sigma_1'}{1+\lambda}\right)_\ell\right)(\sigma_{3h}' - \sigma_{3\ell}')}}$$

$$= \frac{\left(\frac{\sigma_1'}{1+\lambda} - \sigma_3'\right) - \left(\frac{\sigma_3'}{1+\lambda} + \sigma_3'\right)\sin\phi_\varepsilon^*}{2\cos\phi_\varepsilon^*} \qquad (6\text{-}13)$$

These two expressions are similar and by equating like terms,

$$c_f = I_\varepsilon^*$$

if only

$$\phi_f = \phi_\varepsilon^*$$

Since it had been shown that I_ε^* and $\bar{\sigma}_t^{*\prime}$ are not well correlated linearly, a theoretical expression for I_o^* will not be appropriate.

α_s and α_R Parameters

From the linearity of the strain paths in the IDS method, then at each strain, one can write

$$\alpha_s = \frac{\tau_t - I_o + \beta\,\bar{\sigma}_t' \ln \bar{\sigma}_t'}{\bar{\sigma}_t'} \qquad (6\text{-}14)$$

where I_o and β are constants at each strain.

Rowe's α_R parameter is given by

$$\tan\alpha_R = (1+\lambda)\tan(45+\phi_f/2) \qquad (6\text{-}15)$$

which applies to both sand and clay and is independent of c_f.

For cohesive soils, equation (3-19) yields

$$\tan(45+\phi_f/2) = -c_f/\sigma_3' \pm \sqrt{(c_f/\sigma_3')^2 + \frac{\sigma_1'}{\sigma_3'(1+\lambda)}} \qquad (6\text{-}16)$$

Therefore

$$\tan\alpha_R = (1+\lambda)\left[-c_f/\sigma_3' \pm \sqrt{(c_f/\sigma_3')^2 + \frac{\sigma_1'}{\sigma_3'(1+\lambda)}}\right] \qquad (6\text{-}17)$$

For a cohesionless soil, $c_f = 0$,

$$\tan \alpha_R = \sqrt{\frac{\sigma_1'}{\sigma_3'}(1+\lambda)} \qquad (6\text{-}18)$$

Since σ_1' and σ_3' are functions of $\bar{\sigma}_t'$ and τ_t

$$\tan \alpha_R = f(\bar{\sigma}_t', \tau_t, \lambda)$$

Both equations for α, (6-14) and (6-17) are functions of $\bar{\sigma}_t'$ and τ_t with λ as an extra variable in α_R.

ϕ_ε and ϕ_f Parameters

From constant structure envelope,

$$\tan \phi_\varepsilon = \frac{\tau_t - I_o}{\bar{\sigma}_t'} - \beta \qquad (6\text{-}19)$$

$$= f(\bar{\sigma}_t', \tau_t)$$

Rowe's ϕ_f is given by equation (6-16) for cohesive soils, and when $c_f = 0$,

$$\tan(45+\phi_f/2) = \sqrt{\frac{\sigma_1'}{\sigma_3'(1+\lambda)}} = f(\bar{\sigma}_t', \tau_t, \lambda) \qquad (6\text{-}20)$$

It should be noted that c_f and ϕ_f are constant at each strain whereas ϕ_ε is not.

Summary of ϕ and α Parameters

The theoretical relationships of ϕ and α parameters can be expressed by introducing the following terms:

$$R = \sigma_1'/\sigma_3' = \tan^2(45+\phi/2) \qquad (6\text{-}21)$$

$$D = (1 + \lambda) \qquad (6\text{-}22)$$

ϕ Parameters

From equation (6-19)

$$\tan \phi_\varepsilon = \frac{R-1}{2\sqrt{R}} - \beta - \frac{I_o}{\bar{\sigma}'_t} \qquad (6\text{-}23)$$

From equation (6-16)

$$\tan(45+\phi_f/2) = -\frac{c_f}{\sigma'_3} \pm \sqrt{\left(\frac{c_f}{\sigma'_3}\right)^2 + \frac{R}{D}} \qquad (6\text{-}24)$$

α Parameters

From equation (6-14)

$$\alpha_s = \frac{R-1}{2\sqrt{R}} - \frac{I_o}{\bar{\sigma}'_t} + \beta \ln \bar{\sigma}'_t \qquad (6\text{-}25)$$

From equation (6-17)

$$\tan \alpha_R = D \left[-\frac{c_f}{\sigma'_3} \pm \sqrt{\left(\frac{c_f}{\sigma'_3}\right)^2 + \frac{R}{D}} \right] \qquad (6\text{-}26)$$

Relationships between ϕ_ε, ϕ, α_s, ϕ_f and α_R in Cohesionless Materials

For cohesionless materials, the magnitudes of the above parameters may be represented on a Mohr diagram. The slope of the tangent to the Mohr circle for dilating material is given by tan ϕ (Coulomb) with the corresponding slope of the tangent to the Mohr circle modified for no dilation represented by ϕ_f. If one considers α_R as the inclination of the slip line, then ϕ_α represents the corresponding angle of α_R line through the origin.

From geometry, ϕ_α can be computed by

$$\sin \phi_\alpha = \frac{2\tau_t \sin\alpha_R \cos \alpha_R}{\cos \phi \sqrt{\sigma_3'^2 + 4 \cos^2\alpha_R \left(\frac{\tau_t}{\cos \phi}\right)\left(\frac{\tau_t}{\cos \phi} + \sigma_3'\right)}} \qquad (6\text{-}27)$$

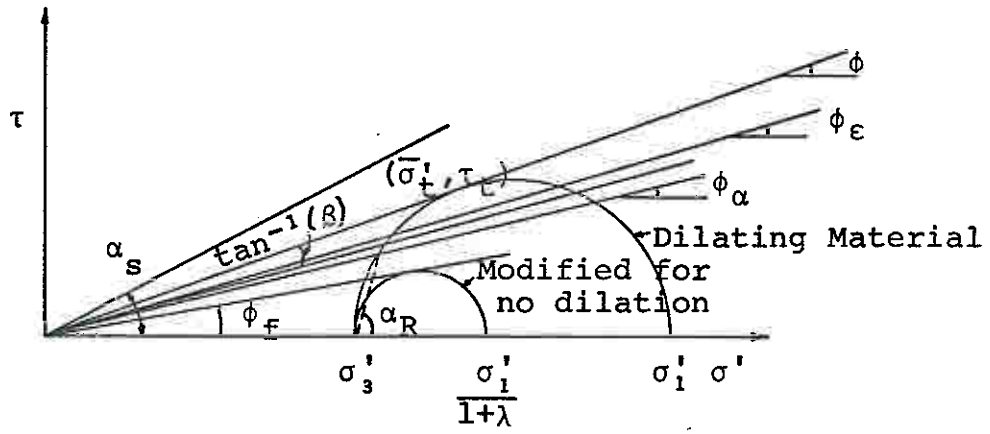

Figure VI-2 Mohr Circles for Cohesionless Element

From constant structure envelope,

$$\alpha_s = \tan \phi + \beta \ln \bar{\sigma}_t' \qquad (6\text{-}28)$$

where

$$\tan \phi = \tau_t / \bar{\sigma}_t'$$

Slope of envelope at point $(\bar{\sigma}_t', \tau_t)$

$$\tan \phi_\varepsilon = \tan \phi - \beta \qquad (6\text{-}29)$$

α_s and ϕ_ε are both represented on the Mohr diagram. However, α_s falls outside the ϕ line and its physical meaning is not too clear at present (1971).

The following two cases were computed for magnitudes of ϕ_ε and α_s:

ϕ (deg)	i) $\beta = 0$		ii) $\beta = 0.2$ $\bar{\sigma}_t' = 2.0 kg/cm^2$	
	ϕ_ε (deg)	α_s (deg)	ϕ_ε (deg)	α_s (deg)
20	20	20.8	9.3	28.8
30	30	33.1	20.7	40.8
40	40	48.1	32.6	56.0
50	50	68.3	44.8	76.2

Table VI-1. ϕ_ε and α_s Values for Two Cases

Comparison of ϕ_ε, ϕ_ε^* and ϕ_f Parameters

The following graphs compare the three ϕ parameters as a function of strain for the three materials. The difference in the definition of the ϕ parameters should be noted.

For the cohesionless glass beads, tan ϕ_ε is greater than tanϕ_ε^* or tan ϕ_f at all strains while tan ϕ_ε^* tend to cluster around tan ϕ_f. ϕ_ε^* and ϕ_f are both corrected for the effect of dilatancy but the former has in addition the effect of envelope curvature β. ϕ_ε includes the effects of both dilatancy and envelope curvature.

The opposite effect is indicated for the N.C. kaolinite with ϕ_f and ϕ_ε^* greater than ϕ_ε which increases with strain. The effect of the artificial bonding of glass beads with hydrocal may be demonstrated by the behaviour of the ϕ parameters with strain. Tanϕ_f is greater than tan ϕ_ε but decreases with increase in strain while ϕ_ε increased

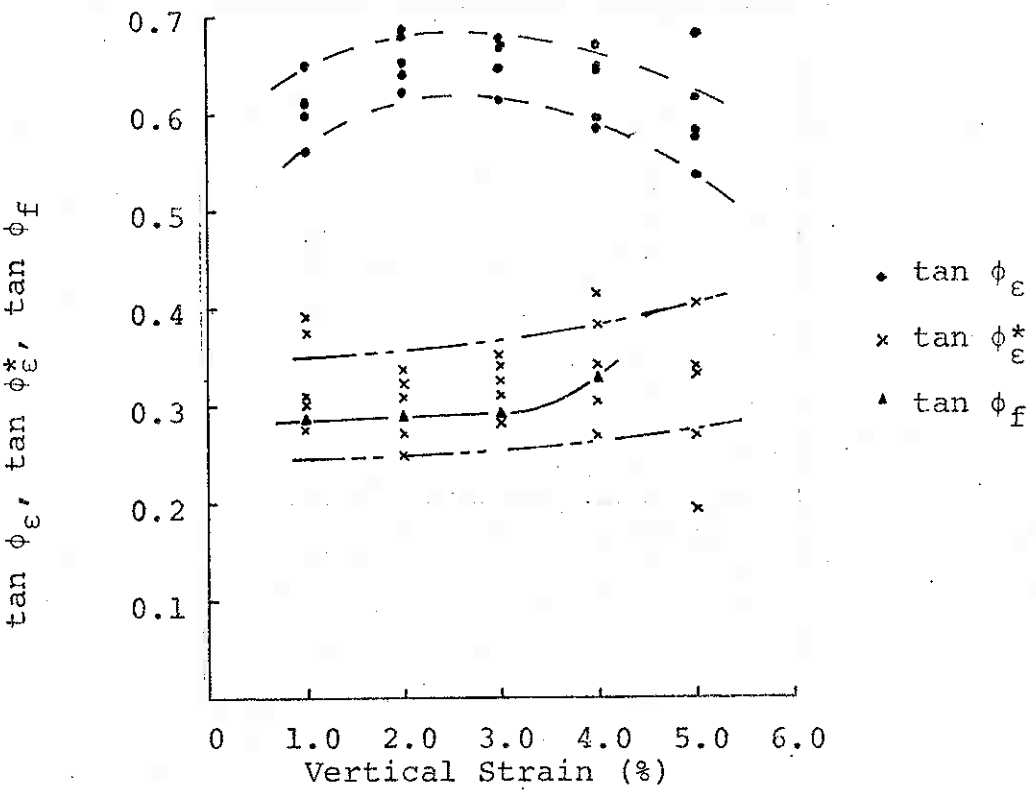

Figure VI-3 ϕ vs Strain Relationships for Glass Beads

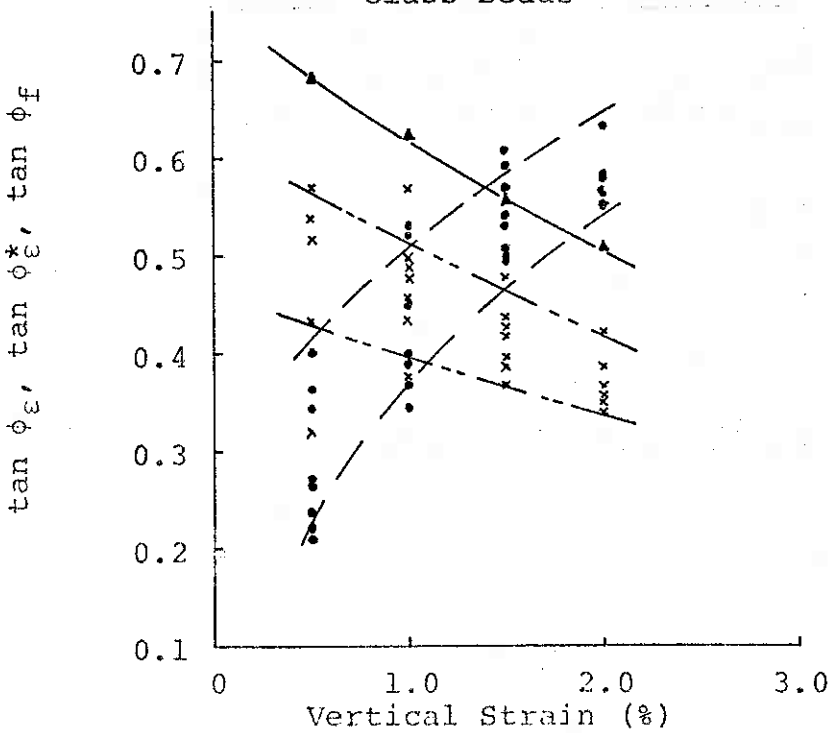

Figure VI-4 ϕ vs Strain Relationships for Glass Beads with Hydrocal

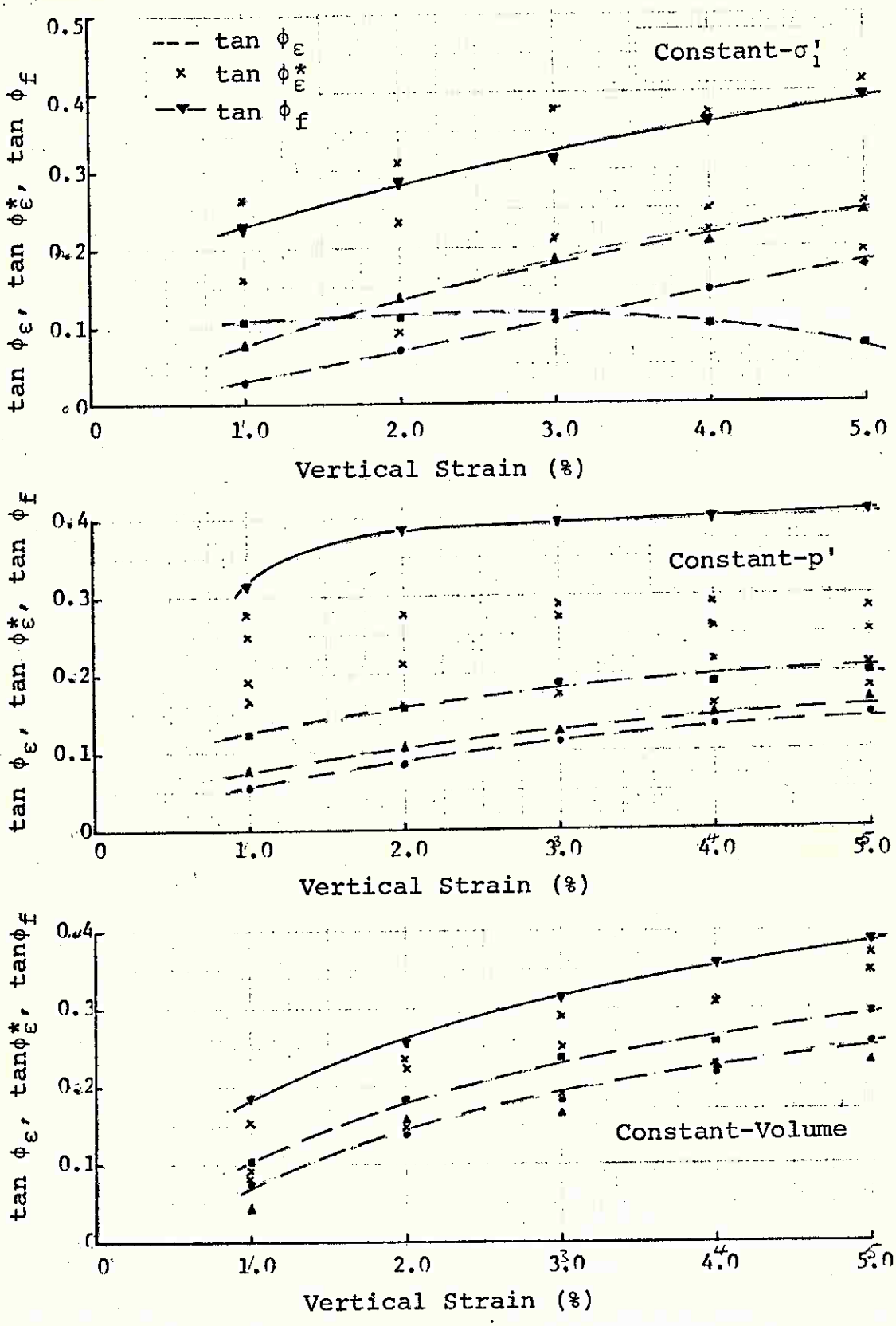

Figure VI-5 ϕ vs Strain Relationships for Three Different Stress Paths on N.C. Kaolinite

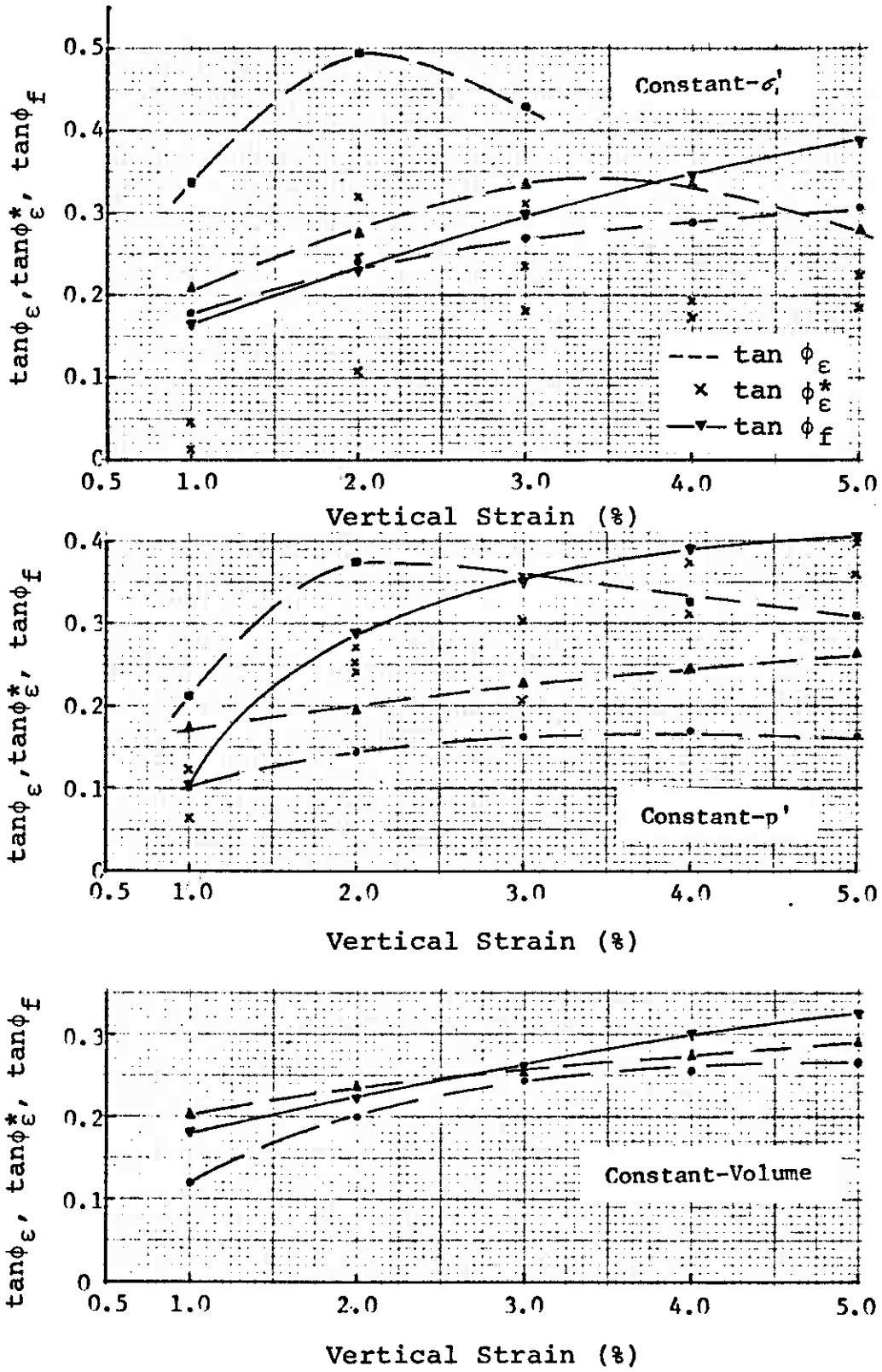

Figure VI-6 ϕ vs Strain Relationships for Three Different Stress Paths on O.C. Kaolinite

becoming ultimately greater than ϕ_f at over 1½% strain. This crossing-over of ϕ_f and ϕ_ε values seems to indicate that at low strains, the samples behave as normally consolidated cohesive material. At higher strains of over 2%, the brittle bonds would have been already broken and the samples would have behaved as cohesionless glass beads. The ϕ_ε^* values follow the same trend as ϕ_f but are generally lower.

ϕ_ε, ϕ_ε^*, ϕ parameters for the three stress paths of N.C. and O.C. kaolinite are presented to give an indication of the variation of the three ϕ parameters with strain, stress path and stress history. For N.C. kaolinite ϕ_f is always greater than ϕ_ε with ϕ_ε^* varying between ϕ_f and ϕ_ε. For the O.C. case, ϕ_f is lower than ϕ_ε at low strains but becomes greater as strain increases.

Of the three stress paths, the constant-volume tests exhibited the smallest difference between ϕ_ε (or ϕ_ε^*) and ϕ_f.

Correlation of α_R and α_s

α_s and α_R parameters were computed from equations (6-14) and (6-15) respectively as a function of strain and then combined to show their correlation. For N.C. kaolinite, the parameters indicate some curvilinear relationship. For the O.C. case they showed a different behaviour.

For cohesionless materials whose I_o and c_f are equal to zero, equation (6-14) reduces to

$$\alpha_s = \frac{\tau_t + \beta\ \bar{\sigma}_t'\ \ln\ \bar{\sigma}_t'}{-,} \qquad (6\text{-}30)$$

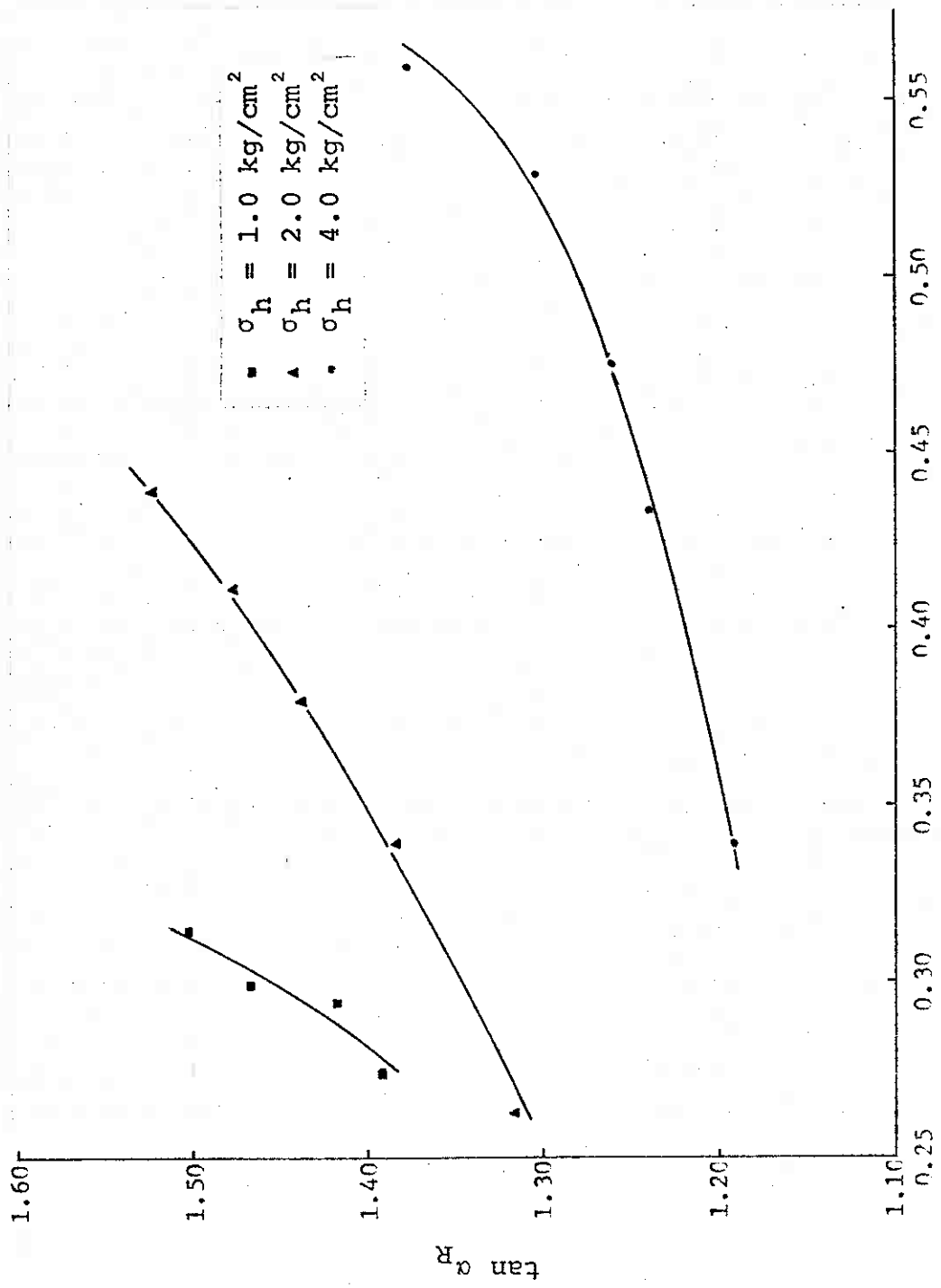

Figure VI-7 tan α_R vs α_s for Constant-σ_1' Test Series on N.C. Kaolinite

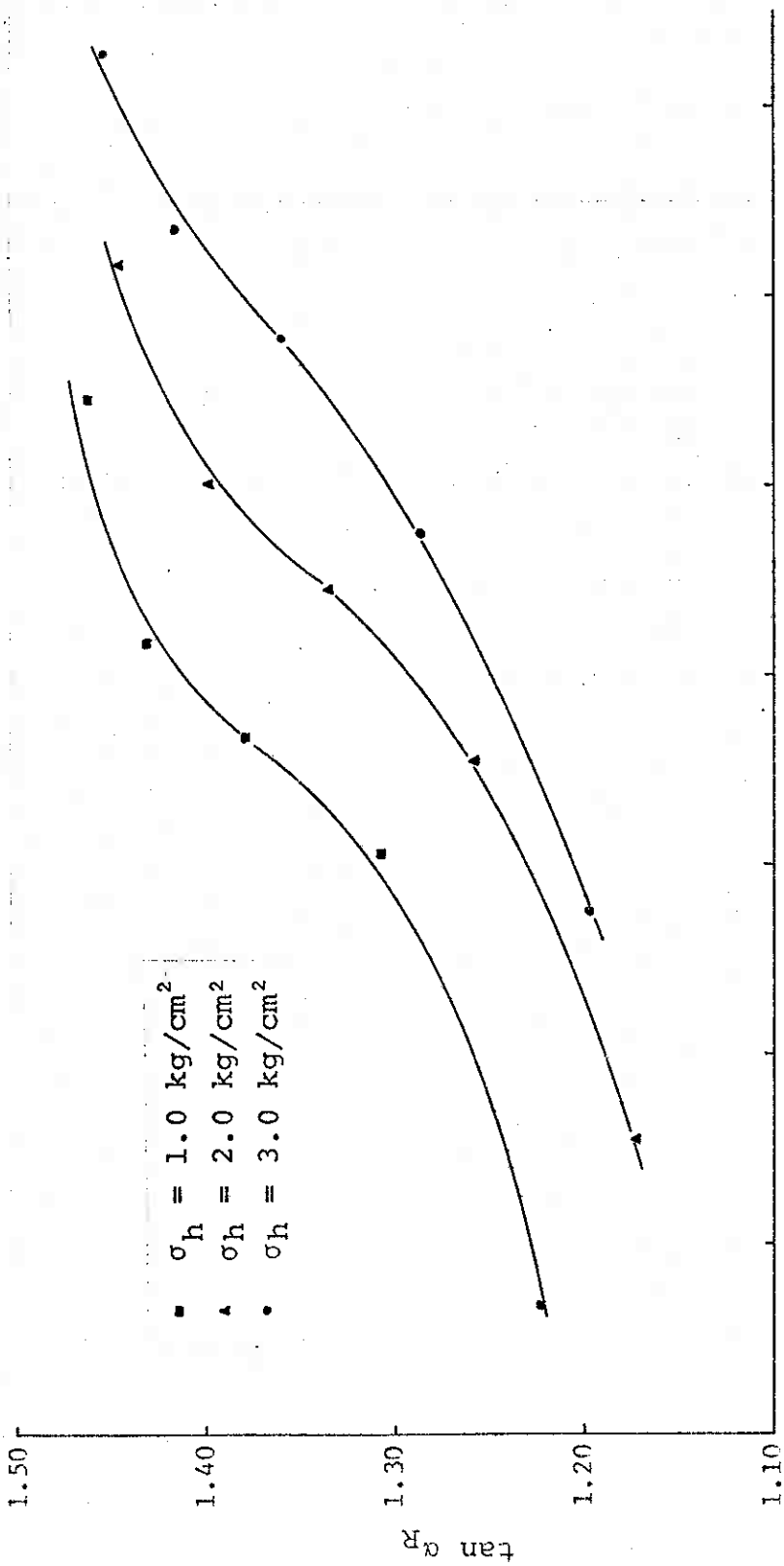

Figure VI-8 tan α_R vs α_s for Constant-Volume Test Series on N.C. Kaolinite

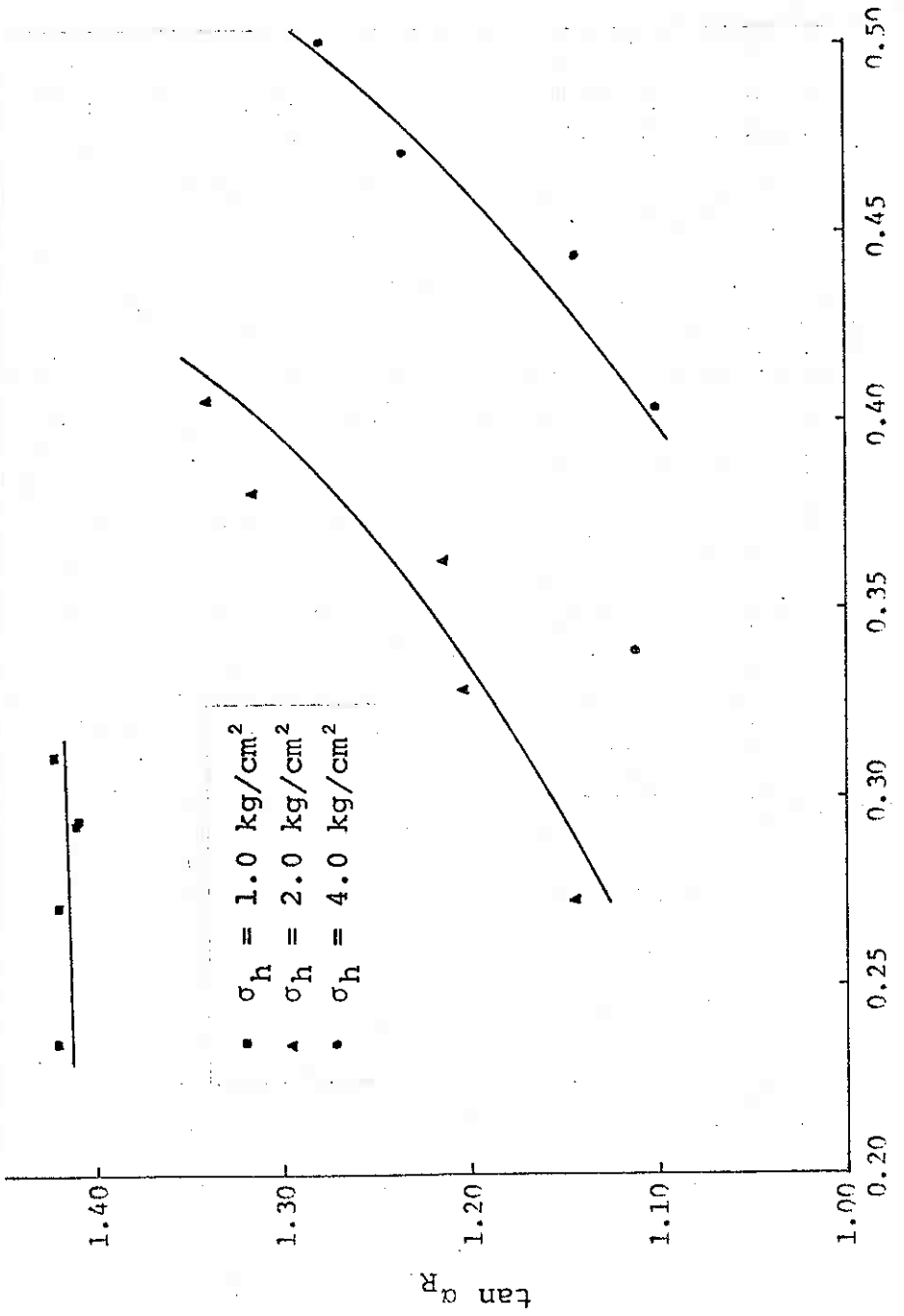

Figure VI-9 tan α_R vs α_s for Constant-p' Test Series on N.C. Kaolinite

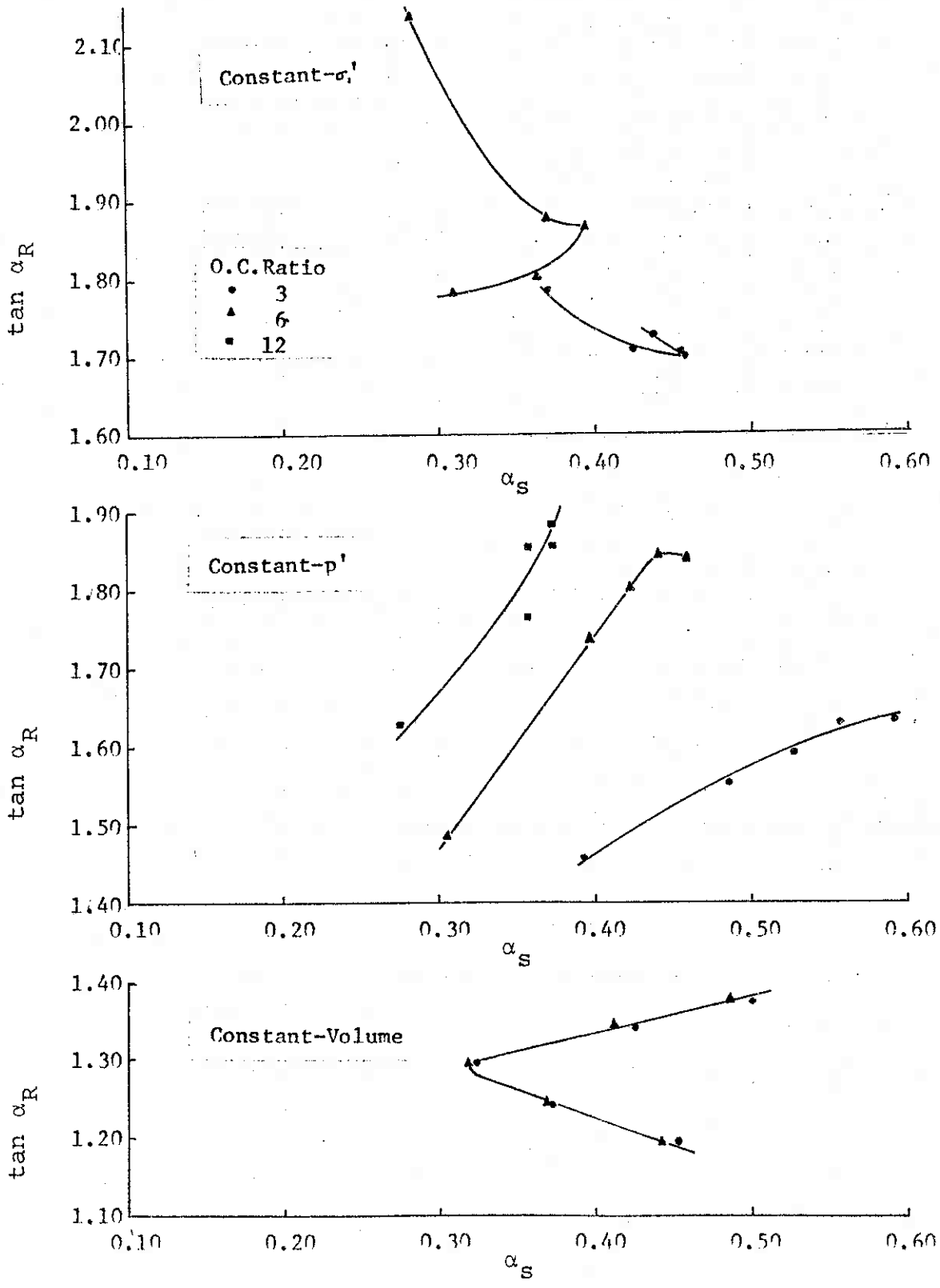

Figure VI-10 tan α_R vs α_s for Three Different Stress Paths on O.C. Kaolinite

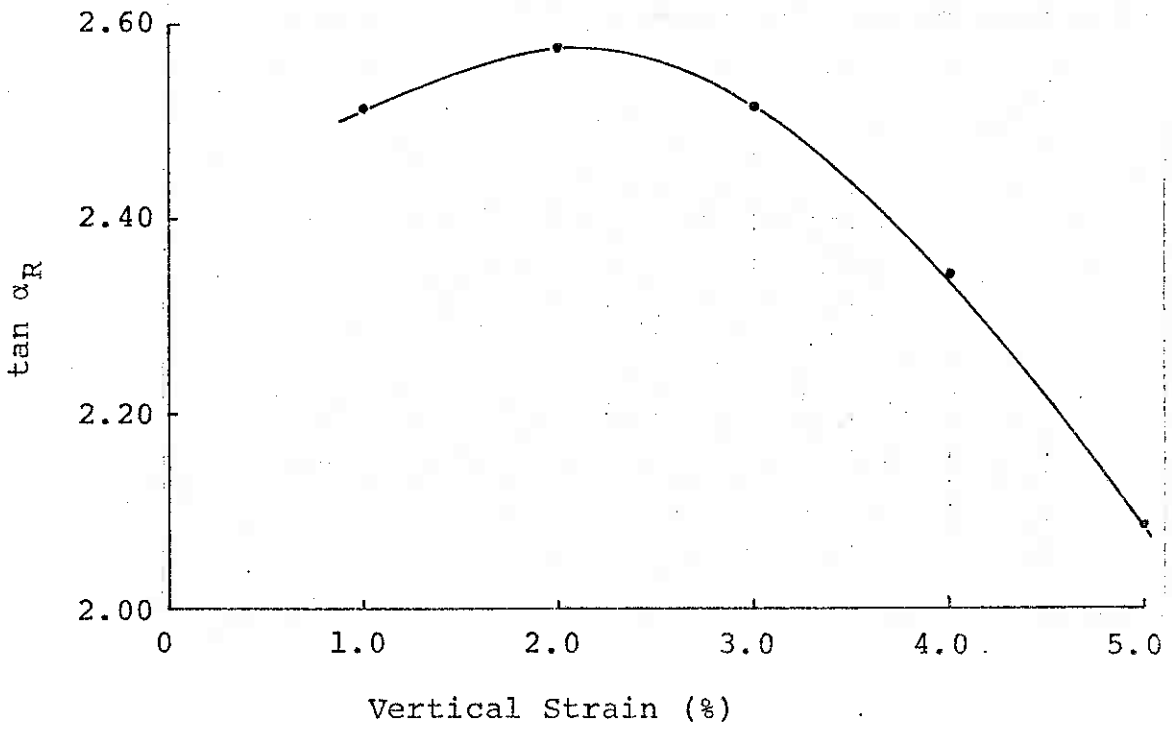

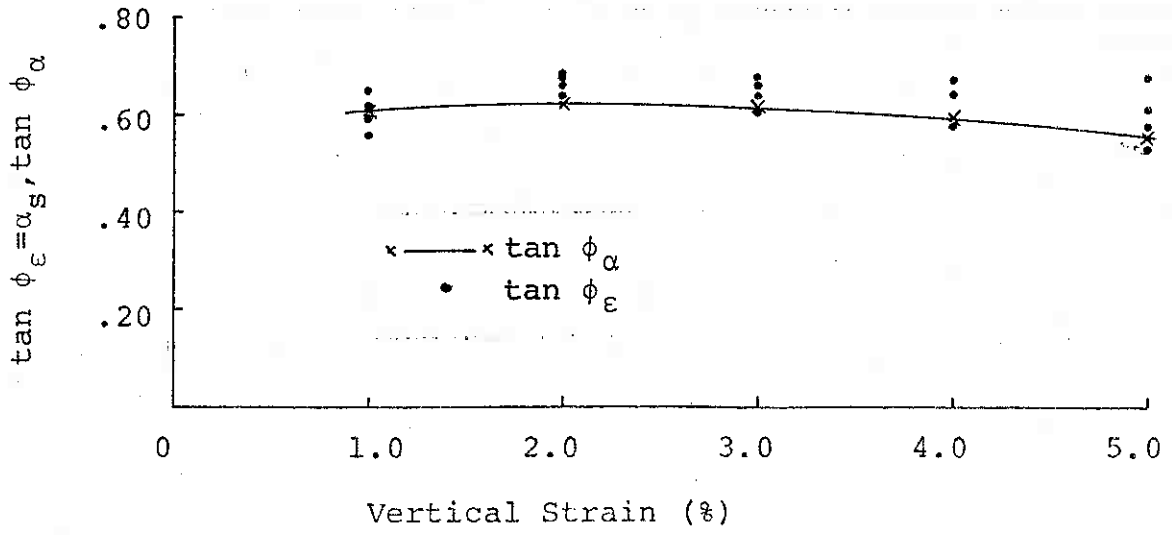

Figure VI-11 tan α_R, tan ϕ_ε, α_s vs Strain Relationships for Glass Beads

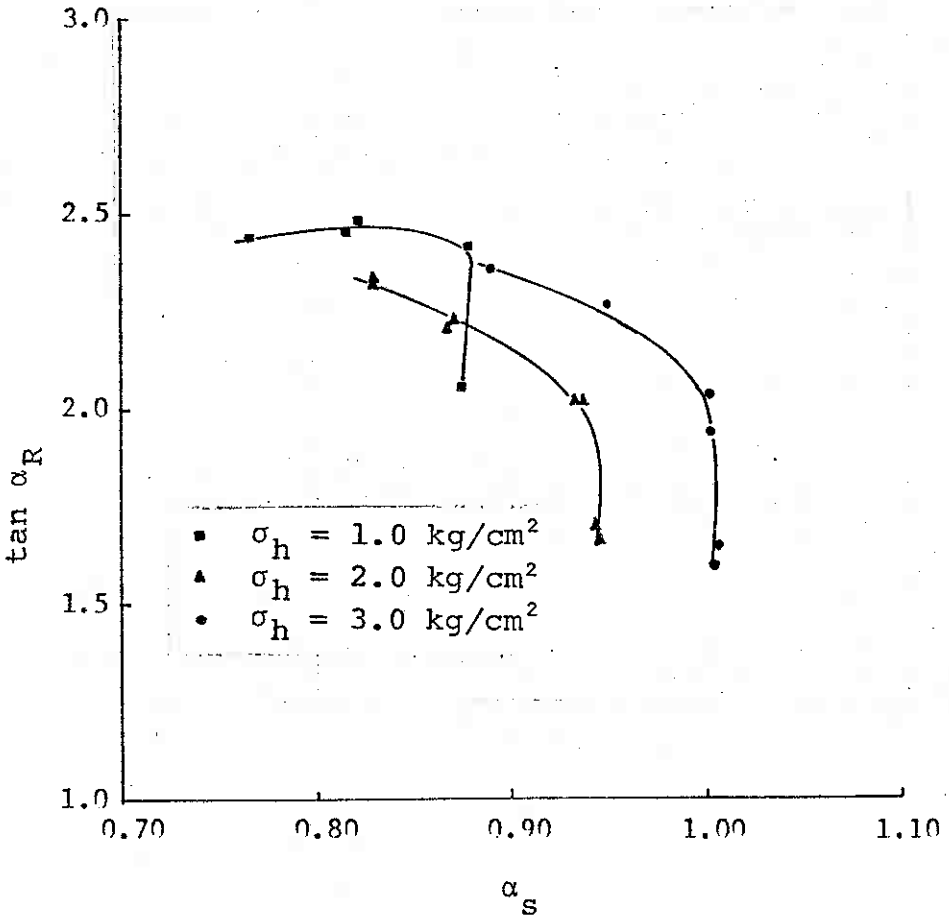

Figure VI-12 tan α_R vs α_s for Glass Beads with Hydrocal

and equation (6-17) is reduced to (6-18).

For glass beads, there is indication that β is close to zero and therefore negligible, then

$$\alpha_s = \tau_f/\bar{\sigma}'_t$$

$$= \tan \phi_\varepsilon = \tan \phi \qquad (6\text{-}31)$$

The plot of tan ϕ_α and tan ϕ_ε (or α_s or tan ϕ) against strain showed that tan ϕ_ε is on the average about 3° greater than tan ϕ_α. (Figure V-11)

For the glass beads with hydrocal, tan α_R increases to a fairly constant value at 1½% strain or greater while α_s decreases with strain. α_s and tan α_R as a function of strain are given in Appendix D for kaolinite and glass beads with hydrocal.

Theoretical Computations of I_o, c_f, ϕ and α Parameters

Cohesionless materials

The following ϕ and α values were computed from equations (6-23), (6-24), (6-25) and (6-26) for the ranges of R and D from 1.0% to 4.0% strain in glass bead tests. The values of β had been shown to be significantly zero for strains greater than 1.0% strain.

$\tan \phi_f$

D \ R	2.9	3.1	3.3	3.5
1.4	.372	.408	.442	.475
1.6	.302	.337	.370	.401
1.8	.241	.275	.308	.339
2.0	.187	.221	.253	.283

$\tan \alpha_R$

D \ R	2.9	3.1	3.3	3.5
1.4	2.015	2.083	2.149	2.214
1.6	2.154	2.227	2.298	2.366
1.8	2.285	2.362	2.437	2.510
2.0	2.408	2.090	2.569	2.646

$\alpha_s = \tan \phi_\varepsilon \ (\beta=0)$

R	2.9	3.1	3.3	3.5
α_s	.558	.596	.633	.668

Table VI-2. Computed ϕ and α Values for Glass Beads

Table VI-2 illustrates the range of values of $\tan \phi_f$, $\tan \alpha_R$, α_s or $\tan \phi_\varepsilon (\beta = 0)$ for various values of R and D encountered in tests on glass beads. α_s or $\tan \phi_\varepsilon$ will be proportional to R when $\beta = 0$. The computed values compare

favourably with the experimental values of tan ϕ_f, tan α_R, and tan ϕ_ε. (Figures VI-3, VI-11) It should be noted that both R and D decrease with increase in strain.

For cohesionless materials whose β is not equal to zero, one has to pick the range of normal effective stress, σ' in addition to R, D, and β in the computation of α_s.

Cohesive Soil

Based on the fact that strain paths are linear, only two points are required. The following four values of τ_t, $\bar{\sigma}'_t$, tan ϕ_ε and λ are selected at each point:
For Constant-σ'_1 IDS test on N.C. kaolinite at 2.0% strain,

Point	τ_t	$\bar{\sigma}'_t$	tanϕ_ε	λ
1	.512	.249	.2227	.10
2	1.325	.420	.1373	-.017

Table VI-3. Two Data Points for N.C. Kaolinite

The following values are computed using equations (6-4), (6-8), (6-19), (6-16), (6-14), and (6-15) respectively:

I_o	c_f	β	tanϕ_f	α_s	tanα_R	Remarks
.070	.085	.127	.264	.283	1.428	computed
.045	.058	.187	.288	.270	1.570	experimental

Table VI-4. Computed Parameters for N.C. Kaolinite

The difference between the computed and the experimental values in Table VI-4 is due to the fact that the computed values are based on only two points whereas the experimental values resulted from the linear regression analysis on 13 test points.

Discussion

Bond Strength I_o and c_f

One of the contributions of this work is the discovery that strain paths are linear for both methods for the materials investigated. Individual values of I_o, c_f and I_o^* at each strain are given in Table VI-5 and 95% confidence intervals for I_o and c_f are given in Table V-7. The confidence intervals for c_f are smaller and they decrease with strain, while those for I_o are more erratic.

Testing the null hypothesis of no difference between I_o and c_f for the two materials, kaolinite and glass beads with hydrocal, at 5% level of significance, it is found that there is insufficient evidence to indicate a difference between I_o and c_f. Thus the effect of dilatancy is not detectable for the sample sizes used. The I_o^* values for the three materials are much different from I_o and c_f and are also more variable. Hypothesis testing has detected a difference in the two methods of computing bond strength, i.e. I_o using I_ε vs $\bar{\sigma}_t'$ and I_o^* using I_ε^* vs $\bar{\sigma}_t'^*$ relationships, with the former having a much smaller confidence interval and therefore greater precision.

Soil Type	Test Type	Strain ε_1 (%)	c_f	I_o	I_o^*	Remarks
Extruded Kaolinite	Constant-σ_1'	1	.0458	.0607	.0241	
		2	.0576	.0415	-.0127	Normally
		3	.0667	.0471	-.0148	Consolidated
		4	.0633	.0494	-.0430	(13 tests)
		5	.0605	.0375	-.0233	
Glass Beads	Constant-σ_3'	1	-.025	-.081	.0615	(6 tests)
		2	-.006	-.064	-.1193	All c_f, I_o &
		3	.010	-.003	.0160	I_o^* values
		4	-.052	.016	.1374	should be 0
Glass Beads with Hydrocal	Constant-σ_3'	0.5	.1831	.2453	.7266	
		1	.1171	.2310	.2535	
		1.5	.1381	.2260	.3330	(9 tests)
		2	.1223	.2118	.1851	

Table VI-5. Comparison of c_f, I_o, I_o^* Values at Each Strain

ϕ and α Parameters

The relationships between Coulomb's ϕ, ϕ_ε, ϕ_f and ϕ_α have been shown on Figure VI-2. The difference between $\tan\phi$ and $\tan\phi_\varepsilon$ is β, which has been shown to be affected by envelope curvature (Schmertmann, 1966a). Table VI-6 shows the range of β for some of the soil types tested. These data, though meager, seem to suggest that β is a function of the sphericity or shape of the grains, i.e. the more angular the particles the higher will be β. However, the range of β varies from about zero for glass beads to just 0.20 for kaolinite

(constant-σ_1' IDS test). The β for the glass beads with hydrocal samples, 0.30 to 0.12,are much higher than that of kaolinite but drops sharply with increase of strain as the bonds are broken.

Soil Type	β	Remarks	Reference
Glass Beads with Hydrocal	.30-.12	At each I_ε	Ho
Kaolinite	.15-.20	At each I_ε	Ho
Fine Beach Sand	.15	At I_m	Schmertmann (1966a)
Ottawa Sand	.036	At I_m	Schmertmann (1966a)
Glass Beads	.055- -.008	At each I_ε	Ho

Table VI-6. Effects of Soil Types on β

ϕ_α, the friction angle corresponding to Rowe's α_R plane for the individual glass bead tests is found to vary from 0^0 to 5^0 below ϕ_ε which is equal to angle ϕ. For sands, Rowe (1971) gave the numerical difference between the α_R plane and $(45 + \phi/2)$ plane as varying from 0^0 to 6^0 for maximum to minimum porosity. This gives a difference in angle between ϕ and ϕ_α of a maximum of 1^0. The interparticle friction angle ϕ_f gives the lower limiting angle of the shearing resistance, while Coulomb's ϕ is the upper limit.

CHAPTER VII
DISCUSSIONS AND CONCLUSIONS

Mobilised Stress-Strain Path

During the shearing of a sample at constant strain rate, it was noted from the movement of the axial deformation dial and the load cell measurements that both readings were not increasing monotonously but rather with the load increasing in a 'saw-tooth' fashion. This phenomenon was carefully observed during the increase of deviator stress with strain. The following figure shows a portion of the observed mobilised stress-strain path for a glass bead with hydrocal sample.

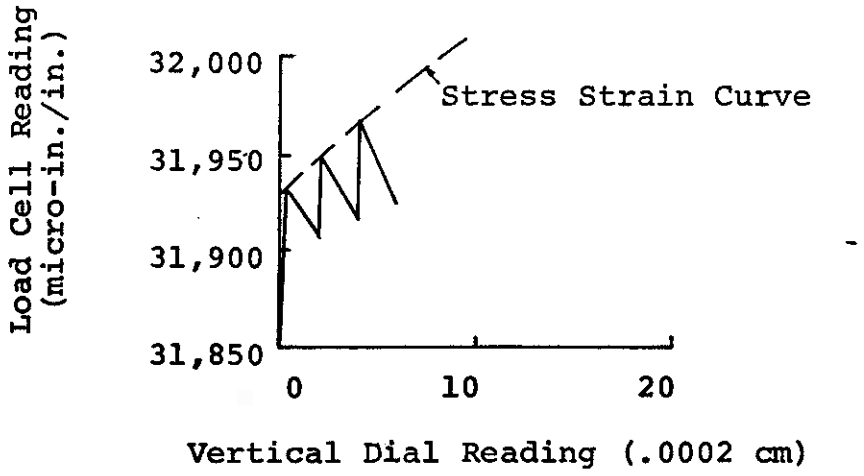

Figure VII-1 Mobilised 'Saw-Tooth' Stress Strain Path

This mode of deformation seems to support the picture presented by Rowe (1962) that groups of particles at critical contacts slide a fraction each time a stress change is made. The soil is said to be in a stage of interparticle slip or 'plastic failure.' The observed phenomenon shows that during the build-up of load at the particle contacts, strain is constant. When the load exceeds the strength of the contacts at the soil structure, these contacts begin to yield,resulting in deformation of the sample. At the same time, the load drops till the groups of particles come to a new stable position when load is again built up at the contacts, this time to a higher ultimate load. This process is repeated, building up each time to a higher 'failure' load,and the joining of the resulting high points of the 'saw-tooth' function will give the stress strain curve. This phenomenon is specially noticeable with the glass beads with hydrocal samples because of the brittle bonds of the hydrocal.

This 'saw-tooth' effect is similar to the 'step-strain' phenemenon during undrained tests described by Trollope and Chan (1960). They suggested that shear strength of clays is entirely frictional in nature and the term 'cohesion' be replaced by 'colloidal friction' so that the mobilised shear strength = colloidal friction + intergranular friction. This concept of frictional strength seems to be demonstrated by the application of Rowe's Stress Dilatancy Theory on the drained strength of two overconsolidated clays (Rowe etal.,

1963) and the writer's drained series on overconsolidated kaolinite resulting in essentially zero values of c_f for isotropically consolidated specimens.

Comments on IDS and Stress Dilatancy Methods of Obtaining Bond Strength

In establishing the linearity of the strain paths of the above two methods, the very minimum number of samples necessary to achieve this will be three which have to be consolidated at different pressures.

In the Stress Dilatancy Method, very precise volume change and vertical deformation measurements are required for the calculation of the dilatancy factor, λ, while no volume change measurements are required in the IDS test. This means that the IDS test can be run on conventional research equipment such as the 'Geonor" triaxial apparatus while high precision volume change equipment had to be specially designed to permit using the Strees Dilatancy Method.

After deciding upon the type of IDS test to perform, whether it be constant-σ_1', constant-p' or constant-volume, the test itself requires continuous manual control to keep the sample at the selected stress or volume condition during the entire shearing stage. Constant-σ_3' tests in the triaxial apparatus do not require such continuous control. On the other hand, if drained tests are used to determine stress dilatancy parameters, then there is no manual control necessary during the test except to take readings at specified intervals.

Without the dilatancy factor to take care of, the compu-

Stress Dilatancy Method.

The accuracy of the two methods can be ascertained from Table V-7(p.85) which lists the confidence intervals for the two parameters. The smaller confidence intervals for c_f establish this method as more precise although for the sample sizes used, one cannot detect any difference between the two parameters at a 5% significance level.

In short, each method has some advantage over the other. For the IDS test, testing requires greater attention but the investigator may use simpler equipment and the computation is less involved. For the Stress Dilatancy Method using drained tests, testing will require less attention but needs more complex equipment and calculation.

Conclusions

1) Employing the IDS curve-hopping technique with precise volume change measurements and vertical deformation readings, one can obtain IDS and stress dilatancy parameters from the same data.

2) For the three materials investigated, the I_ε component vs $\bar{\sigma}'_t$ relationship is linear at each strain, i.e. a 'constant structure envelope' can be computed at each strain for each test.

3) Shear stress τ_t^* vs average normal effective stress $\bar{\sigma}'^*_t$ corrected for dilatancy also produces linear strain paths.

4) The theoretical relationships between the parameters obtained from Schmertmann's IDS technique and those from Rowe's Stress Dilatancy Theory have been derived for both cohesionless and cohesive materials, using the linear

strain path concepts proven experimentally.

5) At most of the strains investigated, the corrected τ_t^* and $\bar{\sigma}_t'^*$ values give higher, though often only slightly higher, correlation coefficients than the corresponding I_ε vs $\bar{\sigma}_t'$ relationships. This results in smaller variance and greater significance in hypothesis testing for the former than the latter for the same number of samples tested.

6) The IDS method of testing requires constant attention during shear but computations are less involved and equipment simpler because no volume change measurements are required. Rowe's method requires very precise measurements of volume change and vertical deformation for the calculation of the dilatancy factor which leads to more complex computation.

7) Both the IDS Method and the Stress Dilatancy Theory can be used to determine the 'bond strength' of a soil as a function of strain although the difference in the two values lies in the effect of dilatancy. No difference was detected using statistical inference technique for the sample sizes used.

8) I_ε^* vs $\bar{\sigma}_t^{*\prime}$ relationships have too much scatter and it is therefore not recommended to correct I_o for dilatancy effects, giving I_o^*. If an investigator goes to the trouble of making sufficiently precise vertical and volumetric strain measurements to permit a dilatancy correction, then he should use Rowe's Stress Dilatancy Method to determine c_f.

9) For cohesionless materials, Coulomb's ϕ, Schmertmann's ϕ_ε and α_s, Rowe's ϕ_α (calculated from α_R) and ϕ_f are

presented on a Mohr diagram.

10) The application of small sample procedures in statistics provides a rational means of drawing conclusions from the data obtained during this work.

Suggestions for Future Research

The following topics are suggested for further research into the shear strength components of cohesive and cohesionless soils:

1) The determination of bond strength should be extended to include undisturbed soils using either the IDS or the Stress Dilatancy Method as only artificially prepared samples are used in this work.

2) The effect of test types, e.g. triaxial extension tests, direct shear tests and plane strain tests on the IDS components and stress dilatancy components should be investigated for both remolded and undisturbed soils.

3) By judicious choice of parameters (e.g. Roscoe et al. 1958; Ladanyi et al., 1965), the strength-deformation characteristics of saturated clays and sands may be predicted with the application of multiple curvilinear or joint regression analysis to the experimental data.

APPENDIX A
PHYSICAL PROPERTIES OF KAOLINITE (EDGAR,FLORIDA) GLASS BEADS AND GLASS BEADS WITH HYDROCAL

The physical properties of the three materials are given below:

Kaolinite (Edgar)

Specific Gravit, G_s	= 2.609
Liquid Limit	= 59.4%
Plastic Limit	= 29.6%
Plasticity Index, P.I.	= 29.8%
Less than .002 mm	= 71.0%
Activity, $\frac{\text{P.I.}}{\%<.002\text{mm}}$	= 0.42

Glass Beads

Specific Gravity, G_s	= 2.43
Shape of Particles	= spherical
Range of Particle Sizes	= between .074mm and .105 mm
Minimum Void Ratio (estimated)	= 0.48
Maximum Void Ratio	= 0.79

Glass Beads with Hydrocal

Specific Gravity, G_s	= 2.50

Table A-1 Water Contents, Degrees of Saturation and Void Ratios of Drained Tests and Constant-σ_i' IDS Tests on Kaolinite

Test Type	Test No.	σ_c' kg/cm^2	σ_h kg/cm^2	Before Test			After Consolidation			After Test		
				w_i	s_i	e_f	w_c	s_c	e_c	w_f	s_f	e_f
Drained	2-3-1D	6.0	2.0	38.2	100.6	.991	31.4	100.7	.812	33.6	99.1	.800
"	2-5-3D	6.0	1.0	37.8	100.3	.984	34.0	100.3	.884	34.6	100.6	.885
"	2-4-2D	6.0	0.5	38.6	100.3	1.004	34.8	100.3	.905	35.8	100.0	.916
Constant-σ_i'	2-9-OC3	6.0	2.0	38.2	99.9	.999	32.3	99.8	.845	35.5	101.2	.893
"	2-10-OC4	6.0	1.0	38.3	100.2	.997	32.9	100.2	.856	36.6	100.3	.919
"	2-11-OC5	6.0	0.5	38.2	100.5	.992	33.6	100.6	.872	37.8	101.5	.945
Constant-σ_i'	2-13-NC1	1.0	1.0	38.6	100.1	1.006	37.2	100.1	.969	38.1	100.5	.990
"	2-12-NC2	2.0	2.0	37.9	100.0	.989	34.3	100.0	.893	36.0	103.9	.904
"	2-14-NC4	4.0	4.0	38.1	100.4	.992	32.7	100.4	.849	34.3	99.4	.845
"	2-17-NC3	3.0	3.0	37.9	99.4	.995	34.0	99.3	.894	34.9	100.5	.906
"	3-16-NC1*	1.0	1.0	36.0	99.4	.944	34.3	99.4	.901	36.5	103.7	.884
"	3-15-NC1	1.0	1.0	36.0	99.2	.947	34.5	99.2	.909	36.6	101.5	.941
"	3-21-NC1	1.0	1.0	34.8	99.1	.917	33.7	99.0	.889	36.0	101.3	.928
"	3-23-NC2	2.0	2.0	36.6	100.0	.955	34.1	100.0	.888	35.2	101.4	.896
"	3-18-NC2	2.0	2.0	35.7	99.6	.936	32.8	99.6	.861	34.9	101.8	.872
"	3-17-NC2*	2.0	2.0	35.7	99.0	.941	34.4	99.0	.908	34.7	100.7	.906
"	3-24-NC4	4.0	4.0	34.7	99.1	.915	31.6	99.0	.832	32.9	98.9	.829
"	3-20-NC4	4.0	4.0	34.3	99.9	.924	30.9	99.5	.834	33.0	99.3	.832
"	3-19-NC4*	4.0	4.0	35.6	99.4	.934	32.5	99.3	.854	32.8	100.7	.850

* without filter strips

Table A-2 Water Contents, Degrees of Saturation and Void Ratios of Constant-p' and Constant-Volume IDS Tests on Kaolinite

Test Type	Test NO.	σ'_c kg/cm^2	σ_h kg/cm^2	Before Test			After Consolidation			After Test		
				w_i	s_i	e_i	w_c	s_c	e_c	w_f	s_f	e_f
Constant-p'	3-30-OC6	6.0	2.0	35.2	100.2	.918	32.1	100.2	.835	33.3	101.5	.857
"	3-31-OC7	6.0	1.0	34.9	99.4	.918	32.6	99.3	.856	34.3	101.6	.880
"	3-32-OC8	6.0	0.5	33.9	98.6	.898	32.4	98.6	.858	35.1	99.2	.896
Constant-p'	3-25-NC1	1.0	1.0	34.8	98.9	.918	33.4	98.8	.883	35.4	101.4	.899
"	3-26-NC2	2.0	2.0	33.8	97.8	.902	30.8	97.6	.823	33.9	99.3	.831
"	3-27-NC4	4.0	4.0	35.1	98.4	.931	31.7	98.3	.843	33.2	99.0	.845
"	3-28-NC2	2.0	2.0	35.0	98.9	.924	32.7	98.8	.864	34.5	99.4	.866
"	3-29-NC4	4.0	4.0	34.1	98.2	.907	30.5	98.0	.812	32.7	99.3	.812
"	3-34-NC4	4.0	4.0	34.9	99.2	.917	29.9	99.0	.788	32.9	99.0	.788
Constant-Volume	2-46-OC9	6.0	2.0	37.9	100.1	.987	32.1	100.1	.836	34.2	100.7	.841
"	2-47-OC10	6.0	1.0	37.4	99.7	.979	32.1	99.7	.841	34.3	99.8	.841
"	3-36-OC11	6.0	0.5	31.7	98.2	.842	30.9	98.1	.821	33.7	100.3	.821
Constant-Volume	2-48-NC2,	2.0	2.0	37.4	101.3	.964	34.5	101.4	.889	35.5	100.5	.894
"	2-49-NC3	3.0	3.0	37.8	99.7	.991	33.2	99.7	.869	34.4	99.2	.869
"	2-50-NC1	1.0	1.0	37.6	98.6	.994	34.9	98.5	.924	36.3	100.7	.929

Table A-3 Water Contents and Void Ratios of Glass Beads

Test Type	Test No.	σ_h kg/cm^2	e_i	w_i	e_c	e_f
Drained	GB-4D	4.0	.558	23.2	.544	.584
"	GB-1D	1.0	.555	23.0	.547	.587
"	GB-2D	2.0	.557	23.1	.534	.581
Constant-σ_3'	GB-1A	1.0	.494	20.5	.473	.531
"	GB-1B	1.0	.484	20.1	.460	.532
"	GB-2B	2.0	.529	22.0	.493	.541
"	GB-2A	2.0	.508	21.1	.502	.563
"	GB-3B	4.0	.534	22.2	.517	.571
"	GB-3A	4.0	.503	20.9	.479	.539

Table A-4 Water Contents and Void Ratios of Glass Beads with Hydrocal

Test Type	Test No.	σ_h kg/cm^2	e_c	w_c	e_f
Constant-σ_3'	GBH-1	1.0	.598	24.4	.611
"	GBH-2	1.0	.614	25.1	.624
"	GBH-3	1.0	.594	24.3	.603
"	GBH-4	2.0	.602	24.6	.612
"	GBH-5	2.0	.609	24.8	.616
"	GBH-6	2.0	.591	24.1	.600
"	GHB-7	3.0	.616	25.1	.624
"	GBH-8	3.0	.592	24.1	.598
"	GBH-9	3.0	.594	24.3	.600

APPENDIX B
CORRECTIONS FOR EXPERIMENTAL DATA

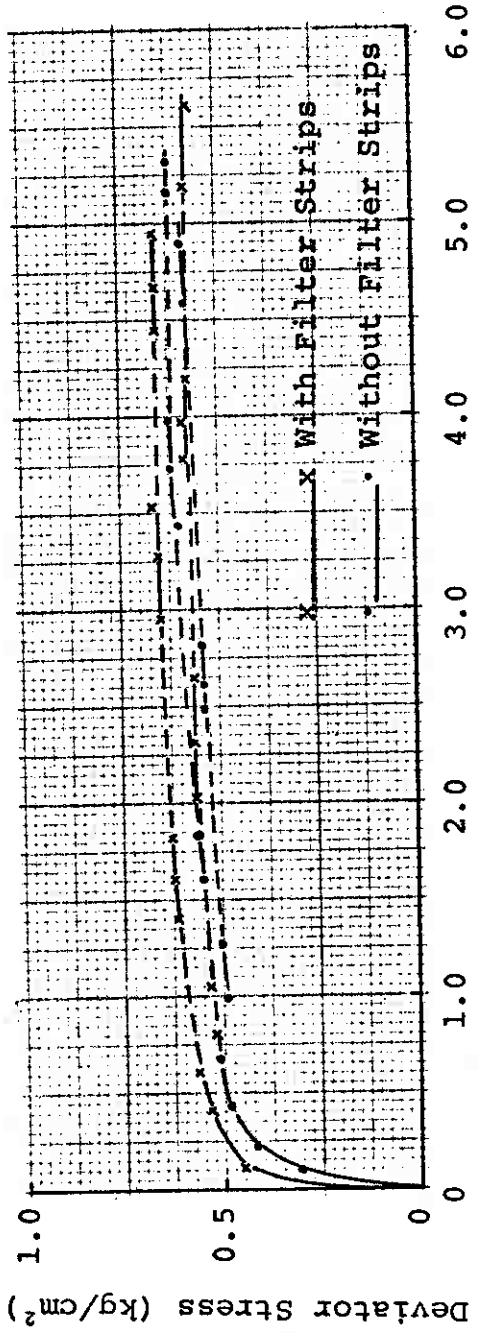

Figure B-1 Effect of Filter Strips, Test Nos. 3-21-NC1 and 3-16-NC1

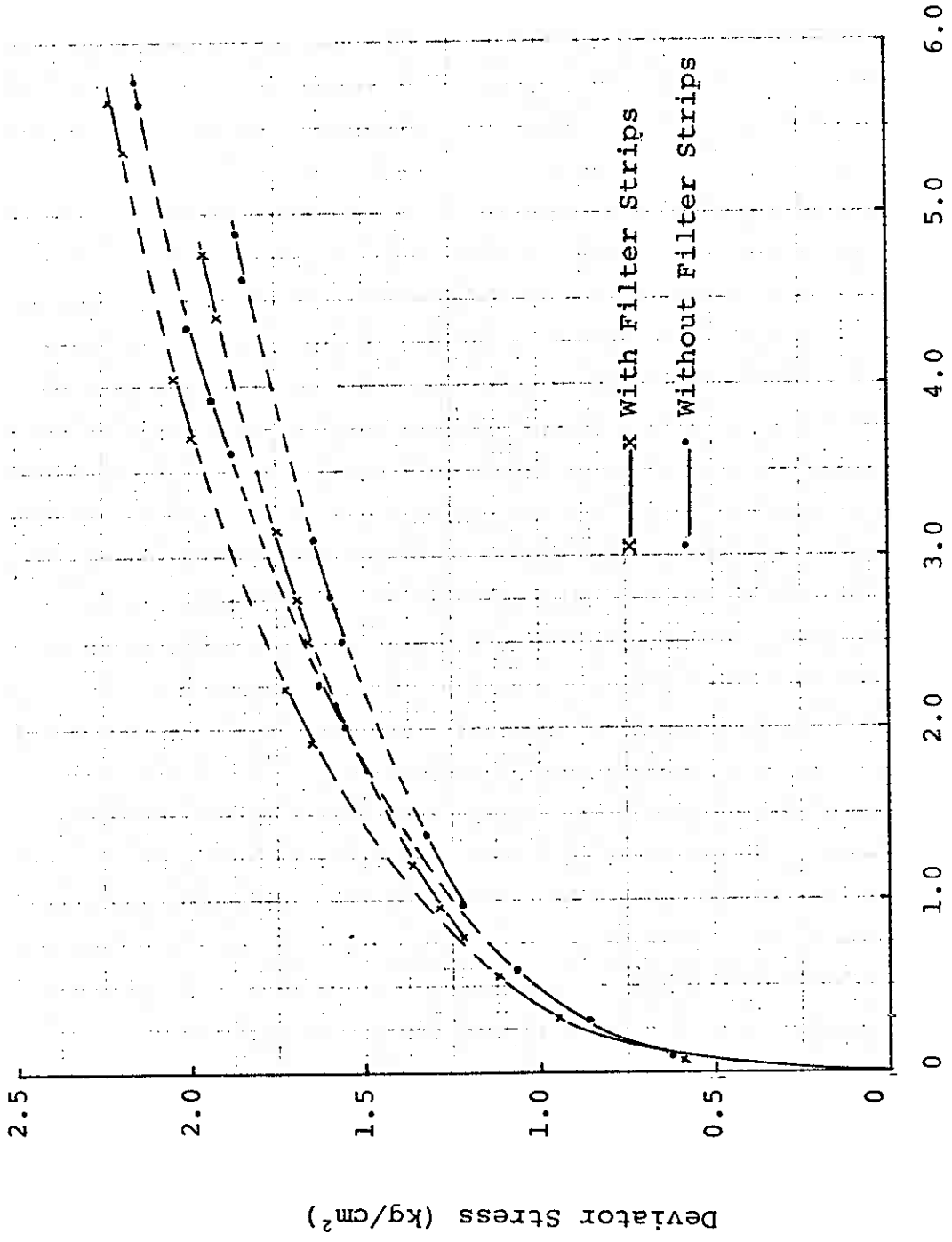

Figure B-2 Effect of Filter Strips, Test Nos. 3-20-NC4 and 3-19-NC4

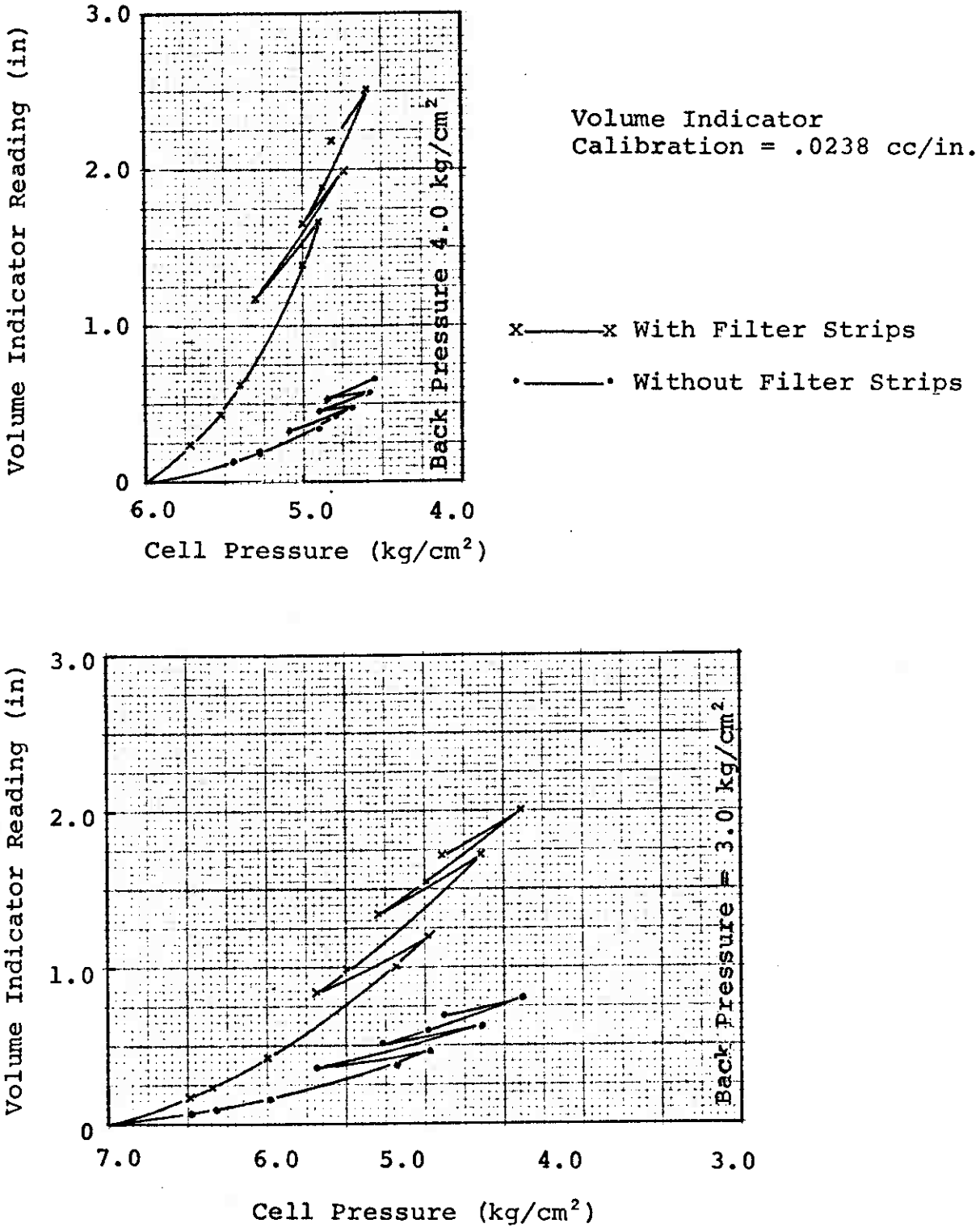

Figure B-3 Apparent Membrane Correction at Normally Consolidated Condition

Volume Indicator
Calibration = .0238 cc/in

Overconsolidation Pressure = 6.0 kg/cm^2

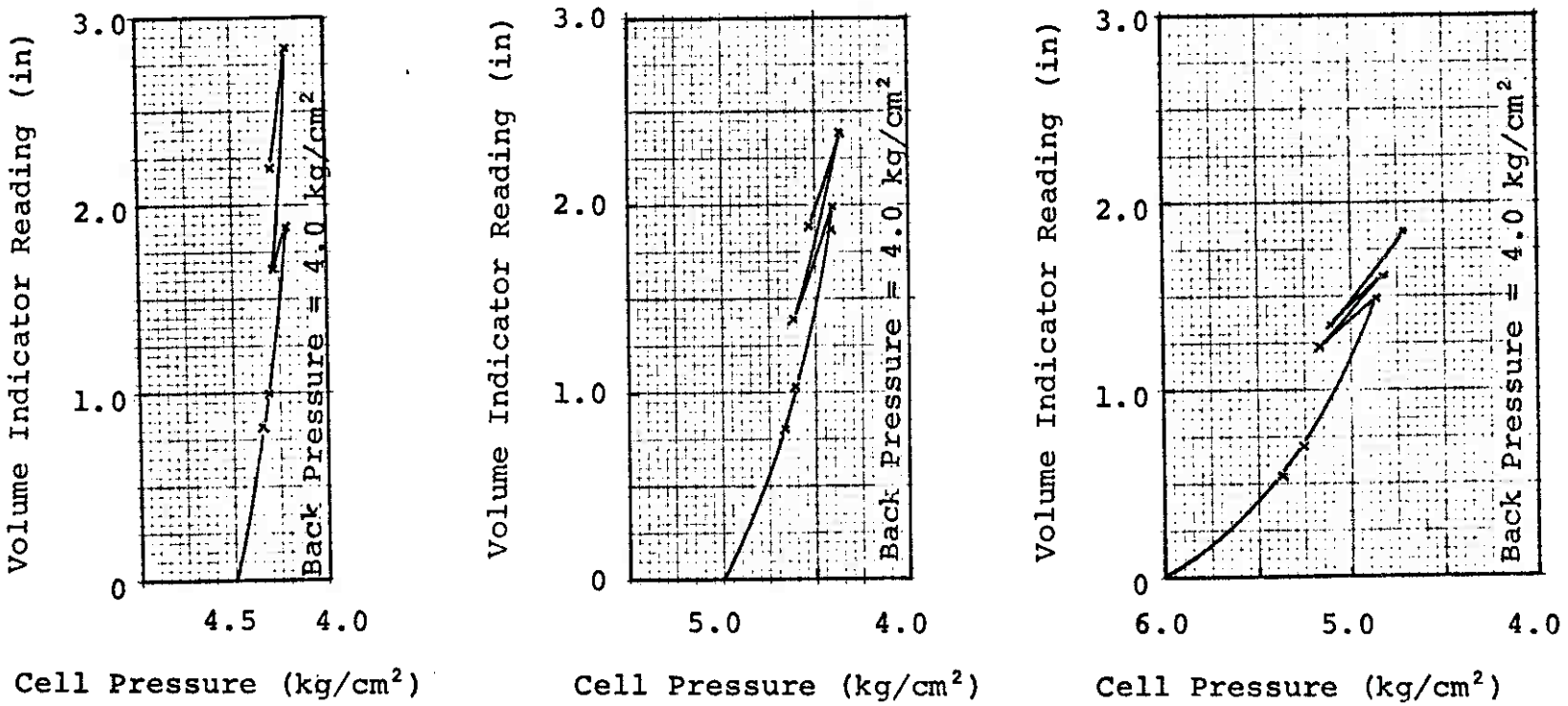

Figure B-4 Apparent Membrane Correction at Overconsolidated Condition

APPENDIX C
ANALYSIS OF EXPERIMENTAL DATA

Stress and Strains and Component Separation

Kaolinite

Glass Beads

Glass Beads with Hydrocal

Legend

PT. NO. = Point number
VOL STRAIN = ε_v
VERT STRAIN = ε_1
DEV STRESS = $(\sigma_1 - \sigma_3)$ (kg/cm^2)
SIGMA 3 = σ_3' (kg/cm^2)
SIGMA 1 = σ_1' (kg/cm^2)
MEAN STRESS = $\frac{\sigma_1' + 2\sigma_3'}{3}$ (kg/cm^2)
STRAIN = ε_1 (%)
TAN ϕ = tan ϕ_ε
I = I_ε (kg/cm^2)
SIG = $\bar{\sigma}_t'$ (kg/cm^2)
D = D_ε (kg/cm^2)
TAU = τ_t (kg/cm^2)
TAN ϕ* = tan ϕ_ε^*
I* = I_ε^* (kg/cm^2)
SIG* = $\bar{\sigma}_t'^*$ (kg/cm^2)
TAU* = τ_t^* (kg/cm^2)

Kaolinite

Drained Test Series on O.C. Kaolinite

TEST NO. 2-3-1D

PT NO.	VOL STRAIN	VERT STRAIN	DEV STRESS	SIGMA 3	SIGMA 1	SIG 1/SIG 3	MEAN STRESS
1	-.00018	.00123	.526	2.000	2.526	1.263	2.175
2	-.00030	.00245	.823	2.000	2.823	1.411	2.274
3	-.00042	.00487	1.085	2.000	3.085	1.542	2.361
4	-.00061	.00756	1.278	2.000	3.278	1.639	2.426
5	-.00114	.01243	1.503	2.000	3.503	1.751	2.501
6	-.00147	.01525	1.607	2.000	3.607	1.803	2.535
7	-.00212	.02001	1.746	2.000	3.746	1.873	2.582
8	-.00322	.02754	1.964	2.000	3.965	1.982	2.655
9	-.00412	.03423	2.132	2.000	4.132	2.066	2.711
10	-.00476	.03917	2.244	2.000	4.245	2.122	2.748
11	-.00513	.04234	2.305	2.000	4.305	2.152	2.768
12	-.00582	.04883	2.438	2.000	4.439	2.219	2.813
13	-.00643	.05591	2.554	2.000	4.555	2.277	2.852
14	-.00685	.06157	2.646	2.000	4.646	2.322	2.882
	ϵ_v	ϵ_a (dec)	$\sigma_1 - \sigma_3$	σ_3'	σ_1'	σ_1'/σ_3'	$\frac{\sigma_1' + 2\sigma_3'}{3}$

TEST NO. 2-5-3D

PT NO.	VOL STRAIN	VERT STRAIN	DEV STRESS	SIGMA 3	SIGMA 1	SIG 1/SIG 3	MEAN STRESS
1	-.00034	.00247	.534	1.000	1.534	1.534	1.178
2	-.00027	.00753	.831	1.000	1.831	1.831	1.277
3	-.00017	.01505	1.049	1.000	2.049	2.049	1.349
4	-.00012	.02162	1.173	1.000	2.173	2.173	1.391
5	-.00008	.02769	1.263	1.000	2.263	2.263	1.421
6	-.00003	.03402	1.350	1.000	2.350	2.350	1.450
7	.00034	.03207	.273	1.000	1.273	1.273	1.091
8	.00025	.02915	-.072	1.000	.927	.927	.975
9	-.00035	.03014	.595	1.000	1.595	1.595	1.198
10	-.00081	.03403	1.250	1.000	2.250	2.250	1.416
11	-.00080	.03536	1.322	1.000	2.322	2.322	1.440
12	-.00059	.04034	1.428	1.000	2.428	2.428	1.476
13	-.00024	.04793	1.499	1.000	2.499	2.498	1.499

TEST NO. 2-4-2D

PT NO.	VOL STRAIN	VERT STRAIN	DEV STRESS	SIGMA 3	SIGMA 1	SIG 1/SIG 3	MEAN STRESS
1	.00000	.00025	-.063	.499	.436	.873	.478
2	-.00025	.00378	.383	.500	.883	1.766	.627
3	-.00016	.00687	.487	.500	.987	1.973	.662
4	.00036	.01209	.614	.499	1.114	2.229	.704
5	.00091	.01734	.698	.499	1.198	2.396	.732
6	.00142	.02170	.752	.499	1.252	2.505	.750
7	.00188	.02304	.369	.499	.869	1.738	.623
8	.00230	.02052	.009	.499	.509	1.018	.503
9	.00241	.01872	.052	.499	.552	1.104	.517
10	.00189	.02097	.487	.499	.987	1.974	.662
11	.00176	.02375	.734	.499	1.234	2.469	.744
12	.00240	.03016	.830	.499	1.330	2.661	.776
13	.00326	.03580	.860	.499	1.360	2.722	.786
14	.00446	.04360	.898	.499	1.397	2.796	.799
15	.00560	.05132	.926	.499	1.426	2.854	.808

Constant-σ_1' Test Series on O.C. Kaolinite

TEST NO. 2-9-0C3

PT NO.	VOL STRAIN	VERT STRAIN	DEV STRESS	SIGMA 3	SIGMA 1	SIG 1/SIG 3	MEAN STRESS
1	.00373	.00122	.598	1.239	1.838	1.483	1.439
2	.00552	.00239	.716	1.139	1.856	1.629	1.378
3	.00759	.00458	.835	1.014	1.850	1.823	1.293
4	.00884	.00771	.954	1.009	1.964	1.945	1.327
5	.01012	.01056	1.009	.934	1.943	2.080	1.270
6	.01129	.01348	1.039	.905	1.945	2.148	1.251
7	.01530	.01582	.922	.619	1.541	2.490	.926
8	.01799	.02103	.943	.598	1.542	2.574	.913
9	.01944	.02427	.953	.578	1.532	2.646	.896
10	.01634	.02715	1.103	.819	1.922	2.346	1.186
11	.01666	.03070	1.153	.799	1.952	2.443	1.183
12	.01752	.03584	1.173	.754	1.927	2.555	1.145
13	.02127	.03767	.993	.523	1.517	2.897	.855
14	.02327	.04196	1.003	.508	1.512	2.972	.843
15	.02426	.04422	.997	.508	1.505	2.960	.841
16	.02078	.04844	1.170	.778	1.949	2.502	1.168
17	.02122	.05280	1.202	.718	1.921	2.672	1.119
18	.02182	.05676	1.210	.698	1.909	2.732	1.102
19	.02615	.06029	1.028	.488	1.517	3.104	.831
20	.02648	.06132	1.026	.488	1.515	3.101	.830

TEST NO. 2-10-OC4

PT NO.	VOL STRAIN	VERT STRAIN	DEV STRESS	SIGMA 3	SIGMA 1	SIG 1/SIG 3	MEAN STRESS
1	-.00009	.00006	.316	1.000	1.316	1.316	1.105
2	.00219	.00109	.429	.534	.963	1.802	.677
3	.00508	.00249	.478	.459	.937	2.039	.619
4	.00914	.00505	.522	.409	.932	2.276	.583
5	.01312	.00660	.480	.279	.759	2.721	.439
6	.01819	.01070	.498	.238	.737	3.084	.404
7	.01774	.01302	.579	.348	.928	2.661	.542
8	.01904	.01659	.605	.318	.924	2.900	.520
9	.01977	.01882	.616	.318	.935	2.934	.524
10	.02332	.02050	.533	.188	.721	3.827	.366
11	.02695	.02558	.527	.188	.716	3.800	.364
12	.02832	.02851	.533	.178	.711	3.992	.356
13	.02650	.03165	.615	.433	1.048	2.419	.638
14	.02720	.03693	.639	.288	.927	3.217	.501
15	.02802	.04137	.648	.288	.936	3.247	.504
16	.03168	.04385	.525	.178	.704	3.951	.353
17	.03315	.04804	.528	.188	.716	3.811	.364
18	.03422	.05227	.517	.188	.705	3.752	.360
19	.03337	.05772	.589	.328	.917	2.796	.524
20	.03334	.06021	.600	.328	.928	2.828	.528

TEST NO. 2-11-OC5

PT NO.	VOL STRAIN	VERT STRAIN	DEV STRESS	SIGMA 3	SIGMA 1	SIG 1/SIG 3	MEAN STRESS
1	.00288	.00111	.247	.189	.437	2.305	.272
2	.00613	.00220	.287	.159	.447	2.801	.255
3	.01002	.00404	.305	.119	.425	3.559	.221
4	.01688	.00666	.282	.048	.331	6.758	.143
5	.02856	.01283	.262	.058	.320	5.493	.145
6	.02837	.01633	.312	.118	.431	3.642	.222
7	.02960	.01978	.326	.088	.414	4.698	.197
8	.03078	.02303	.327	.088	.415	4.708	.197
9	.03398	.02473	.267	.037	.305	8.044	.127
10	.03567	.02652	.246	.057	.304	5.257	.140
11	.03637	.02990	.251	.067	.319	4.708	.151
12	.03683	.03220	.260	.067	.328	4.844	.154
13	.03828	.03584	.246	.067	.313	4.631	.140
14	.03880	.03993	.246	.067	.314	4.642	.149
15	.03802	.04279	.274	.137	.412	2.994	.229
16	.03838	.04725	.274	.117	.392	3.329	.209
17	.03968	.05122	.229	.067	.296	4.383	.144
18	.03972	.05143	.233	.067	.301	4.455	.145

TEST NO. 2-9-0C3

STRAIN	TAN ϕ	I	SIG	D	TAU	TAN ϕ*	I*	SIG*	TAU*
1	.17383	.252	1.192	.207	.460	.16667	.010	.947	.168
2	.24697	.220	1.106	.273	.494	.24382	.043	.932	.270
3	.26843	.226	1.068	.286	.513	.23653	.116	.943	.339
4	.28674	.226	1.030	.295	.521	.17227	.223	.965	.390
5	.30446	.220	1.004	.305	.526	.22325	.203	.947	.415

TEST NO. 2-10-0C4

STRAIN	TAN ϕ	I	SIG	D	TAU	TAN ϕ*	I*	SIG*	TAU*
1	.20846	.151	.517	.107	.259	-.01347	.080	.382	.075
2	.27066	.148	.463	.125	.274	.10806	.107	.387	.149
3	.33531	.128	.436	.146	.274	.18024	.110	.390	.180
4	.33334	.129	.438	.146	.275	.19303	.120	.403	.198
5	.27806	.148	.461	.128	.277	.18447	.135	.430	.215

TEST NO. 2-11-0C5

STRAIN	TAN ϕ	I	SIG	D	TAU	TAN ϕ*	I*	SIG*	TAU*
1	.33562	.078	.176	.059	.137	.01325	.035	.111	.033
2	.49613	.051	.157	.078	.129	.32203	.043	.142	.089
3	.42859	.058	.165	.070	.129	.31172	.052	.154	.100

Constant-σ_1' Test Series on N.C. Kaolinite

TEST NO. 2-13-NC1

PT NO.	VOL STRAIN	VERT STRAIN	DEV STRESS	SIGMA 3	SIGMA 1	SIG 1/SIG 3	MEAN STRESS
1	.00050	.00046	.248	.714	.963	1.347	.797
2	.00176	.00229	.365	.594	.959	1.613	.716
3	.00223	.00359	.430	.539	.970	1.797	.683
4	.00270	.00591	.454	.469	.923	1.966	.621
5	.00480	.00839	.442	.312	.755	2.415	.460
6	.00555	.01082	.452	.297	.750	2.520	.448
7	.00615	.01328	.451	.289	.741	2.559	.440
8	.00407	.01865	.532	.379	.912	2.401	.557
9	.00384	.02130	.545	.359	.905	2.516	.541
10	.00386	.02525	.567	.369	.937	2.535	.558
11	.00716	.03002	.499	.209	.709	3.383	.376
12	.00882	.03503	.494	.213	.708	3.317	.378
13	.00960	.03876	.502	.213	.715	3.352	.380
14	.00675	.04340	.577	.369	.947	2.563	.562
15	.00669	.04748	.591	.318	.910	2.857	.515
16	.00674	.05286	.600	.319	.919	2.877	.519
17	.01063	.05778	.516	.209	.725	3.463	.381
18	.01106	.06013	.526	.211	.737	3.489	.386

TEST NO. 2-12-NC2

PT NO.	VOL STRAIN	VERT STRAIN	DEV STRESS	SIGMA 3	SIGMA 1	SIG 1/SIG 3	MEAN STRESS
1	.00087	.00069	.421	1.589	2.011	1.265	1.730
2	.00141	.00252	.530	1.499	2.030	1.353	1.676
3	.00150	.00370	.582	1.459	2.042	1.398	1.654
4	.00475	.00699	.637	.979	1.617	1.650	1.192
5	.00489	.00876	.665	.949	1.615	1.701	1.171
6	.00488	.01055	.692	.939	1.631	1.736	1.170
7	.00116	.01531	.828	1.189	2.018	1.696	1.466
8	.00071	.01778	.870	1.149	2.020	1.757	1.440
9	.00039	.02030	.912	1.109	2.022	1.821	1.414
10	.00420	.02658	.869	.719	1.589	2.207	1.009
11	.00484	.03308	.891	.709	1.601	2.256	1.007
12	.00510	.03606	.902	.699	1.602	2.289	1.000
13	.00065	.04339	1.087	.920	2.007	2.182	1.282
14	.00061	.04796	1.116	.880	1.996	2.268	1.252
15	.00059	.05185	1.138	.870	2.008	2.308	1.249
16	.00518	.05613	.966	.599	1.566	2.611	.921
17	.00548	.05979	.992	.599	1.592	2.654	.930
18	.00573	.06207	.997	.599	1.596	2.662	.932

TEST NO. 2-14-NC4

PT NO.	VOL STRAIN	VERT STRAIN	DEV STRESS	SIGMA 3	SIGMA 1	SIG 1/SIG 3	MEAN STRESS
1	.00026	.00073	.777	3.359	4.137	1.231	3.619
2	.00046	.00348	1.056	3.079	4.136	1.342	3.432
3	.00319	.00599	1.178	2.159	3.338	1.545	2.552
4	.00379	.00981	1.308	2.059	3.367	1.635	2.495
5	.00384	.01320	1.395	1.949	3.345	1.715	2.414
6	.00149	.01520	1.458	2.709	4.168	1.538	3.196
7	-.00015	.01902	1.622	2.520	4.142	1.643	3.060
8	-.00106	.02236	1.735	2.432	4.167	1.713	3.010
9	.00178	.02588	1.660	1.674	3.335	1.991	2.228
10	.00217	.03022	1.711	1.639	3.351	2.043	2.210
11	.00231	.03329	1.748	1.579	3.328	2.106	2.162
12	-.00146	.03724	1.969	2.180	4.149	1.903	2.836
13	-.00243	.04160	2.085	2.050	4.135	2.017	2.745
14	-.00309	.04660	2.181	2.023	4.204	2.078	2.750
15	-.00036	.04841	1.962	1.340	3.302	2.464	1.994
16	.00138	.05352	1.954	1.355	3.309	2.442	2.006
17	.00202	.05705	1.960	1.327	3.288	2.476	1.981
18	-.00110	.05940	2.139	2.090	4.229	2.023	2.803
19	-.00241	.06150	2.282	1.790	4.072	2.274	2.550
20	-.00242	.06365	2.293	1.770	4.064	2.295	2.534

TEST NO. 2-17-NC3

PT NO.	VOL STRAIN	VERT STRAIN	DEV STRESS	SIGMA 3	SIGMA 1	SIG 1/SIG 3	MEAN STRESS
1	.00046	.00118	.637	2.499	3.137	1.255	2.712
2	.00109	.00305	.761	2.234	2.996	1.340	2.488
3	.00093	.00550	.880	2.234	3.115	1.393	2.528
4	.00387	.00897	.958	1.539	2.498	1.622	1.859
5	.00421	.01049	.993	1.514	2.508	1.656	1.846
6	.00482	.01509	1.122	1.359	2.482	1.825	1.733
7	.00241	.02001	1.279	1.759	3.039	1.727	2.186
8	.00204	.02191	1.323	1.749	3.073	1.756	2.191
9	.00158	.02542	1.388	1.659	3.047	1.836	2.122
10	.00278	.02666	1.327	1.139	2.467	2.164	1.582
11	.00405	.02964	1.323	1.119	2.442	2.181	1.560
12	.00499	.03609	1.362	1.079	2.442	2.261	1.533
13	.00240	.04001	1.509	1.629	3.139	1.926	2.133
14	.00159	.04303	1.578	1.514	3.093	2.041	2.041
15	.00112	.04667	1.625	1.440	3.065	2.128	1.981
16	.00432	.05007	1.463	.919	2.383	2.591	1.407
17	.00533	.05333	1.456	.919	2.376	2.583	1.405

TEST NO. 3-16-NC1

PT NO.	VOL STRAIN	VERT STRAIN	DEV STRESS	SIGMA 3	SIGMA 1	SIG 1/SIG 3	MEAN STRESS
1	.00004	.00079	.300	.729	1.030	1.411	.830
2	.00056	.00191	.420	.569	.990	1.738	.710
3	.00124	.00416	.480	.499	.980	1.961	.660
4	.00174	.00636	.502	.469	.971	2.068	.637
5	.00395	.00967	.492	.299	.792	2.642	.463
6	.00466	.01230	.497	.319	.817	2.555	.485
7	.00375	.01565	.537	.489	1.027	2.097	.668
8	.00357	.01783	.551	.469	1.021	2.174	.653
9	.00358	.01993	.561	.439	1.000	2.275	.626
10	.00548	.02433	.539	.269	.809	3.000	.449
11	.00595	.02555	.539	.259	.799	3.077	.439
12	.00653	.02768	.536	.266	.803	3.013	.445
13	.00544	.03351	.591	.419	1.011	2.409	.616
14	.00540	.03668	.608	.409	1.018	2.484	.612
15	.00539	.03918	.614	.399	1.014	2.537	.604
16	.00786	.04512	.579	.229	.808	3.522	.422
17	.00881	.04820	.577	.234	.811	3.460	.426
18	.00858	.05061	.598	.369	.968	2.620	.569
19	.00854	.05231	.608	.369	.977	2.645	.572

TEST NO. 3-15-NC1

PT NO.	VOL STRAIN	VERT STRAIN	DEV STRESS	SIGMA 3	SIGMA 1	SIG 1/SIG 3	MEAN STRESS
1	.00013	.00097	.374	.569	.944	1.657	.694
2	.00232	.00200	.383	.499	.883	1.768	.627
3	.00348	.00321	.410	.479	.890	1.856	.616
4	.00433	.00594	.464	.479	.944	1.968	.634
5	.00782	.00855	.428	.319	.747	2.340	.462
6	.00942	.01156	.437	.309	.747	2.414	.455
7	.00811	.01778	.514	.399	.913	2.287	.570
8	.00813	.02002	.538	.394	.933	2.365	.574
9	.01244	.02443	.465	.259	.724	2.793	.414
10	.01387	.02709	.456	.259	.716	2.763	.411
11	.01459	.02910	.455	.254	.709	2.793	.406
12	.01220	.03504	.538	.369	.908	2.458	.548
13	.01270	.03945	.547	.349	.896	2.568	.531
14	.01737	.04564	.461	.249	.710	2.852	.402
15	.01803	.04764	.458	.248	.707	2.843	.401
16	.01532	.05110	.543	.364	.907	2.491	.545
17	.01534	.05286	.546	.349	.895	2.565	.531

TEST NO. 3-21-NC1

PT NO.	VOL STRAIN	VERT STRAIN	DEV STRESS	SIGMA 3	SIGMA 1	SIG 1/SIG 3	MEAN STRESS
1	.00158	.00084	.389	.559	.948	1.694	.689
2	.00442	.00386	.468	.479	.947	1.975	.635
3	.00518	.00575	.493	.449	.942	2.096	.614
4	.00781	.00766	.452	.289	.741	2.562	.440
5	.00822	.00811	.452	.289	.742	2.563	.440
6	.00966	.01016	.460	.279	.739	2.647	.432
7	.00742	.01361	.546	.379	.926	2.440	.561
8	.00818	.01574	.548	.374	.923	2.465	.557
9	.00882	.01787	.550	.359	.910	2.531	.543
10	.01171	.01996	.483	.207	.690	3.330	.368
11	.01290	.02264	.492	.229	.721	3.148	.393
12	.01404	.02594	.496	.204	.700	3.430	.369
13	.01157	.02910	.573	.359	.932	2.595	.550
14	.01201	.03198	.579	.319	.898	2.814	.512
15	.01244	.03461	.586	.322	.908	2.818	.517
16	.01547	.03706	.506	.194	.700	3.610	.362
17	.01606	.03908	.512	.200	.712	3.563	.371
18	.01694	.04127	.504	.189	.693	3.666	.357
19	.01513	.04367	.573	.389	.962	2.472	.580
20	.01523	.04578	.576	.294	.870	2.958	.486
21	.01572	.04854	.574	.289	.863	2.986	.480
22	.01788	.05098	.505	.179	.684	3.823	.347
23	.01932	.05517	.490	.190	.681	3.570	.354

TEST NO. 3-23-NC2

PT NO.	VOL STRAIN	VERT STRAIN	DEV STRESS	SIGMA 3	SIGMA 1	SIG 1/SIG 3	MEAN STRESS
1	.00031	.00056	.340	1.699	2.040	1.200	1.813
2	.00131	.00207	.525	1.479	2.005	1.355	1.655
3	.00167	.00458	.645	1.371	2.017	1.470	1.586
4	.00403	.00616	.637	.999	1.637	1.637	1.212
5	.00472	.00835	.696	.939	1.635	1.740	1.171
6	.00504	.01010	.719	.909	1.629	1.791	1.149
7	.00182	.01281	.798	1.304	2.103	1.611	1.570
8	.00183	.01590	.871	1.129	2.001	1.771	1.420
9	.00179	.01818	.901	1.084	1.985	1.830	1.385
10	.00488	.02162	.838	.754	1.593	2.111	1.034
11	.00520	.02390	.858	.739	1.597	2.160	1.025
12	.00558	.02638	.873	.709	1.583	2.230	1.000
13	.00168	.03263	1.038	.929	1.968	2.116	1.276
14	.00181	.03684	1.070	.909	1.980	2.176	1.266
15	.00199	.03961	1.078	.869	1.948	2.239	1.229
16	.00505	.04219	.958	.599	1.558	2.598	.919
17	.00581	.04483	.961	.599	1.561	2.603	.920
18	.00664	.04823	.966	.589	1.556	2.639	.911
19	.00336	.05219	1.111	.829	1.941	2.339	1.200
20	.00333	.05460	1.129	.799	1.929	2.412	1.176

TEST NO. 3-18-NC2

PT NO.	VOL STRAIN	VERT STRAIN	DEV STRESS	SIGMA 3	SIGMA 1	SIG 1/SIG 3	MEAN STRESS
1	.00188	.00185	.564	1.439	2.004	1.392	1.628
2	.00255	.00423	.692	1.274	1.967	1.543	1.505
3	.00561	.00681	.687	.889	1.576	1.772	1.118
4	.00597	.00850	.735	.839	1.575	1.875	1.084
5	.00656	.01047	.749	.829	1.578	1.903	1.079
6	.00368	.01340	.854	1.129	1.983	1.756	1.414
7	.00330	.01733	.923	1.106	2.030	1.834	1.414
8	.00331	.02016	.957	1.004	1.962	1.952	1.323
9	.00605	.02285	.880	.699	1.580	2.258	.993
10	.00664	.02583	.898	.669	1.567	2.341	.968
11	.00710	.02891	.916	.649	1.566	2.411	.955
12	.00425	.03199	1.021	.919	1.941	2.110	1.260
13	.00391	.03486	1.064	.894	1.959	2.190	1.249
14	.00390	.03859	1.092	.857	1.950	2.273	1.222
15	.00742	.04283	.968	.559	1.528	2.731	.882
16	.00829	.04602	.968	.549	1.518	2.762	.872
17	.00513	.04993	1.117	.839	1.957	2.330	1.212
18	.00522	.05346	1.138	.769	1.908	2.478	1.149

TEST NO. 3-17-NC2

PT NO.	VOL STRAIN	VERT STRAIN	DEV STRESS	SIGMA 3	SIGMA 1	SIG 1/SIG 3	MEAN STRESS
1	.00006	.00045	.369	1.739	2.109	1.212	1.863
2	.00068	.00263	.593	1.449	2.043	1.409	1.647
3	.00070	.00528	.681	1.364	2.046	1.499	1.592
4	.00255	.00832	.708	.939	1.648	1.753	1.175
5	.00281	.01016	.737	.939	1.677	1.784	1.185
6	.00048	.01340	.802	1.249	2.052	1.642	1.517
7	.00008	.01579	.843	1.215	2.058	1.693	1.496
8	-.00041	.01875	.888	1.160	2.048	1.765	1.456
9	.00168	.02255	.859	.789	1.649	2.087	1.076
10	.00195	.02507	.873	.769	1.643	2.134	1.061
11	.00220	.02780	.888	.749	1.638	2.184	1.046
12	-.00042	.03215	.984	1.060	2.044	1.928	1.388
13	-.00096	.03489	1.025	1.015	2.041	2.010	1.357
14	-.00133	.03774	1.051	.980	2.031	2.072	1.330
15	.00109	.04171	.977	.640	1.617	2.527	.965
16	.00167	.04484	.983	.629	1.613	2.561	.957
17	.00206	.04742	.987	.619	1.607	2.592	.949
18	-.00048	.05209	1.105	.920	2.025	2.201	1.288
19	-.00091	.05591	1.140	.852	1.992	2.338	1.232

TEST NO. 3-24-NC4

PT NO.	VOL STRAIN	VERT STRAIN	DEV STRESS	SIGMA 3	SIGMA 1	SIG 1/SIG 3	MEAN STRESS
1	.00035	.00157	.633	3.509	4.143	1.180	3.721
2	.00068	.00322	.848	3.249	4.098	1.261	3.532
3	.00064	.00538	1.007	3.109	4.117	1.324	3.445
4	.00359	.00922	1.165	2.139	3.305	1.544	2.528
5	.00392	.01252	1.269	2.019	3.289	1.628	2.443
6	-.00105	.01977	1.565	2.500	4.065	1.626	3.021
7	-.00117	.02294	1.651	2.430	4.081	1.679	2.980
8	.00204	.02842	1.597	1.672	3.270	1.954	2.205
9	.00232	.03217	1.644	1.624	3.269	2.012	2.173
10	-.00198	.04010	1.953	2.090	4.043	1.934	2.741
11	-.00220	.04273	2.004	2.010	4.014	1.997	2.678
12	.00122	.04791	1.825	1.404	3.230	2.299	2.013
13	.00174	.05037	1.835	1.389	3.225	2.320	2.001
14	-.00163	.05560	2.091	1.890	3.981	2.106	2.587
15	-.00191	.05700	2.127	1.905	4.032	2.116	2.614

TEST NO. 3-20-NC4

PT NO.	VOL STRAIN	VERT STRAIN	DEV STRESS	SIGMA 3	SIGMA 1	SIG 1/SIG 3	MEAN STRESS
1	.00011	.00036	.521	3.559	4.081	1.146	3.733
2	.00075	.00263	.879	3.224	4.104	1.272	3.518
3	.00077	.00497	1.046	3.009	4.056	1.347	3.358
4	.00278	.00710	1.141	2.129	3.271	1.536	2.510
5	.00314	.00877	1.210	2.019	3.230	1.599	2.423
6	.00339	.01135	1.287	1.991	3.278	1.646	2.420
7	-.00085	.01827	1.569	2.490	4.059	1.630	3.013
8	-.00090	.02125	1.650	2.370	4.020	1.696	2.920
9	.00145	.02404	1.580	1.654	3.235	1.954	2.181
10	.00190	.02653	1.614	1.609	3.223	2.002	2.147
11	.00214	.03034	1.664	1.541	3.206	2.079	2.096
12	-.00151	.03565	1.912	2.070	3.982	1.923	2.707
13	-.00166	.03885	1.961	2.010	3.971	1.975	2.663
14	.00070	.04265	1.840	1.350	3.190	2.363	1.963
15	.00121	.04632	1.874	1.279	3.154	2.464	1.904
16	-.00152	.05193	2.101	1.820	3.922	2.154	2.520
17	-.00160	.05471	2.136	1.800	3.936	2.186	2.512

TEST NO. 3-19-NC4

PT NO.	VOL STRAIN	VERT STRAIN	DEV STRESS	SIGMA 3	SIGMA 1	SIG 1/SIG 3	MEAN STRESS
1	.00009	.00057	.616	3.579	4.196	1.172	3.785
2	.00054	.00244	.864	3.339	4.204	1.258	3.628
3	.00048	.00535	1.060	3.074	4.135	1.344	3.428
4	.00267	.00910	1.211	2.174	3.386	1.556	2.578
5	.00298	.01314	1.322	2.039	3.362	1.648	2.480
6	-.00098	.01914	1.545	2.683	4.228	1.575	3.198
7	-.00117	.02148	1.620	2.510	4.130	1.645	3.050
8	.00102	.02413	1.556	1.739	3.296	1.894	2.258
9	.00160	.02676	1.590	1.719	3.310	1.924	2.249
10	.00185	.02992	1.627	1.674	3.302	1.971	2.217
11	-.00196	.03485	1.851	2.280	4.131	1.811	2.897
12	-.00220	.03769	1.917	2.150	4.067	1.891	2.789
13	-.00249	.04203	1.987	2.040	4.027	1.974	2.702
14	.00013	.04491	1.829	1.420	3.249	2.288	2.030
15	.00059	.04749	1.843	1.380	3.223	2.335	1.994
16	-.00241	.05489	2.112	1.890	4.002	2.117	2.594
17	-.00248	.05603	2.125	1.880	4.005	2.130	2.588

TEST NO. 2-13-NC1

STRAIN	TAN ϕ	I	SIG	D	TAU	TAN ϕ*	I*	SIG*	TAU*
1	.15542	.145	.563	.087	.233	.34755	.012	.495	.184
2	.22271	.134	.511	.113	.248	.21159	.110	.484	.213
3	.17891	.170	.498	.089	.259	.18704	.137	.468	.225
4	.23412	.149	.480	.112	.261	.24640	.118	.454	.230
5	.29053	.128	.465	.135	.264	.28209	.116	.452	.244

ϵ% $\tan\phi_\epsilon$ I_ϵ $\bar{\sigma}'_\epsilon$ D_ϵ τ_ϵ corr. for dilatancy

TEST NO. 2-12-NC2

STRAIN	TAN ϕ	I	SIG	D	TAU	TAN ϕ*	I*	SIG*	TAU*
1	.07292	.248	1.437	.104	.353	.22592	.046	1.397	.362
2	.13732	.238	1.325	.182	.420	.24125	.117	1.298	.430
3	.19175	.221	1.240	.237	.459	.20157	.207	1.234	.456
4	.23593	.206	1.184	.279	.485	.24564	.192	1.178	.482
5	.26843	.196	1.134	.304	.501	.27790	.184	1.128	.497

TEST NO. 2-14-NC4

STRAIN	TAN ϕ	I	SIG	D	TAU	TAN ϕ*	I*	SIG*	TAU*
1	.03297	.566	3.075	.101	.667	.10904	.402	3.093	.740
2	.07206	.594	2.905	.209	.803	.12500	.626	3.046	1.007
3	.12279	.561	2.750	.337	.899	.25279	.326	2.750	1.021
4	.16761	.528	2.594	.434	.963	.28100	.318	2.567	1.039
5	.19727	.520	2.489	.491	1.011	.26635	.394	2.464	1.050

TEST NO. 2-17-NC3

STRAIN	TAN ϕ	I	SIG	D	TAU	TAN ϕ*	I*	SIG*	TAU*
1	.04089	.415	2.245	.091	.507	.06367	.303	2.173	.442
2	.07587	.460	2.082	.158	.618	.09613	.413	2.064	.611
3	.11337	.464	1.970	.223	.688	.12272	.443	1.961	.684
4	.14078	.467	1.887	.265	.733	.17254	.411	1.868	.734
5	.19006	.421	1.808	.343	.765	.21989	.371	1.790	.765

TEST NO. 3-16-NC1

STRAIN	TAN ϕ	I	SIG	D	TAU	TAN ϕ*	I*	SIG*	TAU*
1	.10178	.191	.610	.062	.253	.16323	.080	.521	.165
2	.10133	.209	.601	.060	.270	.09760	.178	.569	.233
3	.12564	.204	.588	.073	.278	.18641	.147	.550	.250
4	.10874	.230	.580	.063	.293	.25152	.137	.527	.269
5	.07483	.250	.569	.042	.292	.19085	.168	.518	.267

TEST NO. 3-15-NC1

STRAIN	TAN ϕ	I	SIG	D	TAU	TAN ϕ*	I*	SIG*	TAU*
1	.17721	.127	.563	.099	.226	.15589	.038	.468	.111
2	.27156	.093	.520	.141	.234	.49365	-.054	.441	.163
3	.26144	.106	.508	.132	.238	.38849	.004	.444	.177
4	.24228	.120	.502	.121	.242	.33193	.042	.449	.191
5	.29259	.102	.483	.141	.243	.36219	.041	.441	.201

TEST NO. 3-21-NC1

STRAIN	TAN ϕ	I	SIG	D	TAU	TAN ϕ*	I*	SIG*	TAU*
1	.22088	.122	.533	.117	.240	.20932	.043	.451	.137
2	.23469	.139	.486	.114	.253	.14114	.107	.431	.168
3	.25369	.139	.475	.120	.260	.30109	.067	.416	.193
4	.22868	.157	.472	.108	.265	.33452	.068	.409	.205
5	.24581	.149	.453	.111	.261	.34370	.070	.396	.207

TEST NO. 3-23-NC2

STRAIN	TAN ϕ	I	SIG	D	TAU	TAN ϕ*	I*	SIG*	TAU*
1	.07938	.259	1.413	.112	.372	.26119	-.022	1.318	.322
2	.13792	.253	1.298	.179	.432	.31247	.003	1.200	.378
3	.18913	.234	1.196	.226	.460	.38242	-.014	1.092	.402
4	.20480	.259	1.154	.236	.496	.37238	.047	1.055	.441
5	.24514	.238	1.098	.269	.507	.41393	.034	.999	.448

TEST NO. 3-18-NC2

STRAIN	TAN ϕ	I	SIG	D	TAU	TAN ϕ*	I*	SIG*	TAU*
1	.08409	.270	1.341	.112	.383	.29838	-.023	1.249	.349
2	.12779	.286	1.247	.159	.446	.26565	.114	1.185	.429
3	.16304	.278	1.185	.193	.471	.32296	.089	1.110	.448
4	.20987	.265	1.110	.232	.498	.39088	.070	1.028	.472
5	.23717	.254	1.071	.254	.508	.32329	.150	1.019	.480

TEST NO. 3-17-NC2

STRAIN	TAN ϕ	I	SIG	D	TAU	TAN ϕ*	I*	SIG*	TAU*
1	.05068	.301	1.471	.074	.376	.29686	-.031	1.399	.383
2	.09983	.297	1.373	.137	.435	.38837	-.033	1.303	.472
3	.12306	.299	1.316	.162	.461	.44807	-.047	1.236	.507
4	.14270	.325	1.252	.178	.504	.47219	-.004	1.158	.542
5	.20159	.277	1.182	.238	.516	.51885	-.024	1.088	.540

TEST NO. 3-24-NC4

STRAIN	TAN ϕ	I	SIG	D	TAU	TAN ϕ*	I*	SIG*	TAU*
1	.05386	.448	3.066	.165	.613	.28073	-.145	3.016	.701
2	.08452	.517	2.845	.240	.753	.25384	.117	2.795	.827
3	.10801	.532	2.722	.294	.826	.21758	.304	2.698	.891
4	.14539	.542	2.564	.372	.915	.22179	.408	2.554	.974
5	.17422	.532	2.472	.430	.962	.25512	.374	2.435	.995

TEST NO. 3-20-NC4

STRAIN	TAN ϕ	I	SIG	D	TAU	TAN ϕ*	I*	SIG*	TAU*
1	.03812	.519	2.994	.114	.633	.25806	-.036	2.945	.723
2	.07038	.580	2.781	.195	.776	.21758	.263	2.752	.862
3	.09128	.606	2.660	.242	.849	.18770	.423	2.649	.921
4	.11339	.655	2.503	.283	.938	.15988	.612	2.532	1.016
5	.14679	.630	2.413	.354	.984	.22844	.475	2.374	1.018

TEST NO. 3-19-NC4

STRAIN	TAN ϕ	I	SIG	D	TAU	TAN ϕ*	I*	SIG*	TAU*
1	.02685	.541	3.115	.083	.624	.26527	-.095	3.057	.715
2	.06761	.565	2.894	.195	.761	.23861	.158	2.843	.837
3	.09128	.578	2.765	.252	.830	.18100	.408	2.767	.909
4	.11292	.628	2.612	.295	.923	.18042	.519	2.616	.991
5	.15950	.571	2.489	.397	.969	.23988	.414	2.453	1.002

Constant-p' Test Series on O.C. Kaolinite

TEST NO. 3-30-0C6

PT NO.	VOL STRAIN	VERT STRAIN	DEV STRESS	SIGMA 3	SIGMA 1	SIG 1/SIG 3	MEAN STRESS
1	.00234	.00154	.647	1.339	1.987	1.483	1.555
2	.00389	.00346	.847	1.267	2.115	1.668	1.550
3	.00461	.00494	.893	1.249	2.143	1.714	1.547
4	.00761	.00732	.907	.849	1.757	2.068	1.152
5	.00924	.00985	.928	.829	1.757	2.119	1.138
6	.01007	.01186	.951	.824	1.775	2.153	1.141
7	.00793	.01837	1.173	1.143	2.317	2.026	1.534
8	.00803	.02164	1.217	1.112	2.330	2.094	1.518
9	.01121	.02623	1.136	.753	1.890	2.508	1.132
10	.01222	.02964	1.143	.749	1.892	2.526	1.130
11	.00956	.03841	1.354	1.059	2.414	2.278	1.511
12	.00963	.04244	1.390	1.034	2.425	2.344	1.498
13	.01262	.04690	1.273	.695	1.969	2.832	1.119
14	.01324	.04896	1.269	.697	1.967	2.820	1.120
15	.01146	.05427	1.413	1.065	2.478	2.326	1.536
16	.01148	.05762	1.434	1.039	2.474	2.380	1.517

TEST NO. 3-31-0C7

PT NO.	VOL STRAIN	VERT STRAIN	DEV STRESS	SIGMA 3	SIGMA 1	SIG 1/SIG 3	MEAN STRESS
1	.00098	.00352	.500	.644	1.145	1.776	.811
2	.00185	.00655	.602	.604	1.207	1.996	.805
3	.00540	.00959	.580	.414	.995	2.399	.608
4	.00668	.01191	.602	.399	1.001	2.506	.600
5	.00723	.01318	.613	.399	1.013	2.535	.604
6	.00600	.01953	.744	.547	1.291	2.359	.795
7	.00613	.02128	.760	.547	1.308	2.389	.801
8	.01017	.02622	.695	.364	1.060	2.908	.596
9	.01158	.02913	.686	.350	1.036	2.959	.579
10	.00988	.03859	.820	.511	1.332	2.605	.785
11	.01009	.04062	.828	.512	1.340	2.616	.788
12	.01372	.04516	.739	.359	1.099	3.059	.605
13	.01498	.04807	.722	.349	1.071	3.067	.589
14	.01266	.05297	.836	.514	1.350	2.625	.793
15	.01287	.05577	.848	.509	1.357	2.665	.792

TEST NO. 3-32-OC8

PT NO.	VOL STRAIN	VERT STRAIN	DEV STRESS	SIGMA 3	SIGMA 1	SIG 1/SIG 3	MEAN STRESS
1	.00118	.00295	.349	.355	.704	1.980	.472
2	.00262	.00560	.425	.324	.750	2.308	.466
3	.00742	.00976	.437	.222	.659	2.964	.368
4	.00944	.01282	.453	.219	.672	3.065	.370
5	.00990	.02054	.551	.274	.825	3.009	.458
6	.01087	.02308	.555	.285	.840	2.944	.470
7	.01615	.03011	.489	.204	.693	3.398	.367
8	.01736	.03252	.483	.204	.687	3.368	.365
9	.01720	.03938	.544	.279	.823	2.952	.460
10	.01776	.04196	.546	.271	.817	3.017	.453
11	.02061	.04650	.463	.198	.661	3.328	.353
12	.02147	.04879	.447	.198	.646	3.251	.347
13	.02056	.05367	.514	.278	.793	2.843	.450
14	.02072	.05519	.507	.278	.786	2.820	.448

TEST NO. 3-30-OC6

STRAIN	TAN ϕ	I	SIG	D	TAU	TAN ϕ*	I*	SIG*	TAU*
1	.10111	.340	1.449	.146	.486	.06346	.201	1.274	.282
2	.14756	.349	1.433	.211	.561	.27251	.058	1.254	.400
3	.16072	.379	1.426	.229	.608	.30473	.079	1.249	.460
4	.16967	.398	1.421	.241	.639	.37517	.039	1.227	.500
5	.16263	.428	1.430	.232	.661	.35811	.079	1.236	.522

TEST NO. 3-31-OC7

STRAIN	TAN ϕ	I	SIG	D	TAU	TAN ϕ*	I*	SIG*	TAU*
1	.17820	.171	.751	.133	.305	.12243	.088	.644	.167
2	.19624	.199	.742	.145	.345	.25389	.052	.621	.210
3	.22956	.197	.730	.167	.365	.35474	.017	.603	.231
4	.24391	.198	.728	.177	.376	.38721	.012	.600	.244
5	.26077	.189	.722	.188	.378	.40438	.009	.600	.252

TEST NO. 3-32-0C8

STRAIN	TAN ϕ	I	SIG	D	TAU	TAN ϕ*	I*	SIG*	TAU*
1	.21038	.134	.445	.093	.228	.05493	.096	.371	.116
2	.37953	.083	.410	.155	.239	.24388	.051	.352	.137
3	.34995	.101	.417	.146	.248	.20862	.072	.362	.148
4	.32575	.107	.415	.135	.242	.31246	.049	.357	.160
5	.30988	.106	.405	.125	.232	.26788	.071	.363	.168

Constant-p' Test Series on N.C. Kaolinite

TEST NO. 3-25-NC1

PT NO.	VOL STRAIN	VERT STRAIN	DEV STRESS	SIGMA 3	SIGMA 1	SIG 1/SIG 3	MEAN STRESS
1	.00090	.00042	.249	.747	.997	1.333	.831
2	.00166	.00277	.478	.652	1.131	1.732	.812
3	.00195	.00485	.523	.649	1.173	1.805	.824
4	.00373	.00617	.495	.449	.944	2.100	.614
5	.00482	.00861	.512	.449	.962	2.140	.620
6	.00544	.01123	.538	.447	.986	2.202	.627
7	.00297	.01411	.608	.683	1.291	1.889	.886
8	.00313	.01680	.635	.599	1.235	2.060	.811
9	.00305	.01954	.657	.599	1.257	2.095	.818
10	.00558	.02308	.609	.414	1.024	2.470	.617
11	.00638	.02632	.621	.409	1.031	2.517	.616
12	.00369	.03177	.718	.569	1.288	2.260	.809
13	.00367	.03464	.734	.559	1.294	2.312	.804
14	.00641	.03843	.671	.389	1.060	2.722	.613
15	.00746	.04181	.668	.379	1.048	2.760	.602
16	.00482	.04640	.765	.549	1.315	2.391	.804
17	.00472	.04987	.784	.538	1.323	2.455	.800
18	.00722	.05240	.702	.359	1.062	2.954	.593
19	.00825	.05530	.698	.365	1.063	2.909	.598

TEST NO. 3-26-NC2

PT NO.	VOL STRAIN	VERT STRAIN	DEV STRESS	SIGMA 3	SIGMA 1	SIG 1/SIG 3	MEAN STRESS
1	.00143	.00049	.505	1.389	1.895	1.363	1.558
2	.00234	.00252	.710	1.349	2.060	1.526	1.586
3	.00255	.00387	.770	1.309	2.080	1.588	1.566
4	.00499	.00590	.766	.914	1.681	1.837	1.170
5	.00560	.00800	.812	.893	1.706	1.909	1.164
6	.00588	.01029	.861	.799	1.661	2.077	1.086
7	.00297	.01565	1.008	1.234	2.242	1.816	1.570
8	.00268	.01839	1.053	1.196	2.250	1.880	1.548
9	.00473	.02135	1.011	.822	1.834	2.229	1.159
10	.00548	.02468	1.021	.804	1.825	2.268	1.145
11	.00282	.02823	1.142	1.156	2.299	1.987	1.537
12	.00220	.03148	1.197	1.145	2.343	2.045	1.545
13	.00176	.03444	1.238	1.129	2.368	2.096	1.542
14	.00449	.03926	1.160	.751	1.912	2.543	1.138
15	.00502	.04166	1.163	.749	1.913	2.551	1.137
16	.00190	.04848	1.349	1.088	2.438	2.239	1.538
17	.00127	.05084	1.380	1.095	2.475	2.261	1.555
18	.00385	.05434	1.273	.719	1.993	2.768	1.144
19	.00440	.05640	1.271	.721	1.993	2.761	1.145

TEST NO. 3-27-NC4

PT NO.	VOL STRAIN	VERT STRAIN	DEV STRESS	SIGMA 3	SIGMA 1	SIG 1/SIG 3	MEAN STRESS
1	.00214	.00040	.544	2.853	3.398	1.190	3.035
2	.00287	.00243	.916	2.699	3.616	1.339	3.005
3	.00265	.00531	1.095	2.624	3.720	1.417	2.989
4	.00604	.00861	1.161	1.799	2.961	1.645	2.186
5	.00616	.01085	1.233	1.799	3.033	1.685	2.210
6	.00602	.01358	1.305	1.754	3.060	1.744	2.189
7	-.00020	.02077	1.603	2.450	4.053	1.654	2.984
8	-.00102	.02438	1.719	2.412	4.131	1.712	2.985
9	-.00170	.02726	1.801	2.390	4.191	1.753	2.990
10	.00179	.03177	1.710	1.619	3.330	2.055	2.189
11	.00195	.03466	1.754	1.599	3.353	2.096	2.184
12	.00200	.03718	1.783	1.585	3.369	2.124	2.180
13	-.00259	.04550	2.107	2.000	4.108	2.053	2.702
14	-.00293	.04836	2.163	1.990	4.153	2.086	2.711
15	.00050	.05254	1.977	1.291	3.268	2.531	1.950
16	.00101	.05482	1.978	1.276	3.254	2.550	1.935
17	.00133	.05852	2.011	1.270	3.281	2.583	1.940

TEST NO. 3-28-NC2

PT NO.	VOL STRAIN	VERT STRAIN	DEV STRESS	SIGMA 3	SIGMA 1	SIG 1/SIG 3	MEAN STRESS
1	.00190	.00221	.577	1.349	1.926	1.427	1.542
2	.00203	.00356	.632	1.334	1.967	1.474	1.545
3	.00462	.00718	.692	.909	1.602	1.761	1.140
4	.00482	.00915	.723	.901	1.625	1.802	1.142
5	.00018	.01647	.896	1.239	2.136	1.722	1.538
6	-.00009	.01960	.946	1.200	2.146	1.788	1.515
7	.00235	.02395	.915	.829	1.745	2.103	1.135
8	.00262	.02587	.925	.819	1.745	2.128	1.128
9	-.00167	.03368	1.105	1.150	2.255	1.960	1.518
10	-.00206	.03640	1.138	1.148	2.286	1.991	1.527
11	.00087	.04152	1.060	.767	1.827	2.382	1.120
12	.00124	.04415	1.074	.767	1.842	2.398	1.126
13	-.00265	.05075	1.251	1.100	2.351	2.137	1.517
14	-.00295	.05255	1.278	1.096	2.374	2.166	1.522
15	.00027	.05749	1.149	.680	1.830	2.690	1.063
16	.00082	.05967	1.155	.690	1.845	2.673	1.075

TEST NO. 3-29-NC4

PT NO.	VOL STRAIN	VERT STRAIN	DEV STRESS	SIGMA 3	SIGMA 1	SIG 1/SIG 3	MEAN STRESS
1	.00289	.00279	.907	2.699	3.607	1.336	3.002
2	.00285	.00480	1.025	2.619	3.645	1.391	2.961
3	.00641	.00819	1.089	1.805	2.895	1.603	2.168
4	.00645	.01098	1.171	1.783	2.955	1.657	2.174
5	-.00096	.02117	1.564	2.580	4.144	1.606	3.101
6	-.00121	.02348	1.632	2.440	4.072	1.668	2.984
7	-.00167	.02587	1.697	2.402	4.099	1.706	2.968
8	.00210	.03008	1.591	1.639	3.231	1.970	2.170
9	.00228	.03298	1.628	1.632	3.261	1.997	2.175
10	-.00421	.04372	2.059	2.243	4.302	1.917	2.929
11	-.00486	.04756	2.149	2.232	4.382	1.962	2.948
12	-.00032	.05352	1.922	1.512	3.434	2.271	2.152
13	.00000	.05615	1.935	1.512	3.447	2.279	2.157

TEST NO. 3-34-NC4

PT NO.	VOL STRAIN	VERT STRAIN	DEV STRESS	SIGMA 3	SIGMA 1	SIG 1/SIG 3	MEAN STRESS
1	.00223	.00089	.731	2.759	3.490	1.264	3.003
2	.00282	.00327	.938	2.659	3.598	1.352	2.972
3	.00277	.00508	1.030	2.651	3.682	1.388	2.995
4	.00566	.01107	1.186	1.785	2.971	1.664	2.181
5	.00583	.01392	1.246	1.749	2.996	1.712	2.165
6	-.00123	.02358	1.603	2.450	4.053	1.654	2.984
7	-.00170	.02622	1.676	2.400	4.076	1.698	2.958
8	.00167	.03173	1.621	1.626	3.248	1.996	2.167
9	.00189	.03441	1.653	1.603	3.257	2.030	2.154
10	-.00426	.04343	2.026	2.280	4.306	1.888	2.955
11	-.00468	.04547	2.072	2.257	4.329	1.918	2.948
12	-.00052	.05240	1.909	1.510	3.419	2.264	2.146
13	-.00020	.05534	1.931	1.500	3.431	2.287	2.144

TEST NO. 3-25-NC1

STRAIN	TAN ϕ	I	SIG	D	TAU	TAN ϕ*	I*	SIG*	TAU*
1	.12263	.178	.773	.094	.273	.19380	.088	.720	.228
2	.16406	.179	.771	.126	.305	.15876	.158	.748	.277
3	.19402	.185	.765	.148	.333	.18887	.164	.742	.304
4	.18512	.210	.760	.140	.350	.16036	.204	.745	.324
5	.20717	.206	.747	.154	.361	.18231	.201	.732	.334

TEST NO. 3-26-NC2

STRAIN	TAN ϕ	I	SIG	D	TAU	TAN ϕ*	I*	SIG*	TAU*
1	.08216	.319	1.465	.120	.440	.17756	.230	1.472	.492
2	.10350	.360	1.471	.152	.512	.19807	.273	1.474	.565
3	.12413	.382	1.467	.182	.564	.22117	.293	1.464	.617
4	.13947	.403	1.464	.204	.608	.23339	.320	1.461	.661
5	.15588	.413	1.462	.227	.641	.25168	.328	1.454	.694

TEST NO. 3-27-NC4

STRAIN	TAN ϕ	I	SIG	D	TAU	TAN ϕ*	I*	SIG*	TAU*
1	.05380	.477	2.765	.148	.626	.37386	-.192	2.752	.836
2	.09596	.500	2.772	.266	.766	.14439	.708	3.074	1.152
3	.11355	.560	2.784	.316	.876	.13568	.650	2.915	1.046
4	.11915	.629	2.797	.333	.962	.13904	.644	2.848	1.040
5	.14240	.625	2.796	.398	1.023	.19405	.517	2.780	1.057

TEST NO. 3-28-NC2

STRAIN	TAN ϕ	I	SIG	D	TAU	TAN ϕ*	I*	SIG*	TAU*
1	.07542	.268	1.435	.108	.377	.17342	.234	1.501	.494
2	.10232	.305	1.425	.145	.451	.21630	.258	1.485	.579
3	.11957	.337	1.430	.171	.508	.17281	.355	1.496	.613
4	.14329	.345	1.419	.203	.549	.22190	.278	1.419	.593
5	.16380	.350	1.405	.230	.581	.21133	.313	1.407	.611

TEST NO. 3-29-NC4

STRAIN	TAN ϕ	I	SIG	D	TAU	TAN ϕ*	I*	SIG*	TAU*
1	.05061	.457	2.742	.138	.596	.28116	.130	2.889	.943
2	.08454	.499	2.747	.232	.731	.21221	.481	2.976	1.113
3	.12544	.490	2.746	.344	.834	.28976	.281	2.838	1.103
4	.16774	.462	2.713	.455	.918	.29630	.309	2.783	1.134
5	.19076	.479	2.707	.516	.995	.25780	.441	2.781	1.159

TEST NO. 3-34-NC4

STRAIN	TAN ϕ	I	SIG	D	TAU	TAN ϕ*	I*	SIG*	TAU*
1	.04547	.467	2.760	.125	.593	.25203	.151	2.876	.876
2	.07546	.518	2.759	.208	.726	.27983	.337	2.973	1.169
3	.10665	.537	2.748	.293	.831	.27367	.391	2.907	1.187
4	.13555	.550	2.740	.371	.921	.26282	.402	2.817	1.143
5	.16150	.553	2.725	.440	.993	.28384	.381	2.759	1.164

Constant-Volume Test Series on O.C. Kaolinite

TEST NO. 2-46-OC9

PT NO.	VOL STRAIN	VERT STRAIN	DEV STRESS	SIGMA 3	SIGMA 1	SIG 1/SIG 3	MEAN STRESS
1	.00000	.00093	.599	1.944	2.544	1.308	2.144
2	.00000	.00227	.902	1.939	2.842	1.465	2.240
3	.00000	.00457	1.137	1.937	3.074	1.587	2.316
4	.00253	.00899	1.269	1.576	2.846	1.805	2.000
5	.00251	.01243	1.388	1.569	2.958	1.884	2.032
6	-.00011	.01591	1.579	1.970	3.549	1.801	2.496
7	-.00002	.01890	1.660	1.779	3.439	1.933	2.332
8	-.00004	.02298	1.748	1.705	3.453	2.025	2.288
9	-.00007	.02470	1.775	1.705	3.480	2.041	2.296
10	.00257	.02871	1.672	1.406	3.079	2.189	1.964
11	.00250	.03157	1.737	1.401	3.139	2.239	1.981
12	.00248	.03420	1.782	1.407	3.190	2.266	2.002
13	.00249	.03727	1.830	1.399	3.230	2.307	2.010
14	-.00007	.04295	2.042	1.630	3.672	2.253	2.310
15	-.00008	.04523	2.071	1.610	3.681	2.286	2.300
16	-.00005	.04840	2.100	1.576	3.677	2.333	2.276
17	-.00009	.05101	2.138	1.560	3.698	2.370	2.272
18	.00243	.05437	1.961	1.259	3.221	2.557	1.913
19	.00245	.05643	2.018	1.331	3.350	2.515	2.004
20	.00248	.05917	2.050	1.340	3.390	2.529	2.023

TEST NO. 2-47-0C10

PT NO.	VOL STRAIN	VERT STRAIN	DEV STRESS	SIGMA 3	SIGMA 1	SIG 1/SIG 3	MEAN STRESS
1	-.00004	.00085	.416	.965	1.381	1.432	1.103
2	-.00001	.00235	.634	.990	1.624	1.640	1.201
3	.00001	.00399	.753	.989	1.743	1.761	1.241
4	-.00001	.00515	.856	1.000	1.856	1.856	1.285
5	.00256	.00903	.940	.859	1.800	2.093	1.173
6	.00257	.01195	1.040	.886	1.927	2.173	1.233
7	.00257	.01467	1.107	.888	1.996	2.246	1.258
8	-.00004	.01819	1.277	1.164	2.441	2.097	1.589
9	-.00001	.02100	1.339	1.097	2.436	2.221	1.543
10	-.00001	.02354	1.384	1.091	2.475	2.269	1.552
11	.00259	.02853	1.343	.899	2.242	2.492	1.347
12	.00260	.03320	1.414	.917	2.332	2.540	1.389
13	-.00002	.03659	1.571	1.126	2.697	2.395	1.649
14	-.00001	.03970	1.615	1.102	2.717	2.465	1.640
15	-.00002	.04432	1.665	1.092	2.758	2.525	1.647
16	.00260	.04875	1.579	.926	2.506	2.703	1.453
17	.00263	.05084	1.600	.939	2.540	2.702	1.473
18	.00263	.05380	1.638	.979	2.618	2.671	1.526
19	-.00001	.05849	1.814	1.160	2.974	2.564	1.765
20	.00000	.05992	1.822	1.150	2.973	2.584	1.757

TEST NO. 3-36-0C11

PT NO.	VOL STRAIN	VERT STRAIN	DEV STRESS	SIGMA 3	SIGMA 1	SIG 1/SIG 3	MEAN STRESS
1	.00000	.00028	.175	.475	.650	1.368	.533
2	-.00000	.00310	.473	.495	.968	1.956	.652
3	-.00000	.00569	.600	.523	1.123	2.148	.723
4	.00249	.00842	.636	.439	1.076	2.447	.652
5	.00250	.01026	.696	.455	1.152	2.527	.687
6	.00249	.01177	.728	.467	1.196	2.557	.710
7	-.00000	.01596	.878	.660	1.538	2.331	.952
8	-.00000	.01761	.912	.655	1.567	2.393	.959
9	-.00000	.01949	.952	.650	1.602	2.465	.967
10	.00251	.02344	.909	.549	1.459	2.654	.853
11	.00252	.02488	.931	.550	1.482	2.691	.861
12	-.00000	.03001	1.075	.753	1.828	2.427	1.111
13	-.00000	.03190	1.096	.747	1.843	2.467	1.112
14	.00252	.03638	1.049	.634	1.684	2.653	.984
15	.00253	.03841	1.071	.641	1.713	2.669	.999
16	-.00000	.04326	1.205	.825	2.030	2.460	1.226
17	-.00000	.04495	1.220	.830	2.050	2.470	1.236
18	.00253	.04958	1.157	.719	1.877	2.607	1.105
19	.00252	.05010	1.162	.718	1.881	2.616	1.106
20	-.00001	.05318	1.279	.880	2.160	2.454	1.306
21	-.00000	.05365	1.284	.880	2.164	2.459	1.308

TEST NO. 2-46-0C9

STRAIN	TAN ϕ	I	SIG	D	TAU	TAN ϕ*	I*	SIG*	TAU*
1	.11866	.394	2.318	.275	.669	.11866	.394	2.318	.669
2	.19950	.339	2.264	.451	.790	.19950	.339	2.264	.790
3	.24219	.333	2.233	.541	.874	.24219	.333	2.233	.874
4	.25374	.374	2.223	.564	.938	.25374	.374	2.223	.938
5	.26504	.400	2.221	.588	.989	.26504	.400	2.221	.989

TEST NO. 2-47-0C10

STRAIN	TAN ϕ	I	SIG	D	TAU	TAN ϕ*	I*	SIG*	TAU*
1	.20412	.219	1.355	.276	.496	.20412	.219	1.355	.496
2	.23862	.265	1.473	.351	.616	.23862	.265	1.473	.616
3	.25301	.302	1.550	.392	.694	.25301	.302	1.550	.694
4	.27229	.314	1.601	.436	.750	.27229	.314	1.601	.750
5	.28980	.323	1.637	.474	.798	.28980	.323	1.637	.798

TEST NO. 3-36-0C11

STRAIN	TAN ϕ	I	SIG	D	TAU	TAN ϕ*	I*	SIG*	TAU*
1	.22154	.173	.792	.175	.348	.22154	.173	.792	.348
2	.21071	.243	.959	.202	.445	.21071	.243	.959	.445
3	.21786	.272	1.073	.233	.506	.21786	.272	1.073	.506
4	.21753	.296	1.176	.255	.552	.21753	.296	1.176	.552
5	.25750	.261	1.247	.321	.583	.25750	.261	1.247	.583

Constant-Volume Test Series on N.C. Kaolinite

TEST NO. 2-48-NC2

PT NO.	VOL STRAIN	VERT STRAIN	DEV STRESS	SIGMA 3	SIGMA 1	SIG 1/SIG 3	MEAN STRESS
1	-.00003	.00048	.447	1.835	2.282	1.243	1.984
2	-.00012	.00421	.673	1.560	2.233	1.431	1.784
3	.00221	.00726	.737	1.129	1.867	1.653	1.375
4	.00221	.00948	.791	1.083	1.875	1.730	1.347
5	.00217	.01184	.827	1.047	1.875	1.790	1.323
6	-.00035	.01685	.946	1.154	2.100	1.820	1.469
7	-.00038	.02010	.990	1.080	2.070	1.917	1.410
8	-.00041	.02360	1.029	1.020	2.049	2.009	1.363
9	.00198	.02956	.999	.779	1.779	2.281	1.113
10	.00191	.03248	1.029	.764	1.794	2.345	1.108
11	.00196	.03452	1.050	.769	1.820	2.364	1.119
12	-.00055	.04021	1.136	.750	1.886	2.515	1.129
13	-.00056	.04175	1.165	.844	2.009	2.380	1.232
14	-.00055	.04523	1.192	.837	2.029	2.424	1.234
15	-.00056	.04800	1.215	.830	2.045	2.464	1.235
16	.00187	.05074	1.108	.650	1.759	2.702	1.020
17	.00189	.05263	1.139	.681	1.821	2.670	1.061
18	.00191	.05767	1.181	.707	1.889	2.668	1.101
19	.00190	.06074	1.202	.710	1.912	2.693	1.110

TEST NO. 2-49-NC3

PT NO.	VOL STRAIN	VERT STRAIN	DEV STRESS	SIGMA 3	SIGMA 1	SIG 1/SIG 3	MEAN STRESS
1	-.00001	-.00003	.367	2.879	3.247	1.127	3.002
2	-.00004	.00144	.687	2.715	3.402	1.253	2.944
3	-.00006	.00345	.877	2.482	3.359	1.353	2.774
4	.00241	.00558	.965	1.885	2.851	1.512	2.207
5	.00237	.00796	1.076	1.806	2.883	1.595	2.165
6	.00233	.01082	1.163	1.711	2.875	1.679	2.099
7	-.00021	.01450	1.311	1.929	3.240	1.679	2.366
8	-.00024	.01658	1.365	1.833	3.198	1.745	2.288
9	-.00029	.02038	1.445	1.703	3.148	1.848	2.184
10	.00218	.02258	1.354	1.342	2.697	2.008	1.794
11	.00220	.02570	1.420	1.347	2.768	2.054	1.821
12	.00219	.02950	1.481	1.314	2.796	2.126	1.808
13	-.00028	.03326	1.635	1.310	2.945	2.248	1.855
14	-.00038	.03821	1.673	1.431	3.104	2.169	1.988
15	-.00040	.04052	1.708	1.408	3.116	2.213	1.977
16	.00208	.04346	1.591	1.147	2.739	2.386	1.678
17	.00209	.04587	1.628	1.154	2.783	2.409	1.697
18	.00209	.04848	1.658	1.161	2.820	2.427	1.714
19	.00209	.05114	1.678	1.178	2.857	2.423	1.738
20	-.00043	.05326	1.814	1.397	3.211	2.298	2.001
21	-.00043	.05577	1.852	1.345	3.197	2.377	1.962
22	-.00045	.05780	1.868	1.325	3.193	2.409	1.947

TEST NO. 2-50-NC1

PT NO.	VOL STRAIN	VERT STRAIN	DEV STRESS	SIGMA 3	SIGMA 1	SIG 1/SIG 3	MEAN STRESS
1	-.00005	.00023	.291	.910	1.201	1.319	1.007
2	-.00012	.00214	.439	.837	1.276	1.525	.983
3	-.00014	.00346	.487	.781	1.268	1.624	.943
4	.00160	.00705	.561	.559	1.121	2.002	.746
5	.00155	.01023	.599	.529	1.128	2.130	.729
6	-.00030	.01429	.672	.602	1.274	2.117	.826
7	-.00033	.01697	.699	.573	1.272	2.220	.806
8	.00201	.02045	.664	.413	1.078	2.606	.635
9	.00198	.02431	.700	.418	1.119	2.672	.652
10	.00199	.02652	.714	.420	1.135	2.696	.658
11	-.00049	.03015	.786	.530	1.316	2.483	.792
12	-.00043	.03399	.808	.500	1.308	2.617	.769
13	-.00042	.03604	.817	.496	1.313	2.647	.768
14	.00185	.03827	.744	.369	1.114	3.012	.618
15	.00189	.04145	.776	.408	1.185	2.899	.667
16	.00193	.04474	.796	.404	1.201	2.967	.670
17	-.00040	.04724	.873	.512	1.386	2.706	.803
18	-.00043	.05015	.887	.502	1.389	2.766	.797
19	-.00044	.05394	.903	.496	1.399	2.821	.797
20	.00193	.05747	.832	.396	1.229	3.098	.674
21	.00194	.06000	.852	.406	1.258	3.099	.690

TEST NO. 2-48-NC2

STRAIN	TAN ϕ	I	SIG	D	TAU	TAN ϕ*	I*	SIG*	TAU*
1	.04032	.343	1.597	.064	.407	.10137	.248	1.574	.407
2	.15939	.251	1.401	.223	.475	.22718	.159	1.371	.470
3	.16554	.301	1.296	.214	.516	.24588	.200	1.258	.509
4	.22417	.266	1.225	.274	.541	.30851	.166	1.183	.531
5	.29085	.219	1.189	.346	.565	.37160	.126	1.149	.553

TEST NO. 2-49-NC3

STRAIN	TAN ϕ	I	SIG	D	TAU	TAN ϕ*	I*	SIG*	TAU*
1	.07468	.399	2.461	.183	.583	.08036	.396	2.469	.594
2	.13585	.392	2.187	.297	.689	.14191	.389	2.193	.700
3	.18043	.389	2.032	.366	.756	.18677	.386	2.036	.766
4	.21908	.378	1.949	.427	.805	.22550	.375	1.953	.816
5	.25403	.357	1.904	.483	.840	.26040	.353	1.908	.850

TEST NO. 2-50-NC1

STRAIN	TAN ϕ	I	SIG	D	TAU	TAN ϕ*	I*	SIG*	TAU*
1	.10450	.213	.860	.089	.303	.15988	.165	.844	.300
2	.18283	.201	.780	.142	.344	.23549	.161	.762	.340
3	.23535	.191	.749	.176	.368	.28800	.152	.731	.363
4	.24987	.201	.754	.188	.390	.30601	.160	.734	.384
5	.29701	.182	.751	.223	.405	.34920	.143	.732	.399

Glass Beads

Drained Test Series on Glass Beads

TEST NO. GB-4D

PT NO.	VOL STRAIN	VERT STRAIN	DEV STRESS	SIGMA 3	SIGMA 1	SIG 1/SIG 3	MEAN ...
1	-.00022	.00123	1.683	4.000	5.683	1.420	4.561
2	-.00062	.00257	4.518	4.000	8.518	2.129	5.506
3	-.00009	.00518	6.978	4.000	10.978	2.744	6.326
4	.00362	.01087	8.603	3.999	12.603	3.150	6.867
5	.00789	.01634	8.880	3.999	12.880	3.220	6.959
6	.01420	.02437	8.687	3.999	12.687	3.172	6.895
7	.02273	.03765	7.844	3.998	11.843	2.961	6.613
8	.02500	.04411	7.038	3.998	11.036	2.760	6.344
9	.02624	.06502	6.103	3.998	10.101	2.526	6.033

TEST NO. GB-1D

PT NO.	VOL STRAIN	VERT STRAIN	DEV STRESS	SIGMA 3	SIGMA 1	SIG 1/SIG 3	MEAN STRESS
1	-.00002	.00017	.767	1.000	1.767	1.767	1.255
2	.00136	.00334	1.873	.999	2.873	2.873	1.624
3	.00261	.00516	2.041	.999	3.041	3.041	1.680
4	.00517	.00808	2.125	.999	3.125	3.126	1.708
5	.00915	.01252	2.130	.999	3.130	3.131	1.709
6	.01274	.01707	2.088	.999	3.088	3.090	1.695
7	.01814	.02480	1.987	.998	2.986	2.989	1.661
8	.02290	.03368	1.806	.998	2.805	2.808	1.600
9	.02486	.04032	1.595	.998	2.593	2.597	1.530

TEST NO. GB-2D

PT NO.	VOL STRAIN	VERT STRAIN	DEV STRESS	SIGMA 3	SIGMA 1	SIG 1/SIG 3	MEAN STRESS
1	.00001	.00214	.384	1.999	2.384	1.192	2.128
2	-.00022	.00419	2.194	2.000	4.194	2.097	2.731
3	.00176	.00882	3.715	1.999	5.714	2.857	3.238
4	.00616	.01463	4.032	1.999	6.031	3.016	3.343
5	.01007	.01995	4.053	1.999	6.052	3.027	3.350
6	.01780	.03137	3.905	1.999	5.904	2.953	3.300
7	.02306	.04067	3.736	1.998	5.735	2.869	3.244
8	.02560	.04625	3.627	1.998	5.625	2.814	3.207
9	.02802	.05229	3.497	1.998	5.495	2.750	3.164
10	.02995	.05903	3.292	1.998	5.290	2.647	3.095
11	.03088	.06598	2.911	1.998	4.909	2.456	2.968

Constant-σ_3' Test Series on Glass Beads

TEST NO. GB-1A

PT NO.	VOL STRAIN	VERT STRAIN	DEV STRESS	SIGMA 3	SIGMA 1	SIG 1/SIG 3	MEAN STRESS
1	.00000	.00025	.130	.999	1.130	1.130	1.043
2	.00024	.00293	1.581	.999	2.581	2.581	1.527
3	.00215	.00573	2.049	.999	3.049	3.050	1.683
4	.00437	.00749	1.649	.749	2.399	3.200	1.299
5	.00764	.01123	1.706	.749	2.455	3.276	1.318
6	.00993	.01391	1.708	.749	2.457	3.279	1.318
7	.00997	.01467	2.241	.999	3.240	3.242	1.746
8	.01246	.01761	2.254	.999	3.253	3.255	1.750
9	.01574	.02190	2.225	.999	3.224	3.226	1.740
10	.01804	.02432	1.658	.748	2.407	3.214	1.301
11	.02245	.03081	1.625	.748	2.374	3.170	1.290
12	.02465	.03403	1.596	.748	2.345	3.132	1.280
13	.02487	.03518	2.104	.998	3.103	3.107	1.700
14	.02627	.03773	2.081	.998	3.080	3.084	1.692
15	.03159	.04793	1.942	.998	2.940	2.945	1.645
16	.03380	.05147	1.457	.748	2.205	2.947	1.233
17	.03614	.05742	1.417	.747	2.165	2.894	1.220
18	.03738	.06086	1.404	.747	2.152	2.877	1.216
19	.03724	.06188	1.832	.997	2.830	2.836	1.608
20	.03929	.06913	1.774	.997	2.772	2.778	1.589

TEST NO. GB-1B

PT NO.	VOL STRAIN	VERT STRAIN	DEV STRESS	SIGMA 3	SIGMA 1	SIG 1/SIG 3	MEAN STRESS
1	.00009	.00335	1.719	.999	2.719	2.719	1.573
2	.00207	.00614	2.165	.999	3.165	3.165	1.721
3	.00354	.00700	1.648	.749	2.398	3.199	1.299
4	.00948	.01269	1.742	.749	2.492	3.325	1.330
5	.01337	.01658	1.752	.749	2.501	3.338	1.333
6	.01488	.01881	2.388	.999	3.387	3.390	1.795
7	.02289	.02686	2.350	.998	3.349	3.353	1.782
8	.02675	.03034	1.722	.748	2.471	3.301	1.322
9	.03452	.03905	1.661	.748	2.409	3.220	1.301
10	.03697	.04271	2.195	.997	3.193	3.200	1.729
11	.04156	.04843	2.124	.997	3.122	3.129	1.705
12	.04353	.05030	1.545	.747	2.293	3.067	1.262
13	.04627	.05425	1.519	.747	2.267	3.033	1.254
14	.04796	.05519	2.032	.997	3.029	3.038	1.674
15	.04953	.06013	1.989	.997	2.986	2.994	1.660

TEST NO. GB-2B

PT NO.	VOL STRAIN	VERT STRAIN	DEV STRESS	SIGMA 3	SIGMA 1	SIG 1/SIG 3	MEAN STRESS
1	.00008	.00012	.145	1.999	2.145	1.072	2.048
2	-.00012	.00173	1.669	2.000	3.669	1.834	2.556
3	.00005	.00363	3.007	1.999	5.007	2.503	3.002
4	.00156	.00577	3.335	1.749	5.085	2.906	2.861
5	.00309	.00792	3.606	1.749	5.355	3.060	2.951
6	.00557	.01048	3.789	1.749	5.538	3.165	3.012
7	.00662	.01205	4.380	1.999	6.380	3.190	3.459
8	.01094	.01679	4.471	1.999	6.470	3.236	3.489
9	.01366	.01964	4.458	1.999	6.458	3.230	3.485
10	.01465	.02025	3.859	1.749	5.608	3.206	3.035
11	.01864	.02487	3.841	1.748	5.590	3.196	3.029
12	.02296	.03007	3.765	1.748	5.514	3.153	3.003
13	.02329	.03080	4.288	1.998	6.286	3.145	3.428
14	.02699	.03569	4.199	1.998	6.197	3.101	3.398
15	.03109	.04100	4.083	1.998	6.081	3.043	3.359
16	.03244	.04256	3.527	1.748	5.275	3.018	2.924
17	.03687	.04977	3.376	1.747	5.124	2.931	2.873
18	.03897	.05372	3.295	1.747	5.043	2.885	2.846
19	.03907	.05449	3.722	1.997	5.720	2.863	3.238
20	.04176	.06007	3.590	1.997	5.587	2.797	3.194
21	.04239	.06135	3.096	1.747	4.844	2.771	2.779
22	.04436	.06598	3.016	1.747	4.764	2.726	2.753

TEST NO. GB-2A

PT NO.	VOL STRAIN	VERT STRAIN	DEV STRESS	SIGMA 3	SIGMA 1	SIG 1/SIG 3	MEAN STRESS
1	-.00005	.00444	2.834	2.000	4.834	2.417	2.944
2	.00124	.00696	3.802	1.999	5.802	2.901	3.267
3	.00369	.00957	3.717	1.749	5.467	3.124	2.989
4	.00931	.01592	3.992	1.749	5.741	3.281	3.080
5	.00980	.01682	4.615	1.999	6.614	3.308	3.537
6	.01715	.02459	4.663	1.999	6.662	3.332	3.553
7	.01886	.02595	4.043	1.748	5.792	3.311	3.096
8	.02481	.03231	3.986	1.748	5.735	3.279	3.077
9	.02507	.03301	4.577	1.998	6.575	3.290	3.524
10	.03103	.03994	4.444	1.998	6.442	3.224	3.479
11	.03255	.04130	3.826	1.748	5.574	3.188	3.023
12	.03744	.04761	3.624	1.747	5.372	3.073	2.956
13	.03749	.04815	4.113	1.997	6.111	3.058	3.369
14	.03873	.05018	3.970	1.997	5.967	2.987	3.321
15	.03955	.05117	3.383	1.747	5.131	2.935	2.875

TEST NO. GB-3B

PT NO.	VOL STRAIN	VERT STRAIN	DEV STRESS	SIGMA 3	SIGMA 1	SIG 1/SIG 3	MEAN STRESS
1	-.00006	.00250	.764	4.000	4.764	1.191	4.254
2	-.00055	.00465	5.051	4.000	9.051	2.262	5.683
3	.00058	.00719	6.892	3.499	10.392	2.969	5.797
4	.00217	.00928	7.666	3.499	11.165	3.190	6.055
5	.00479	.01195	8.063	3.499	11.563	3.304	6.187
6	.00477	.01265	9.190	3.999	13.189	3.297	7.063
7	.00547	.01344	9.337	3.999	13.337	3.334	7.112
8	.00847	.01682	9.462	3.999	13.461	3.365	7.153
9	.01285	.02156	9.447	3.999	13.446	3.362	7.148
10	.01450	.02277	8.230	3.499	11.729	3.351	6.242
11	.01715	.02575	8.159	3.499	11.658	3.331	6.218
12	.01980	.02847	8.058	3.498	11.557	3.303	6.185
13	.02256	.03243	9.040	3.998	13.039	3.260	7.012
14	.02621	.03705	8.847	3.998	12.845	3.212	6.947
15	.02885	.04073	8.634	3.998	12.632	3.159	6.876
16	.03128	.04344	7.336	3.498	10.835	3.097	5.943
17	.03357	.04756	6.805	3.498	10.303	2.945	5.766
18	.03548	.05208	6.313	3.498	9.811	2.804	5.602
19	.03527	.05565	7.127	3.998	11.125	2.782	6.373
20	.03529	.05729	7.007	3.998	11.005	2.752	6.334

TEST NO. GB-3A

PT NO.	VOL STRAIN	VERT STRAIN	DEV STRESS	SIGMA 3	SIGMA 1	SIG 1/SIG 3	MEAN STRESS
1	-.00033	.00169	2.777	4.000	6.777	1.694	4.925
2	.00027	.00499	7.896	3.999	11.896	2.974	6.632
3	.00280	.00754	8.065	3.499	11.565	3.304	6.188
4	.00633	.01113	8.592	3.499	12.092	3.455	6.363
5	.00906	.01388	8.741	3.499	12.240	3.497	6.413
6	.01028	.01564	10.057	3.999	14.057	3.514	7.352
7	.01872	.02393	10.060	3.998	14.059	3.515	7.352
8	.02089	.02557	8.764	3.498	12.263	3.505	6.420
9	.02859	.03334	8.541	3.498	12.039	3.441	6.345
10	.02956	.03484	9.666	3.998	13.664	3.417	7.220
11	.03497	.04138	9.051	3.998	13.049	3.263	7.015
12	.03715	.04386	7.656	3.497	11.154	3.188	6.050
13	.04062	.04980	7.047	3.497	10.545	3.015	5.847
14	.04120	.05232	7.570	3.997	11.567	2.893	6.521

TEST NO. GB-1A

STRAIN	TAN ϕ	I	SIG	D	TAU	TAN ϕ*	I*	SIG*	TAU*
1	.60754	.022	1.348	.819	.841	.27663	.005	1.113	.313
2	.61418	.013	1.344	.825	.839	.30125	.010	1.137	.352
3	.60010	.009	1.333	.800	.810	.34738	-.023	1.140	.373
4	.57735	.014	1.325	.764	.779	.33282	.011	1.162	.398
5	.52805	.053	1.331	.702	.756	.33175	.036	1.185	.429

TEST NO. GB-1B

STRAIN	TAN ϕ	I	SIG	D	TAU	TAN ϕ*	I*	SIG*	TAU*
1	.64019	-.030	1.321	.845	.815	.38855	-.116	1.083	.304
2	.66815	-.030	1.335	.892	.861	.28347	-.021	1.092	.288
3	.65777	-.026	1.333	.877	.850	.33863	-.066	1.092	.303
4	.66125	-.060	1.307	.864	.803	.33705	-.068	1.089	.299
5	.60754	-.016	1.314	.798	.781	.26505	.027	1.126	.326

TEST NO. GB-2A

STRAIN	TAN ϕ	I	SIG	D	TAU	TAN ϕ*	I*	SIG*	TAU*
1	.60010	.011	2.849	1.710	1.721	.30344	-.106	2.317	.596
2	.67158	-.103	2.834	1.903	1.799	.31518	-.097	2.346	.642
3	.65777	-.070	2.846	1.872	1.802	.27715	-.003	2.372	.653
4	.63305	-.042	2.841	1.799	1.756	.26632	.044	2.400	.684
5	.57349	.004	2.811	1.612	1.616	.19147	.251	2.474	.725

TEST NO. GB-2B

STRAIN	TAN ϕ	I	SIG	D	TAU	TAN ϕ*	I*	SIG*	TAU*
1	.55785	.132	2.903	1.619	1.752	.21300	.095	2.359	.598
2	.64374	-.070	2.830	1.821	1.751	.33307	-.141	2.332	.635
3	.60383	.008	2.851	1.721	1.730	.28182	.006	2.389	.679
4	.58501	.005	2.826	1.653	1.659	.30068	-.022	2.393	.697
5	.56961	-.017	2.787	1.588	1.570	.33382	-.043	2.427	.766

TEST NO. GB-3A

STRAIN	TAN ϕ	I	SIG	D	TAU	TAN ϕ*	I*	SIG*	TAU*
1	.60383	.270	5.920	3.574	3.845	.36936	-.430	4.645	1.285
2	.67499	-.015	5.834	3.938	3.922	.28938	-.011	4.781	1.372
3	.66815	-.026	5.811	3.882	3.855	.28347	-.018	4.754	1.328
4	.63663	-.021	5.745	3.657	3.635	.40926	-.490	4.716	1.439
5	.52352	.299	5.754	3.012	3.312	.40088	-.270	4.893	1.691

TEST NO. GB-3B

STRAIN	TAN ϕ	I	SIG	D	TAU	TAN ϕ*	I*	SIG*	TAU*
1	.59447	.213	5.849	3.477	3.690	.30112	-.092	4.742	1.335
2	.63125	.071	5.812	3.669	3.740	.26985	.051	4.776	1.340
3	.63841	-.063	5.714	3.648	3.585	.32003	-.143	4.756	1.378
4	.63305	-.192	5.593	3.540	3.348	.37734	-.208	4.879	1.633
5	.67669	-.689	5.280	3.573	2.883	.58662	-1.031	4.757	1.759

Glass Beads with Hydrocal

Constant-σ_3' Test Series on

Glass Beads with Hydrocal

TEST NO. GBH-1

PT NO.	VOL STRAIN	VERT STRAIN	DEV STRESS	SIGMA 3	SIGMA 1	SIG 1/SIG 3	MEAN STRESS
1	-.00017	.00055	.739	1.000	1.739	1.739	1.246
2	-.00073	.00209	2.596	1.000	3.596	3.596	1.865
3	-.00062	.00368	3.128	.800	3.928	4.910	1.842
4	-.00054	.00452	3.283	.800	4.083	5.103	1.894
5	-.00071	.00600	3.701	1.000	4.701	4.701	2.233
6	-.00059	.00707	3.857	1.000	4.857	4.857	2.285
7	.00000	.00791	3.642	.799	4.442	5.553	2.014
8	.00066	.00932	3.655	.799	4.455	5.570	2.018
9	.00069	.01027	3.983	.999	4.983	4.983	2.327
10	.00174	.01288	4.024	.999	5.024	5.024	2.341
11	.00254	.01370	3.570	.799	4.370	5.463	1.989
12	.00324	.01470	3.521	.799	4.320	5.402	1.973
13	.00396	.01678	3.873	.999	4.873	4.874	2.291
14	.00487	.01859	3.777	.999	4.777	4.778	2.258
15	.00568	.01932	3.260	.799	4.060	5.077	1.886
16	.00665	.02068	3.163	.799	3.962	4.955	1.854
17	.00674	.02165	3.496	.999	4.495	4.497	2.165
18	.00725	.02278	3.422	.999	4.422	4.424	2.140
19	.00765	.02383	3.265	.999	4.265	4.267	2.088

TEST NO. GBH-2

PT NO.	VOL STRAIN	VERT STRAIN	DEV STRESS	SIGMA 3	SIGMA 1	SIG 1/SIG 3	MEAN STRESS
1	-.00020	.00032	.954	1.000	1.954	1.954	1.318
2	-.00054	.00065	2.352	1.000	3.352	3.352	1.784
3	-.00093	.00203	3.355	1.000	4.355	4.354	2.118
4	-.00069	.00313	3.417	.800	4.217	5.271	1.939
5	-.00051	.00441	3.492	.800	4.292	5.365	1.964
6	-.00060	.00606	3.829	1.000	4.829	4.829	2.276
7	-.00046	.00692	3.859	1.000	4.859	4.859	2.286
8	.00031	.00825	3.563	.799	4.363	5.454	1.987
9	.00075	.00944	3.549	.799	4.349	5.437	1.983
10	.00123	.01179	3.847	.999	4.847	4.847	2.282
11	.00163	.01276	3.824	.999	4.824	4.824	2.274
12	.00280	.01420	3.348	.799	4.148	5.186	1.915
13	.00319	.01487	3.304	.799	4.104	5.132	1.901
14	.00359	.01655	3.592	.999	4.592	4.593	2.197
15	.00415	.01783	3.511	.999	4.511	4.512	2.170
16	.00560	.01983	2.919	.799	3.718	4.650	1.772
17	.00581	.02015	2.878	.799	3.677	4.599	1.759
18	.00625	.02220	3.067	.999	4.067	4.068	2.022
19	.00636	.02243	3.022	.999	4.022	4.023	2.007

TEST NO. GBH-3

PT NO.	VOL STRAIN	VERT STRAIN	DEV STRESS	SIGMA 3	SIGMA 1	SIG 1/SIG 3	MEAN STRESS
1	-.00051	-.00002	1.613	1.000	2.613	2.613	1.537
2	-.00084	.00069	2.419	1.000	3.419	3.419	1.806
3	-.00115	.00188	2.954	1.000	3.954	3.954	1.985
4	-.00108	.00377	3.113	.800	3.913	4.892	1.838
5	-.00104	.00445	3.187	.800	3.987	4.984	1.862
6	-.00119	.00610	3.537	1.000	4.537	4.536	2.179
7	-.00113	.00755	3.675	1.000	4.675	4.675	2.225
8	-.00048	.00900	3.434	.800	4.234	5.292	1.944
9	-.00000	.01031	3.440	.799	4.240	5.300	1.946
10	.00007	.01252	3.768	1.000	4.768	4.768	2.256
11	.00062	.01349	3.757	.999	4.757	4.757	2.252
12	.00155	.01482	3.327	.799	4.127	5.159	1.909
13	.00221	.01617	3.280	.799	4.080	5.101	1.893
14	.00290	.01865	3.532	.999	4.531	4.532	2.177
15	.00340	.02007	3.485	.999	4.484	4.485	2.161
16	.00446	.02159	2.989	.799	3.788	4.737	1.796
17	.00494	.02247	2.903	.799	3.703	4.631	1.767
18	.00530	.02407	3.159	.999	4.159	4.160	2.052
19	.00552	.02469	3.117	.999	4.117	4.118	2.038

TEST NO. GBH-4

PT NO.	VOL STRAIN	VERT STRAIN	DEV STRESS	SIGMA 3	SIGMA 1	SIG 1/SIG 3	MEAN STRESS
1	-.00002	.00015	.451	2.000	2.451	1.225	2.150
2	-.00019	.00073	2.473	2.000	4.473	2.236	2.824
3	-.00039	.00187	4.450	2.000	6.450	3.225	3.483
4	-.00023	.00305	5.130	1.600	6.730	4.206	3.310
5	-.00011	.00421	5.505	1.600	7.105	4.441	3.435
6	-.00031	.00551	6.214	2.000	8.214	4.107	4.071
7	-.00020	.00650	6.384	2.000	8.384	4.192	4.128
8	.00056	.00777	5.868	1.599	7.468	4.667	3.556
9	.00094	.00880	5.901	1.599	7.501	4.688	3.567
10	.00113	.01072	6.574	1.999	8.574	4.287	4.191
11	.00128	.01119	6.597	1.999	8.597	4.299	4.199
12	.00171	.01240	6.586	1.999	8.586	4.293	4.195
13	.00325	.01441	5.661	1.599	7.261	4.538	3.486
14	.00362	.01501	5.630	1.599	7.230	4.519	3.476
15	.00409	.01703	6.254	1.999	8.254	4.127	4.084
16	.00456	.01806	6.165	1.999	8.165	4.083	4.054
17	.00606	.02026	4.968	1.599	6.567	4.105	3.255
18	.00640	.02091	4.794	1.599	6.394	3.997	3.197
19	.00634	.02179	5.289	1.999	7.288	3.644	3.762
20	.00664	.02322	4.657	1.999	6.657	3.329	3.552

TEST NO. GBH-5

PT NO.	VOL STRAIN	VERT STRAIN	DEV STRESS	SIGMA 3	SIGMA 1	SIG 1/SIG 3	MEAN STRESS
1	-.00005	.00033	.421	2.000	2.421	1.210	2.140
2	-.00038	.00107	2.059	2.000	4.059	2.029	2.686
3	-.00081	.00198	3.371	2.000	5.371	2.685	3.123
4	-.00099	.00318	3.996	1.600	5.596	3.497	2.932
5	-.00119	.00450	4.315	1.600	5.915	3.696	3.038
6	-.00175	.00645	4.967	2.000	6.968	3.483	3.656
7	-.00180	.00681	5.050	2.000	7.050	3.525	3.683
8	-.00154	.00833	4.897	1.600	6.497	4.060	3.232
9	-.00146	.00926	4.950	1.600	6.550	4.093	3.250
10	-.00172	.01190	5.640	2.000	7.640	3.819	3.880
11	-.00160	.01300	5.742	2.000	7.742	3.870	3.914
12	-.00062	.01495	5.220	1.600	6.820	4.263	3.340
13	-.00034	.01578	5.254	1.600	6.854	4.284	3.351
14	-.00018	.01820	5.954	2.000	7.954	3.977	3.984
15	.00004	.01901	5.967	2.000	7.967	3.983	3.989
16	.00166	.02165	5.126	1.599	6.726	4.204	3.308
17	.00192	.02224	5.148	1.599	6.748	4.218	3.316
18	.00229	.02461	5.795	1.999	7.795	3.898	3.931
19	.00262	.02543	5.777	1.999	7.777	3.889	3.925
20	.00371	.02671	4.981	1.599	6.581	4.113	3.260
21	.00416	.02755	4.943	1.599	6.543	4.090	3.247

TEST NO. GBH-6

PT NO.	VOL STRAIN	VERT STRAIN	DEV STRESS	SIGMA 3	SIGMA 1	SIG 1/SIG 3	MEAN STRESS
1	-.00002	.00030	.311	2.000	2.311	1.155	2.103
2	-.00039	.00097	1.910	2.000	3.910	1.955	2.636
3	-.00087	.00192	3.208	2.000	5.208	2.604	3.069
4	-.00105	.00328	3.962	1.600	5.562	3.476	2.921
5	-.00119	.00423	4.233	1.600	5.833	3.645	3.011
6	-.00181	.00581	4.814	2.000	6.814	3.407	3.604
7	-.00204	.00713	5.133	2.000	7.133	3.566	3.711
8	-.00160	.00880	4.980	1.600	6.580	4.112	3.260
9	-.00140	.01013	5.094	1.600	6.695	4.184	3.298
10	-.00167	.01209	5.717	2.000	7.717	3.858	3.905
11	-.00150	.01339	5.849	2.000	7.849	3.924	3.950
12	-.00031	.01550	5.267	1.600	6.867	4.291	3.355
13	.00004	.01632	5.279	1.600	6.879	4.299	3.359
14	.00022	.01868	5.927	2.000	7.927	3.963	3.975
15	.00078	.02032	5.951	1.999	7.951	3.975	3.983
16	.00200	.02165	5.133	1.599	6.733	4.208	3.311
17	.00293	.02332	5.078	1.599	6.678	4.174	3.292
18	.00316	.02520	5.777	1.999	7.777	3.889	3.925
19	.00371	.02644	5.779	1.999	7.779	3.890	3.926

TEST NO. GBH-7

PT NO.	VOL STRAIN	VERT STRAIN	DEV STRESS	SIGMA 3	SIGMA 1	SIG 1/SIG 3	MEAN STRESS
1	-.00035	.00053	2.177	3.000	5.177	1.725	3.725
2	-.00097	.00188	4.260	3.000	7.260	2.420	4.420
3	-.00113	.00335	5.078	2.400	7.478	3.116	4.092
4	-.00128	.00410	5.347	2.400	7.747	3.228	4.182
5	-.00218	.00653	6.487	3.000	9.487	3.162	5.162
6	-.00230	.00736	6.757	3.000	9.757	3.252	5.252
7	-.00233	.00766	6.860	3.000	9.860	3.286	5.286
8	-.00159	.00985	6.594	2.400	8.994	3.747	4.598
9	-.00137	.01095	6.725	2.400	9.125	3.802	4.641
10	-.00159	.01354	7.904	3.000	10.905	3.634	5.635
11	-.00125	.01509	7.966	3.000	10.966	3.655	5.655
12	.00058	.01805	6.869	2.399	9.269	3.862	4.689
13	.00093	.01884	6.858	2.399	9.258	3.857	4.686
14	.00090	.02073	7.918	2.999	10.918	3.639	5.639
15	.00127	.02170	7.893	2.999	10.893	3.631	5.631
16	.00154	.02268	7.666	2.999	10.666	3.555	5.555
17	.00317	.02468	6.507	2.399	8.907	3.711	4.569
18	.00342	.02513	6.503	2.399	8.903	3.709	4.567

TEST NO. GBH-8

PT NO.	VOL STRAIN	VERT STRAIN	DEV STRESS	SIGMA 3	SIGMA 1	SIG 1/SIG 3	MEAN STRESS
1	-.00009	.00042	1.641	3.000	4.641	1.547	3.547
2	-.00033	.00108	3.332	3.000	6.332	2.110	4.111
3	-.00062	.00177	4.330	3.000	7.330	2.443	4.443
4	-.00074	.00307	5.343	2.400	7.743	3.226	4.181
5	-.00092	.00406	5.826	2.400	8.226	3.427	4.342
6	-.00149	.00580	6.765	3.000	9.766	3.255	5.255
7	-.00162	.00641	7.029	3.000	10.029	3.343	5.343
8	-.00140	.00735	6.952	2.400	9.352	3.896	4.717
9	-.00122	.00885	7.217	2.400	9.617	4.007	4.805
10	-.00154	.01066	8.195	3.000	11.195	3.731	5.731
11	-.00144	.01185	8.487	3.000	11.488	3.829	5.829
12	-.00027	.01360	7.691	2.400	10.091	4.204	4.963
13	.00033	.01502	7.699	2.399	10.099	4.208	4.966
14	.00093	.01841	8.819	2.999	11.819	3.939	5.939
15	.00121	.01913	8.821	2.999	11.821	3.940	5.940
16	.00300	.02126	7.521	2.399	9.921	4.134	4.906
17	.00340	.02201	7.506	2.399	9.906	4.127	4.901
18	.00377	.02407	8.564	2.999	11.564	3.855	5.854
19	.00421	.02497	8.526	2.999	11.525	3.842	5.841

TEST NO. GBH-9

PT NO.	VOL STRAIN	VERT STRAIN	DEV STRESS	SIGMA 3	SIGMA 1	SIG 1/SIG 3	MEAN STRESS
1	.00000	.00003	1.072	2.999	4.072	1.357	3.357
2	-.00027	.00056	3.421	3.000	6.421	2.140	4.140
3	-.00075	.00195	4.987	3.000	7.987	2.662	4.662
4	-.00075	.00302	5.485	2.400	7.885	3.285	4.228
5	-.00088	.00424	5.942	2.400	8.342	3.476	4.380
6	-.00150	.00603	6.815	3.000	9.815	3.271	5.271
7	-.00160	.00654	7.027	3.000	10.027	3.342	5.342
8	-.00119	.00782	6.791	2.400	9.192	3.829	4.664
9	-.00104	.00908	6.961	2.400	9.361	3.900	4.720
10	-.00133	.01105	7.930	3.000	10.930	3.643	5.643
11	-.00120	.01221	8.111	3.000	11.111	3.703	5.703
12	-.00031	.01370	7.302	2.400	9.702	4.042	4.834
13	.00013	.01491	7.344	2.399	9.744	4.060	4.848
14	.00047	.01817	8.403	2.999	11.403	3.801	5.801
15	.00061	.01869	8.410	2.999	11.410	3.803	5.803
16	.00183	.02014	7.250	2.399	9.650	4.021	4.816
17	.00253	.02148	7.178	2.399	9.578	3.991	4.792
18	.00299	.02428	8.074	2.999	11.074	3.691	5.691
19	.00347	.02552	7.990	2.999	10.990	3.663	5.663
20	.00481	.02716	6.632	2.399	9.031	3.763	4.610
21	.00497	.02755	6.628	2.399	9.028	3.762	4.609

TEST NO. GBH-1

STRAIN	TAN ϕ	I	SIG	D	TAU	TAN ϕ*	I*	SIG*	TAU*
.5	.34015	.941	2.081	.707	1.649	.42949	.625	1.829	1.411
1.0	.52248	.687	1.926	1.006	1.693	.37307	.527	1.708	1.164
1.5	.60569	.507	1.800	1.090	1.597	.39427	.379	1.583	1.003
2.0	.62855	.384	1.704	1.071	1.455	.41971	.226	1.456	.837

TEST NO. GBH-2

STRAIN	TAN ϕ	I	SIG	D	TAU	TAN ϕ*	I*	SIG*	TAU*
.5	.39836	.869	2.040	.813	1.682	.41898	.604	1.804	1.360
1.0	.52764	.645	1.890	.997	1.642	.40356	.472	1.674	1.148
1.5	.58881	.469	1.761	1.036	1.506	.38682	.366	1.566	.972
2.0	.57735	.372	1.672	.965	1.338	.33807	.329	1.500	.836

TEST NO. GBH-3

STRAIN	TAN ϕ	I	SIG	D	TAU	TAN ϕ*	I*	SIG*	TAU*
.5	.36014	.850	2.004	.722	1.572	.37072	.748	1.914	1.458
1.0	.47985	.700	1.920	.921	1.621	.56479	.264	1.572	1.152
1.5	.56277	.527	1.801	1.013	1.541	.36178	.439	1.619	1.025
2.0	.54792	.479	1.753	.960	1.440	.34727	.399	1.572	.945

TEST NO. GBH-4

STRAIN	TAN ϕ	I	SIG	D	TAU	TAN ϕ*	I*	SIG*	TAU*
.5	.37953	1.345	3.696	1.403	2.748	.42806	.869	3.307	2.285
1.0	.51729	.967	3.486	1.803	2.771	.45380	.509	3.007	1.874
1.5	.58691	.672	3.291	1.931	2.604	.36659	.575	2.960	1.661
2.0	.57735	.526	3.156	1.822	2.349	.36247	.433	2.821	1.456

TEST NO. GBH-5

STRAIN	TAN ϕ	I	SIG	D	TAU	TAN ϕ*	I*	SIG*	TAU*
.5	.26077	1.292	3.504	.913	2.206	.53225	.757	3.314	2.521
1.0	.38587	1.106	3.480	1.342	2.448	.43097	.789	3.237	2.184
1.5	.49613	.827	3.341	1.657	2.485	.41612	.605	3.050	1.874
2.0	.55241	.650	3.239	1.789	2.440	.38657	.559	2.971	1.708

TEST NO. GBH-6

STRAIN	TAN ϕ	I	SIG	D	TAU	TAN ϕ*	I*	SIG*	TAU*
.5	.23717	1.359	3.538	.839	2.198	.56109	.737	3.324	2.602
1.0	.36667	1.190	3.537	1.297	2.488	.34041	1.020	3.346	2.159
1.5	.50201	.825	3.345	1.679	2.504	.39378	.630	3.046	1.830
2.0	.54038	.687	3.260	1.761	2.449	.35591	.580	2.950	1.631

TEST NO. GBH-7

STRAIN	TAN ϕ	I	SIG	D	TAU	TAN ϕ*	I*	SIG*	TAU*
.5	.27097	1.482	4.836	1.310	2.793	.71743	.137	4.385	3.283
1.0	.44802	1.068	4.779	2.141	3.210	.49358	.539	4.378	2.700
1.5	.52764	.821	4.686	2.472	3.294	.42938	.532	4.254	2.359
2.0	.55950	.650	4.586	2.566	3.216	.38045	.533	4.158	2.115

TEST NO. GBH-8

STRAIN	TAN ϕ	I	SIG	D	TAU	TAN ϕ*	I*	SIG*	TAU*
.5	.21535	1.978	5.202	1.120	3.098	.30983	2.167	5.569	3.893
1.0	.39753	1.556	5.143	2.044	3.601	.47206	.866	4.636	3.055
1.5	.53616	1.017	4.872	2.612	3.629	.47729	.389	4.214	2.400
2.0	.57574	.810	4.749	2.734	3.545	.36643	.671	4.259	2.231

TEST NO. GBH-9

STRAIN	TAN ϕ	I	SIG	D	TAU	TAN ϕ*	I*	SIG*	TAU*
.5	.20695	1.923	5.130	1.061	2.985	.51163	.915	4.744	3.342
1.0	.37099	1.530	5.073	1.882	3.412	.48338	.818	4.611	3.047
1.5	.49434	1.079	4.864	2.404	3.483	.43266	.720	4.433	2.639
2.0	.54925	.836	4.733	2.599	3.436	.41892	.547	4.248	2.327

APPENDIX D
α_s AND TAN α_R VS STRAIN RELATIONSHIPS

Normally Consolidated Kaolinite

Overconsolidated Kaolinite

Glass Beads with Hydrocal

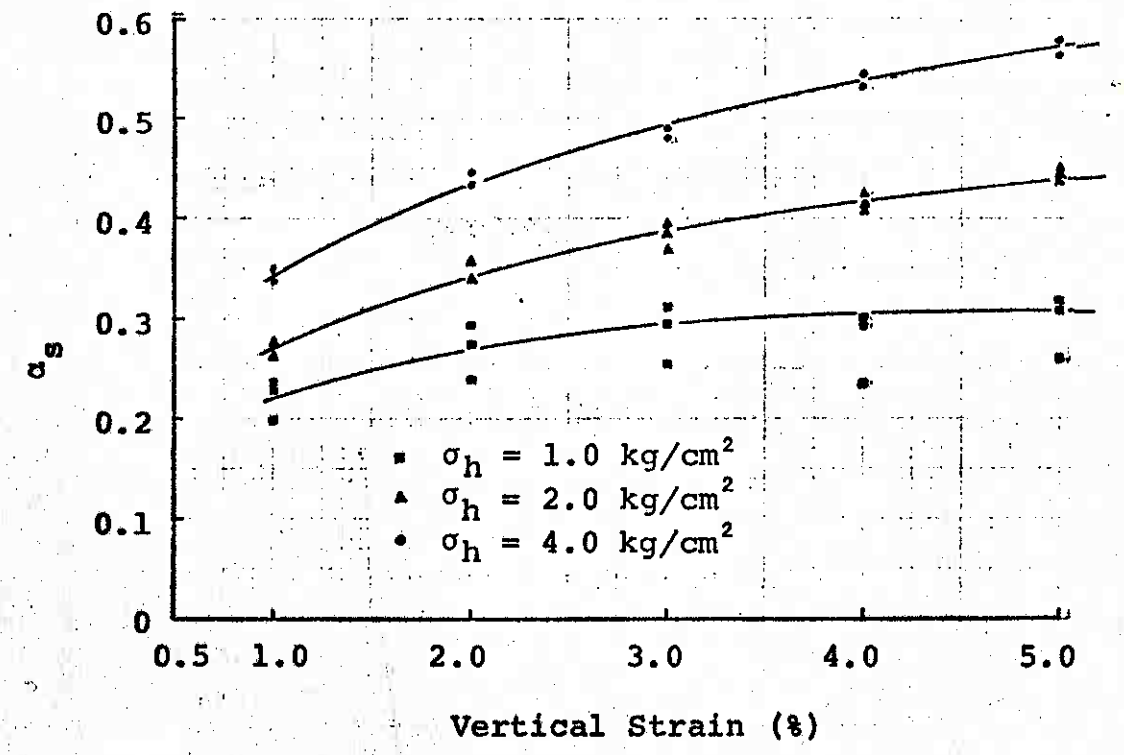

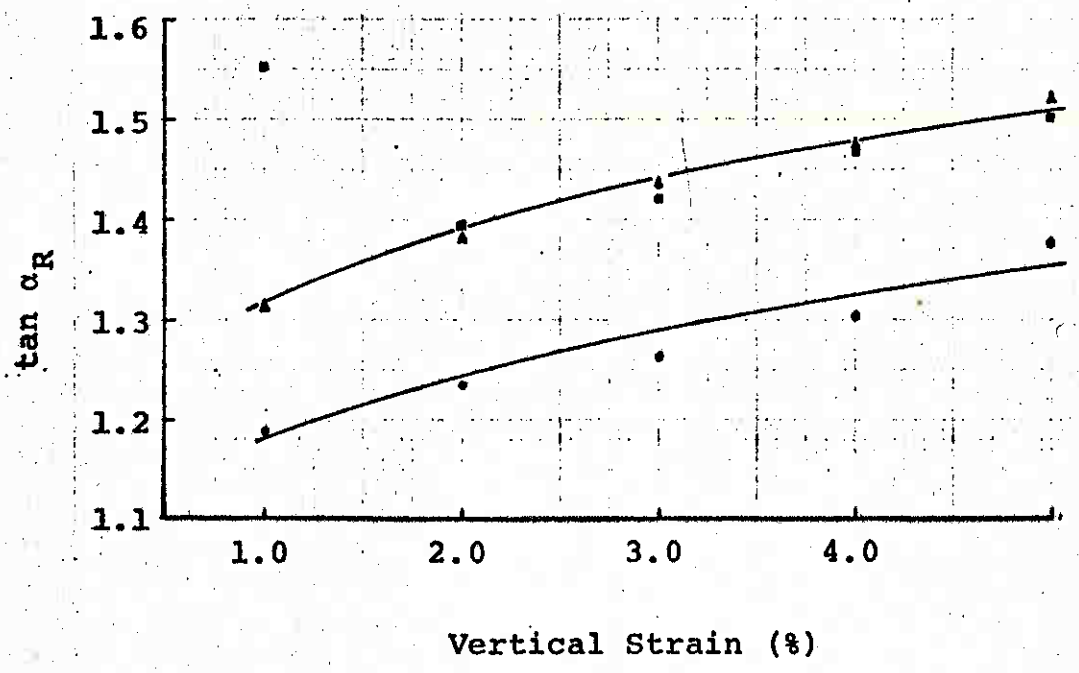

Figure D-1 α_s and tan α_R vs Strain, Constant-σ_1' Test Series On N.C. Kaolinite

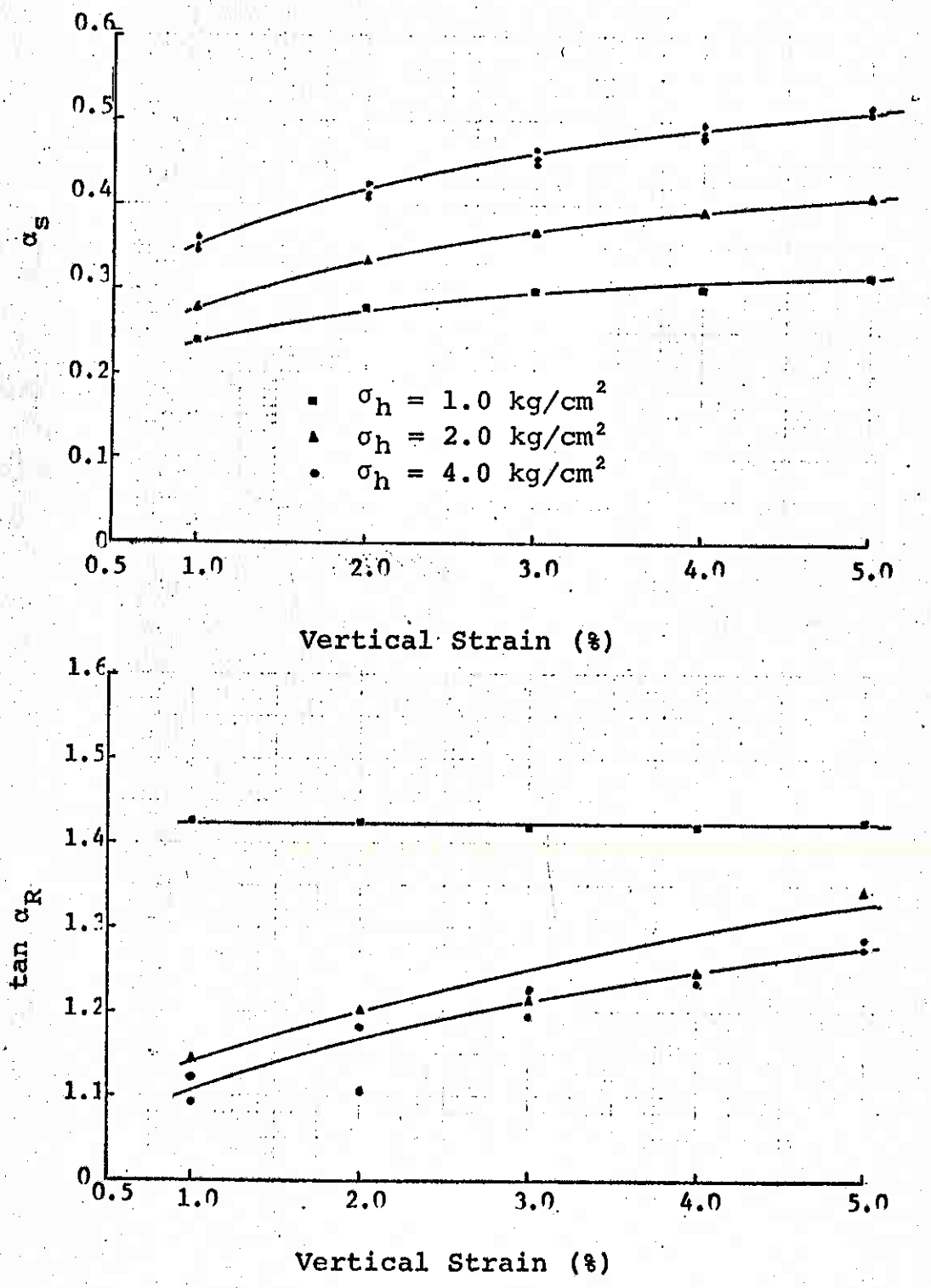

Figure D-2 α_s and tan α_R vs Strain, Constant-p' Test Series on N.C. Kaolinite

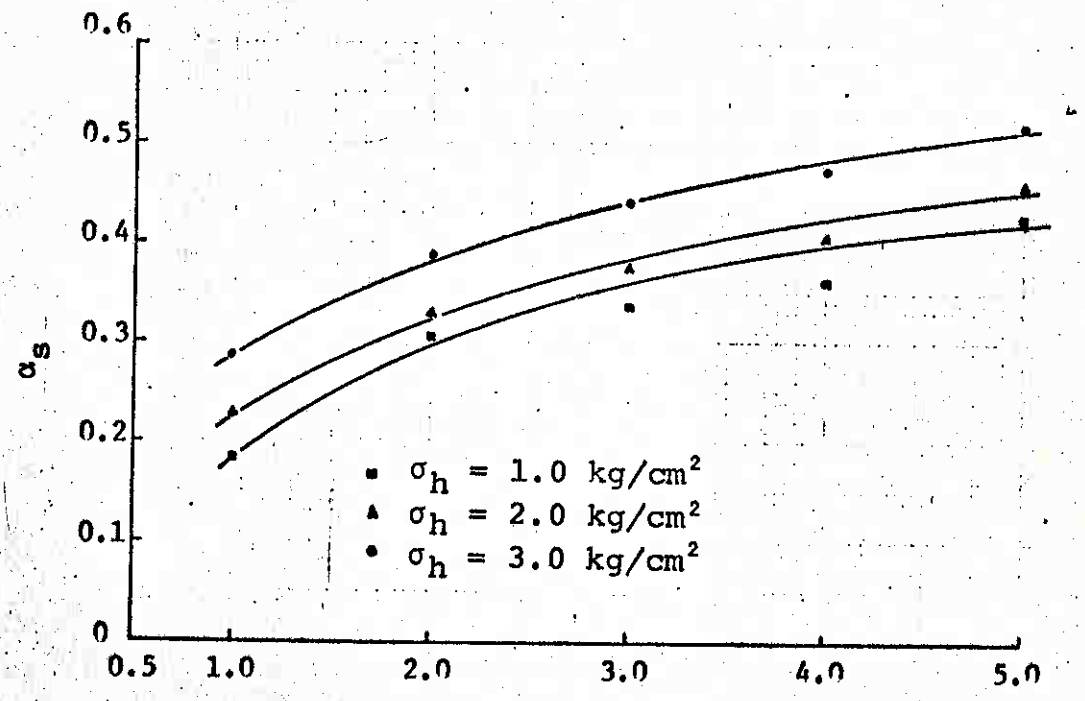

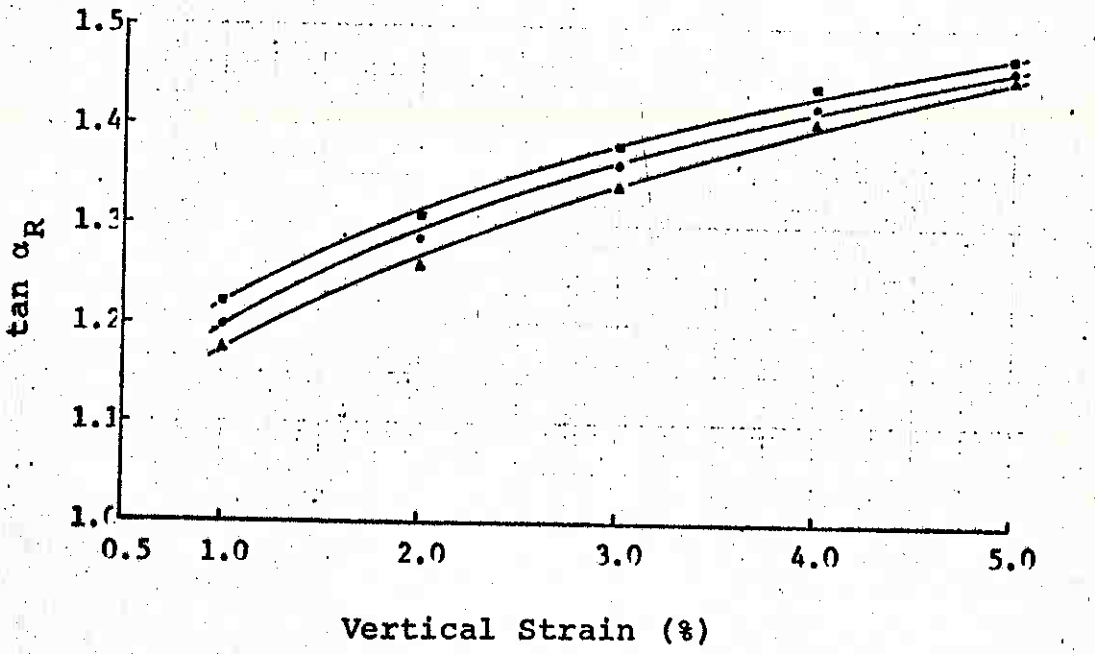

Figure D-3 α_s and tan α_R vs Strain, Constant-Volume Test Series on N.C. Kaolinite

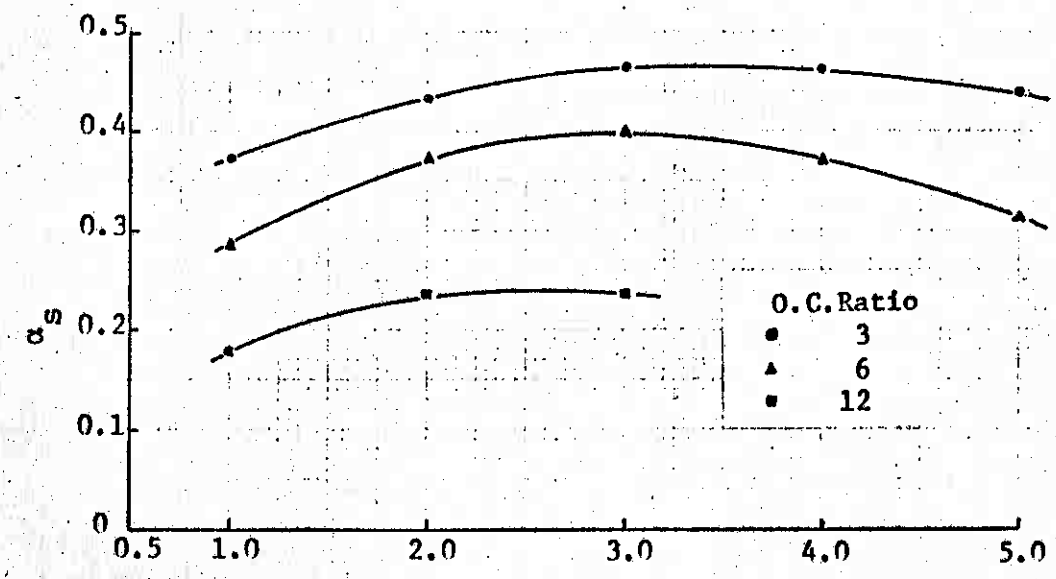

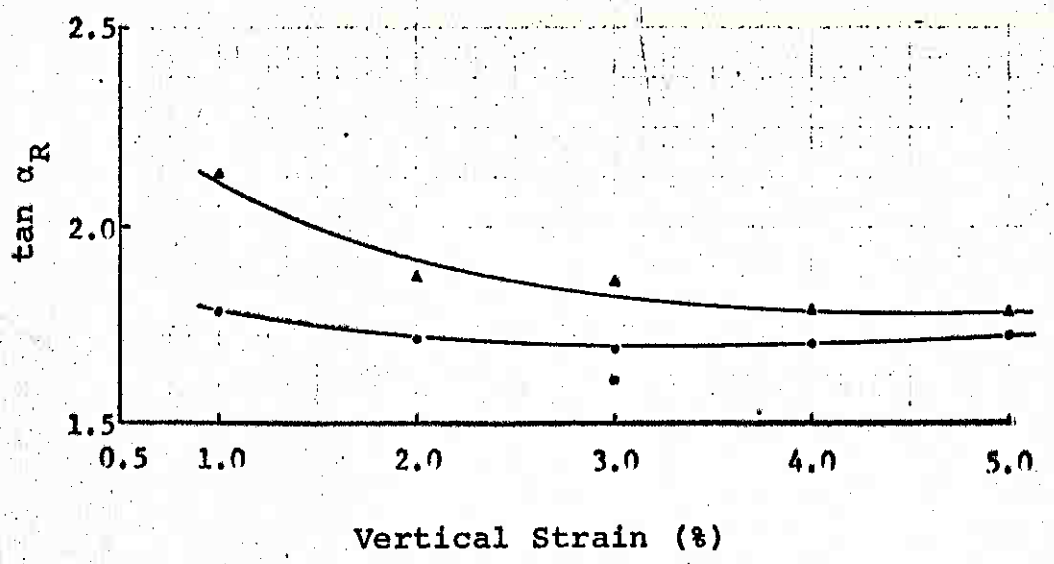

Figure D-4 α_s and tan α_R vs Strain, Constant-σ_1' Test Series on O.C. Kaolinite

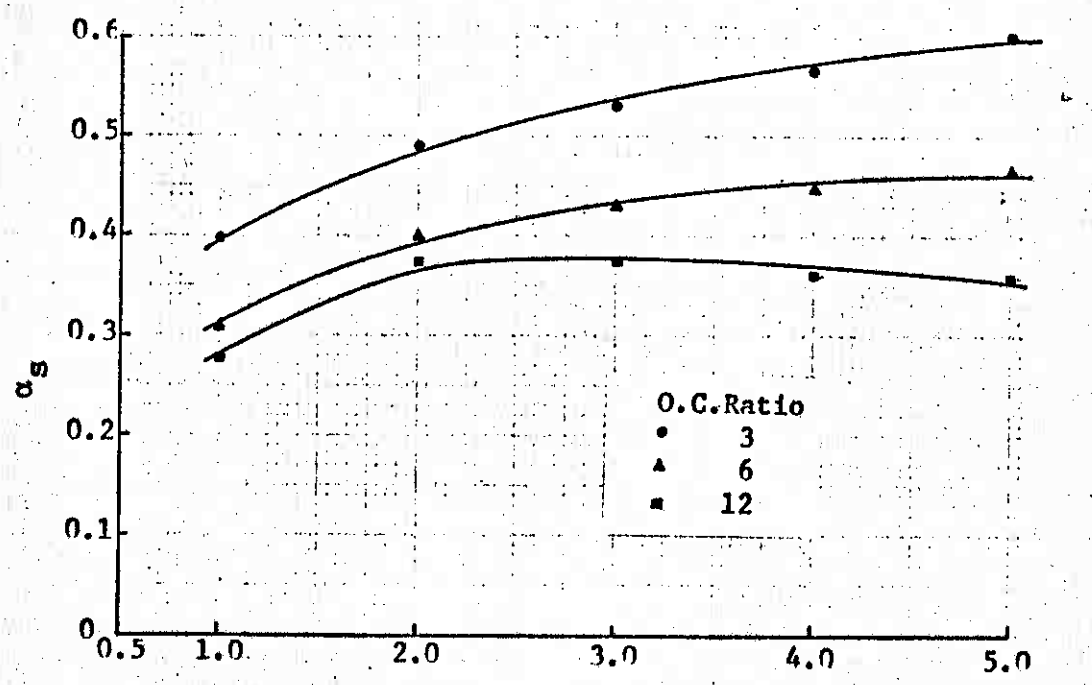

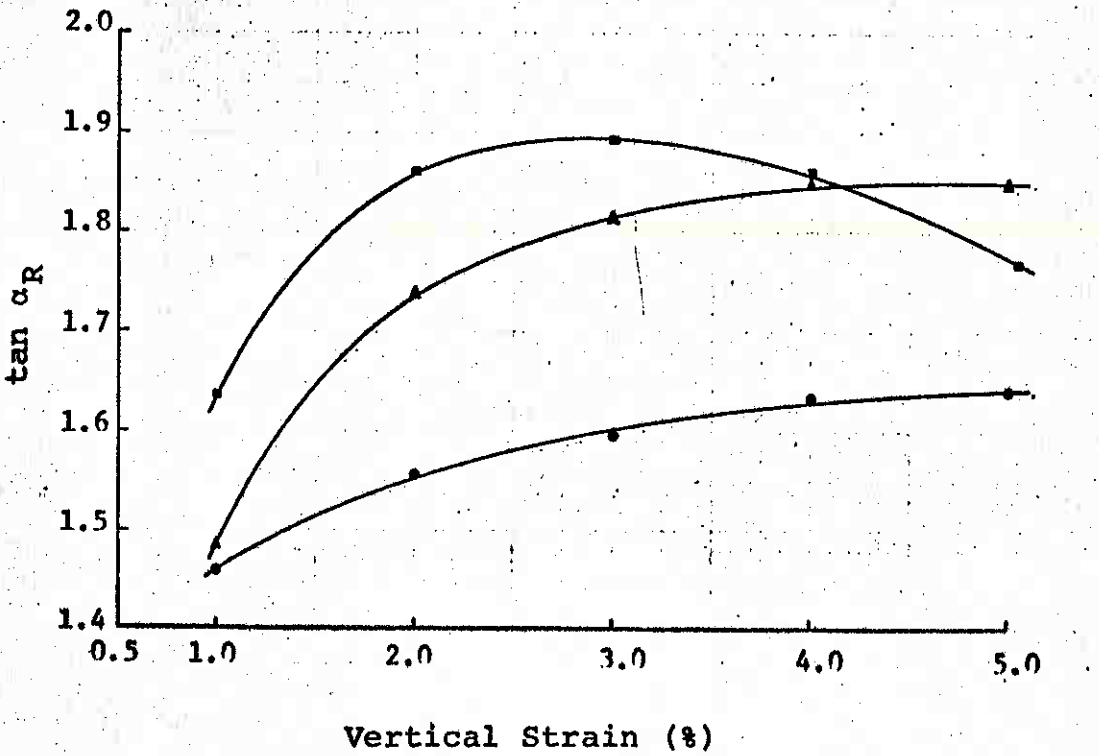

Figure D-5 α_s and tan α_R vs Strain, Constant-p' Test Series on O.C. Kaolinite

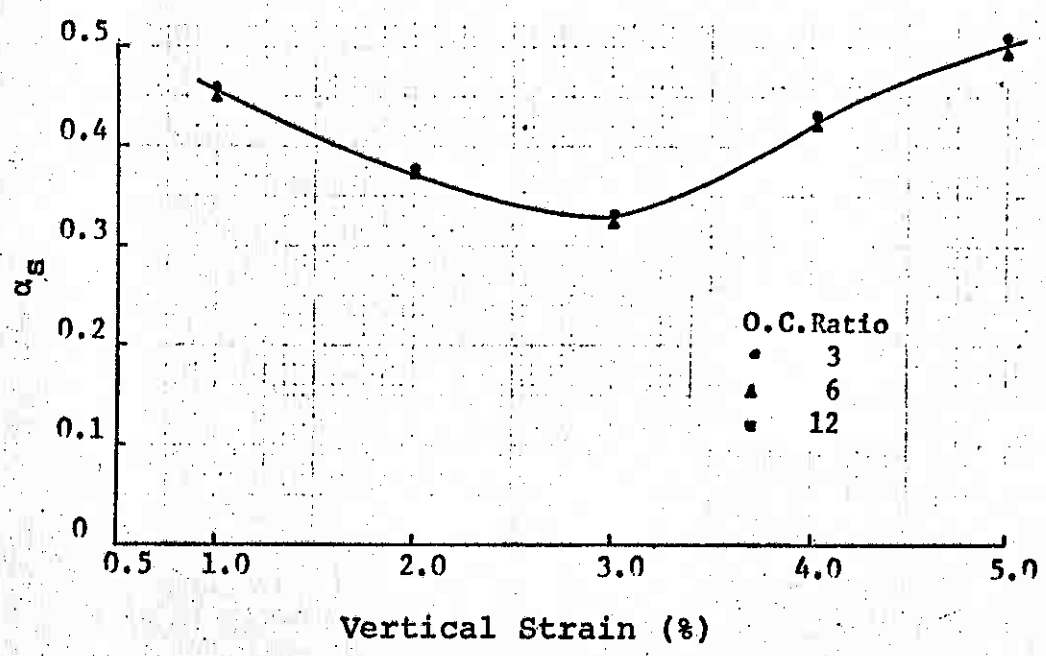

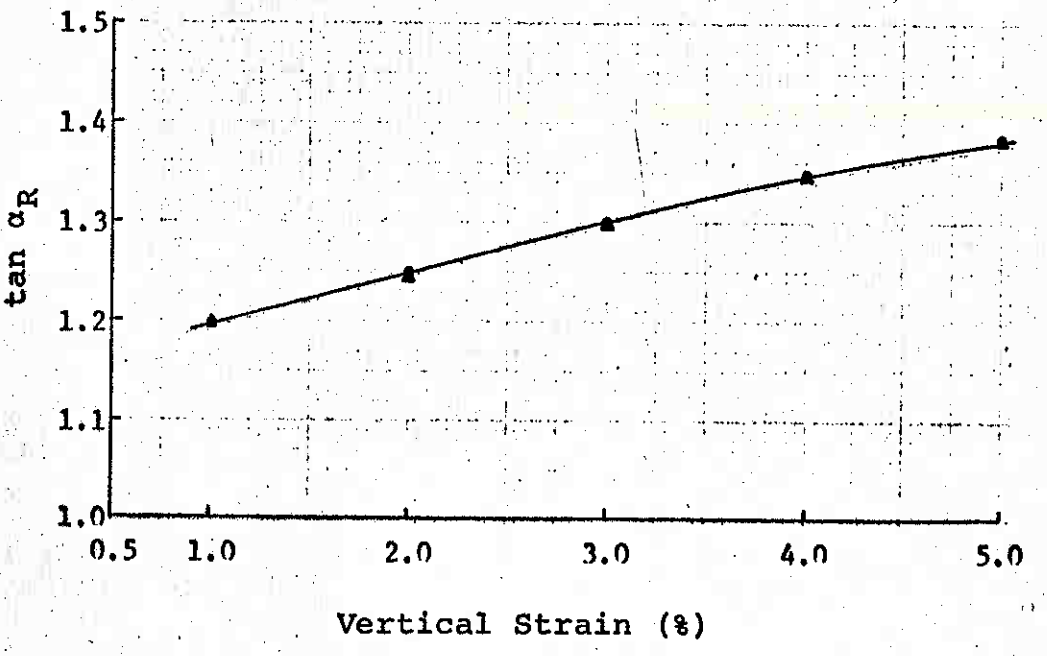

Figure D-6 α_s and tan α_R vs Strain, Constant-Volume Tests on O.C. Kaolinite

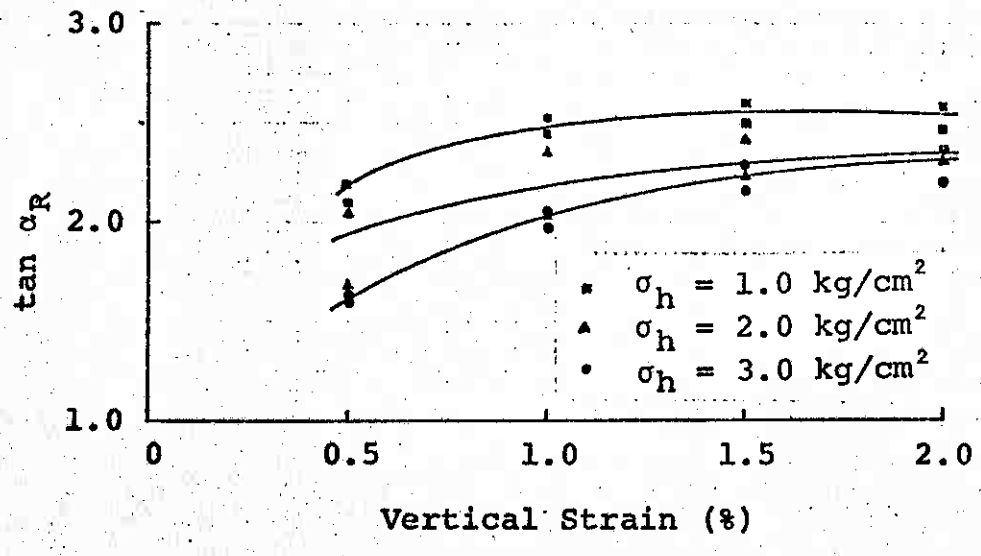

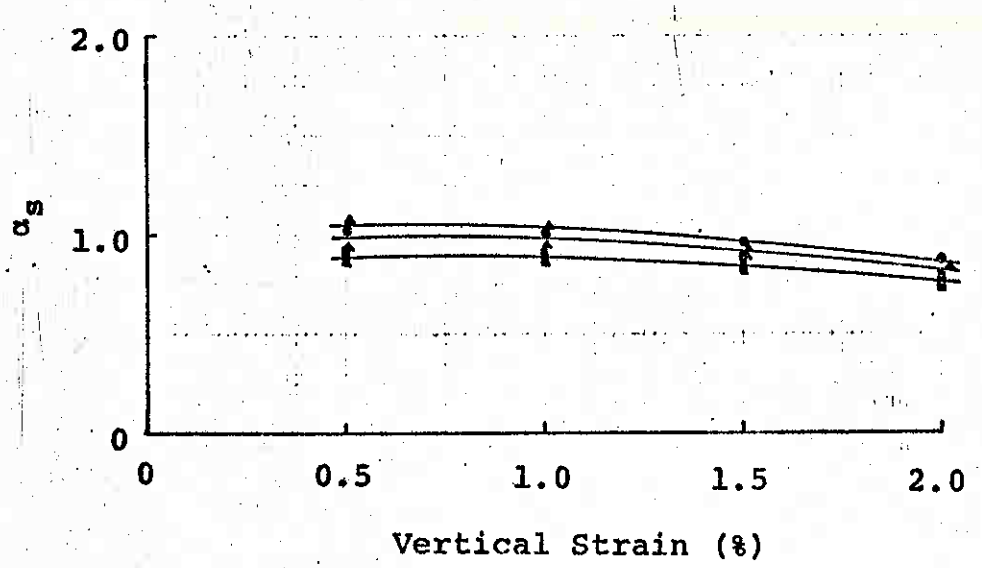

Figure D-7 α_s and tanα_R vs Strain, Constant-σ_3' Test Series on Glass Beads with Hydrocal

LIST OF REFERENCES

Andresen, A. and Simons, N.E., 1960. "Norwegian Triaxial Equipment and Technique," Research Conference on Shear Strength of Cohesive Soils, Boulder, Colorado. Pp. 695-709.

Barden, L. and Khayatt, A.J., 1966. "Incremental Strain Rate Ratios and Strength of Sand in the Triaxial Test," Geotechnique, Vol. 16, No. 4, pp. 338-357.

Barden, L., Khayatt, A.J. and Wightman, A., 1969. "Elastic and Slip Components of the Deformation of Sand," Canadian Geotechnical Journal, Vol. 6, No. 3, August, pp. 227-240.

Bishop, A.W., 1954. Correspondence on a paper by A.D.M. Penman. Geotechnique, Vol. 4, No. 1, pp. 43-45.

Bishop, A.W. and Henkel, D.J., 1964. The Measurement of Soil Properties in the Triaxial Test, Edward Arnold Ltd., London.

Bjerrum, L., 1954. "Theoretical and Experimental Investigations on the Shear Strength of Soils." Norwegian Geotech. Inst. Pub. No. 5.

Bjerrum, L., 1961. "The Effective Shear Strength Parameters of Sensitive Clays," Proc. 5th Int. Conf. Soil Mech., Vol. 1, pp. 23-28.

Caquot, A., 1934. "Equilibre des Massifs a Fronttement Interne," Stabilite des Terres Pulverents et Coherentes, Paris, Gauthier Villars.

Casagrande, A., 1932. "The Structure of Clay and Its Importance in Foundation Engineering," Contributions to Soil Mechanics, B.S.C.E. 1925-1940, pp. 72-112.

Christensen, R.W. and Wu, T.H., 1964. "Analysis of Clay Deformation as a Rate Process," Journal of Soil Mechanics and Foundations Division, ASCE, Vol. 90. No. SM6, November, pp. 125-157.

Crawford, C.B., 1961. "The Influence of Strain on Shearing Resistance of Sensitive Clay," Proc. A.S.T.M., pp. 1250-1276.

Crawford, C.B., 1963. "Cohesion in an Undisturbed Sensitive Clay," Geotechnique, Vol. 13, No. 2, pp. 132-146.

Duncan, J.M. and Seed, H.B., 1967. "Corrections for Strength Test Data," Journal of Soil Mechanics and Foundations Division, Vol. 93, No. SM6, September, pp. 121-137.

El-Sohby, M.A., 1964. "The Behaviour of Particulate Materials Under Stress," Ph.D. Thesis, Manchester University.

Gibson, R.E., 1953. "Esperimental Determination of the True Cohesion and Angle of Internal Friction in Clays," Proc. 3rd Int. Conf. Soil Mech., Vol. 1, pp. 126-130.

Henkel, D.J. and Gilbert, G.C., 1952. "The Effect of Rubber Membranes on the Measured Triaxial Compression Strength of Clay Samples," Geotechnique, Vol. 3, pp. 20-29.

Horne, M.R., 1965a. "The Behaviour of an Assembly of Rotund, Rigid, Cohesionless Particles, Part I," Proc. Royal Soc., A., Vol. 286, pp. 62-78.

Horne, M.R., 1965b. "The Behaviour of an Assembly of Rotund, Rigid, Cohesionless Particles, Part II," Proc. Royal Soc. A, Vol. 286, pp. 79-97.

Horne, M.R., 1969. "The Behaviour of an Assembly of Rotund, Rigid, Cohesionless Particles, Part III," Proc. Royal Soc. A, Vol. 310, pp. 21-34.

King, G.J.W. and Dickin, E.A., 1970. "Comparison of Stress Dilatancy Theories," Journal of Soil Mechanics and Foundation Division, ASCE, Vol. 96, No. SM5, September, pp. 1697-1714.

Kruyt, H.R., 1952. Colloid Science, Vol. I, Elsevier Publishing Co.

Ladanyi, B., Larochelle, P. and Tanguay, L., 1965. "Some Factors Controlling the Predictability of Stress-Strain Behaviour of Clay," Canadian Geotechnical Journal, Vol. 2, No. 2, May, pp. 60-83.

Lambe, T.W., 1953. "The Structure of Inorganic Soil," Proc. ASCE, Vol. 79, Separate No. 315, October, pp. 1-49.

Lambe, T.W., 1960. "A Mechanistic Picture of Shear Strength in Clay," Research Conf. on Shear Strength of Cohesive Soils, Boulder, Colorado, pp. 555-580.

Lambe, T.W. and Whitman, R.V., 1969. Soil Mechanics, John Wiley and Sons, New York.

Lee, I.K., 1966. "Stress Dilatancy Performance of Feldspar," Journal of Soil Mechanics and Foundations Division, ASCE, Vol. 92, No. SM2, March, pp. 79-103.

Lowe, III, J. and Johnson, T.C., 1960. "Use of Back Pressure to Increase Degree of Saturation of Triaxial Test Specimens," Research Conference on Shear Strength of Cohesive Soils, Boulder, Colorado, pp. 819-836.

Mendenhall, W., 1967. Introduction to Probability and Statistics, Wadsworth Publishing Co., Belmont, California.

Mitchell, J.K., 1964. "Shearing Resistance of Soils as a Rate Process," Journal of Soil Mechanics and Foundations Division, ASCE, Vol. 90, No. SM1, January, pp. 29-61.

Mitchell, J.K., Campanella, R.G., and Singh, A., 1968. "Soil Creep as a Rate Process," Journal of Soil Mechanics and Foundations Division, ASCE, Vol. 94, No. SM1, January, pp. 231-253.

Mitchell, J.K., Singh, A., and Campanella, R.G., 1969. "Bonding, Effective Stresses, and Strength of Soils," Journal of Soil Mechanics and Foundations Division, ASCE, Vol. 95, No. SM5, September, pp. 1219-1246.

Newland, P. L. and Allely, B.H., 1957. "Volume Changes in Drained Triaxial Tests on Granular Materials," Geotechnique, Vol. 7, No. 1, pp. 17-34.

Penman, A.D.M., 1953. "Shear Characteristics of a Saturated Silt," Geotechnique, Vol. 3, No. 8, pp. 312-328.

Roscoe, K.H., Schofield, A.N., and Wroth, C.P., 1958. "On the Yielding of Soils," Geotechnique, Vol. 8, No. 1, pp. 22-53.

Rosenquist, I. Th., 1959. "Physico-Chemical Properties of Soils: Soil Water Systems," Journal of Soil Mechanics and Foundations Division, ASCE, Vol. 85, No. SM2, April, pp. 31-53.

Rowe, P.W., 1962. "The Stress-Dilatancy Relation for Static Equilibrium of an Assembly of Particles in Contact," Proc. of Royal Society, A, Vol. 269, pp. 500-527.

Rowe, P.W., Oates, D.B., and Skermer, N.A., 1963. "The Stress Dilatancy Performance of Two Clays," Laboratory Shear Testing of Soils, ASTM, STP No. 361, pp. 134-143.

Rowe, P.W., 1963. "Stress Dilatancy, Earth Pressures and Slopes," Journal of Soil Mechanics and Foundations Division, ASCE, Vol. 89, No. SM3, May, pp. 37-61.

Rowe, P.W., 1964. Closure to discussion on paper by Rowe, 1963, Journal of Soil Mechanics and Foundations Division, ASCE, Vol. 90, No. SM4, July, pp. 145-180.

Rowe, P.W., Barden, L. and Lee, I.K., 1964. "Energy Components During the Triaxial Cell and Direct Shear Tests," Geotechnique, Vol. 14, No. 3, pp. 247-261.

Rowe, P.W., 1971. Discussion to paper by King and Dickin, 1970., Journal of Soil Mechanics and Foundations Div., Vol. 97, No. SM4, April, pp. 704-709.

Schmertmann, J.H., and Osterberg, J.O., 1960. "An Experimental Study of the Development of Cohesion and Friction iwth Axial Strain in Saturated Cohesive Soils," Research Conf. on Shear Strength of Cohesive Soils, Boulder, Colorado, p. 646.

Schmertmann, J.H., 1962. "Comparisons of One and Two-Specimen CFS Tests," Journal of Soil Mechanics and Foundations Division, ASCE, Vol. 88, No. SM6, December, pp. 169-205.

Schmertmann, J.H., 1963a. "Generalizing and Measuring the Hvorslev Effective Components of Shear Resistance," Laboratory Shear Testing of Soils, ASTM, STP No. 361, pp. 147-157.

Schmertmann, J.H., 1963b. Discussion on paper by Wu et al., 1962., Journal of Soil Mechanics and Foundation Division, ASCE, February, pp. 260-268.

Schmertmann, J.H., 1963c. "Study of the Reconsolidation Behaviour of Manglerud Quick Clay by Means of Constant-Volume IDS Tests," NGI Internal Report, F.234.1, July.

Schmertmann, J.H., 1966a. "The I-component of a Soil's Shear Resistance," Internal Report, Department of Civil Engineering, University of Florida. (Two copies of report in Dept. files).

Schmertmann, J.H., 1966b. "A Laboratory Test for Bond Strength," Internal Report, Department of Civil Engineering, University of Florida. (Two copies of report in Dept. files).

Scott, R.F., 1963. Principles of Soil Mechanics, Addison-Wesley, Mass.

Steel, R.G.D. and Torrie, J.H., 1960. Principles and Procedures of Statistics, McGraw-Hill Co., New York.

Taylor, D.W., 1948. Fundamentals of Soil Mechanics, J. Wiley and Sons, New York.

Terzaghi, K., 1920. "Old Earth-Pressure Theories and New Test Results," Engineering News Record, 85, No. 14, p. 633. (1960 Reprinted in From Theory to Practice in Soil Mechanics, J. Wiley and Sons, New York).

Topshoj, A., 1970. "Bond Strength of Extruded Kaolinite by Triaxial Extension Testing," M. Sc. Thesis, U. of Florida.

Trollope, D.H. and Chan, C.K., 1960. "Soil Structure and the Step-Strain Phenomenon," Journal of Soil Mechanics and Foundations Division, ASCE, Vol. 86, No. SM2, April, pp. 1-39.

Trollope, D.H., 1961. "Effective Contact Stresses and Friction," Nature, Vol. 191, pp. 376-377.

Trollope, D.H., Rosengren, K.J. and Brown, E.T., 1965. "The Mechanics of Brown Coal," Geotechnique, Vol. 15, No. 4, pp. 363-386.

Yong, R.N. and Vey, E., 1962. "The Use of Stress Loci for Determination of Effective Stress Parameters," Highway Research Board, Bulletin No. 342, pp. 38-49.

BIOGRAPHICAL SKETCH

Kum-Hung Ho was born in Malacca, Malaya, Malaysia on April 20, 1932. Upon graduation from High School, Malacca he entered the University of Hong Kong where he obtained a Bachelor of Science degree in Civil Engineering with honours in May, 1957. He then joined the British Consulting Firm of Scott and Wilson, Kirkpatrick and Partners as an assistant engineer until he left for graduate study in Canada in September, 1959. While at McGill University, Montreal he held teaching and research assistantships, graduating with a Master of Engineering degree in May, 1962. He was employed by Terratech Limited, Montreal as a soils engineer and later worked for St. Lawrence Seaway Authority Montreal in the same capacity till December, 1966.

He was enrolled at the University of Florida in 1967 and held a research assistantship during his course of study for the degree of Doctor of Philosophy.

He is an Associate Member of the American Society of Civil Engineers and is married to the former Nancy Lin-Hee Yip of Singapore and has a son and a daughter.

I certify that I have read this study and that in my opinion it conforms to acceptable standards of scholarly presentation and is fully adequate, in scope and quality, as a dissertation for the degree of Doctor of Philosophy.

John H. Schmertmann, Chairman
Professor of Civil Engineering

I certify that I have read this study and that in my opinion it conforms to acceptable standards of scholarly presentation and is fully adequate, in scope and quality, as a dissertation for the degree of Doctor of Philosophy.

Morris W. Self
Professor of Civil Engineering

I certify that I have read this study and that in my opinion it conforms to acceptable standards of scholarly presentation and is fully adequate, in scope and quality, as a dissertation for the degree of Doctor of Philosophy.

Frank G. Martin
Associate Professor of Statistics

This dissertation was submitted to the Dean of the College of Engineering and to the Graduate Council, and was accepted as partial fulfillment of the requirements for the degree of Doctor of Philosophy.

August, 1971

Dean, College of Engineering

Dean, Graduate School